

Impacts of Heatwaves and Hypoxia on Gene Expression in the Pacific Oyster and the
Development of Monitoring and Mitigation Tools for Summer Mortality

by

Andrew Bickell

B.Sc., Simon Fraser University, 2023

A Thesis Submitted in Partial Fulfillment of the Requirements for the Degree of

MASTER OF SCIENCE

in the Department of Biology

© Andrew Bickell, 2025

University of Victoria

All rights reserved. This thesis may not be reproduced in whole or in part, by photocopy or other means, without the permission of the author.

We acknowledge and respect the Ləkʷəŋən (Songhees and Xʷsepsəm/Esquimalt) Peoples on whose territory the university stands, and the Ləkʷəŋən and W̱SÁNEĆ Peoples whose historical relationships with the land continue to this day.

Impacts of Heatwaves and Hypoxia on Gene Expression in the Pacific Oyster and the
Development of Monitoring and Mitigation Tools for Summer Mortality

by

Andrew Bickell

B.Sc., Simon Fraser University, 2023

Supervisory Committee:

Dr. Christopher Pearce – Co-Supervisor
Department of Geography

Dr. Amanda Bates – Co-Supervisor
Department of Biology

Dr. Timothy Green – Outside Member
Vancouver Island University, Centre for Shellfish Research

Abstract

Marine heatwaves and coastal hypoxic events are increasing in frequency and intensity under anthropogenic climate change, resulting in widespread mass mortalities of the Pacific oyster (*Crassostrea gigas*). Those mortality events threaten the economic stability of global aquaculture, yet strategies to monitor oyster health and mitigate losses during periods of environmental stress are largely limited. Changes in gene expression of *C. gigas* in response to laboratory-simulated heatwaves and hypoxic events were assessed to identify candidate monitoring genes and explore artificial aeration as a potential mortality mitigation strategy. Two laboratory experiments were performed, exposing farmed *C. gigas* to simulated 10-day heatwave and hypoxic conditions similar to a 2021 marine heatwave that triggered farmed oyster mortality in Baynes Sound, British Columbia, Canada. Gill tissues were periodically sampled during the experiments and total RNA was extracted to explore patterns of gene expression via RNAseq and qPCR. Five candidate genes were consistently differentially expressed in both experiments—death-associated inhibitor of apoptosis 2 (A2I), high mobility group protein DSP1 (DSP1), high mobility group box 1 (HMGB1), heat shock protein 90 (HSP90), and peptidyl-prolyl cis-trans isomerase (PPCTI)—demonstrating potential for monitoring summer mortality. No significant differences in expression of the general stress marker genes heat shock protein 70 (HSP70) and heat shock protein 20 (HSP20) were detected, suggesting that genes related to immune function and regulation of transcription may be more appropriate for monitoring summer mortality. In addition, the presence of artificial aeration resulted in significantly lower HSP90 relative expression, suggesting some potential utility in stress mitigation during heatwaves. The present work provides insights into the role of heatwaves and hypoxia in Pacific oyster summer mortality

and will inform effective monitoring and mitigation practices to support the adaptation of shellfish aquaculture to the growing impacts of climate change.

Table of Contents

Supervisory Committee	ii
Abstract	iii
Table of Contents	v
List of Tables	viii
List of Figures	ix
Acknowledgements	xvii
Chapter 1. Introduction	1
1.1 Climate change	1
1.2 Marine heatwaves	5
1.3 Coastal hypoxic events	7
1.4 Aquaculture	10
1.5 Pacific oyster summer mortality	13
1.6 Mortality monitoring and mitigation	16
1.7 Objectives	18
Chapter 2. Simulated marine heatwave alters gene expression in the Pacific oyster (<i>Crassostrea gigas</i>): potential monitoring tools for summer mortality	20
2.1 Introduction	20
2.2 Materials and methods	25
2.2.1 Oyster collection and acclimation	25
2.2.2 Experimental conditions	26
2.2.3 Experimental monitoring	27
2.2.4 Oyster sampling	27
2.2.5 Condition index	28
2.2.6 RNA extraction and purification	28
2.2.7 cDNA synthesis	30
2.2.8 RNA sequencing and analysis	30
2.2.9 Candidate gene selection	31
2.2.10 Primer design	33
2.2.11 qPCR verification	34
2.2.12 qPCR statistical analysis	35

2.3 Results	36
2.3.1 Experimental monitoring	36
2.3.2 Condition index	37
2.3.3 RNA sequencing	37
2.3.4 qPCR single-gene responses	38
2.3.5 qPCR multivariate response	42
2.4 Discussion	44
2.4.1 Identification of candidate genes for summer mortality monitoring	44
2.4.2 Genes involved in stress response	47
2.4.3 Genes involved in regulation of transcription	49
2.4.4 Genes involved in immune function	50
2.4.5 Conclusion	54
2.5 Tables and figures	56
Chapter 3. Simulated heatwave and hypoxic event alter gene expression in the Pacific oyster (<i>Crassostrea gigas</i>): potential monitoring and mitigation strategies for summer mortality	70
3.1 Introduction	70
3.2 Materials and methods	76
3.2.1 Oyster collection and acclimation	76
3.2.2 Experimental conditions	77
3.2.3 Experimental monitoring	78
3.2.4 Oyster sampling	79
3.2.5 Condition index	79
3.2.6 RNA extraction and purification	80
3.2.7 cDNA synthesis	81
3.2.8 RNA sequencing and analysis	82
3.2.9 Candidate gene selection	83
3.2.10 Primer design	84
3.2.11 qPCR verification	85
3.2.12 qPCR statistical analysis	86
3.3 Results	88
3.3.1 Experimental monitoring	88

3.3.2 Condition index	89
3.3.3 RNA sequencing	89
3.3.4 qPCR single-gene responses	91
3.3.5 qPCR multivariate response	94
3.4 Discussion	96
3.4.1 Identification of candidate genes for summer mortality monitoring	97
3.4.2 Genes involved in stress response	100
3.4.3 Genes involved in regulation of transcription	102
3.4.4 Genes involved in immune function	103
3.4.5 Conclusion	106
3.5 Tables and figures	108
Chapter 4. Conclusions and perspectives	124
4.1 Candidate genes for summer mortality monitoring	124
4.2 Simulated heatwaves impact immune function	126
4.3 Artificial aeration may mitigate stress response during heatwaves	128
4.4 Conclusion	130
4.5 Tables and figures	132
References	133

List of Tables

Table 2.1 Primer sequences used in qPCR verification and associated gene IDs for cDNA sequences used in primer design	56
Table 2.2 Numbers of differently expressed genes (DEGs) at each heatwave timepoint and corresponding temperature including both upregulated and downregulated DEGs	57
Table 3.1 Primer sequences used in qPCR verification and associated gene IDs for cDNA sequences used in primer design	108
Table 3.2 Numbers of differently expressed genes (DEGs) in each treatment and timepoint with corresponding temperature, including both upregulated and downregulated DEGs	109

List of Figures

Figure 2.1 Heat map of changes in gene expression (Log₂FC) for the 246 DEGs detected by RNAseq at the height of the heatwave (T5, 26°C) at each timepoint during the experiment. Hierarchical clustering was performed for genes (rows) using Euclidean distance and complete linkage. A colour gradient from blue (low) to red (high) represents Log₂FC values 58

Figure 2.2 Heat map of changes in gene expression (Log₂ fold change) detected by RNAseq for the 10 genes of interest (GOIs) — peptidyl-prolyl cis-trans isomerase (PPCTI), high mobility group protein DSP1 (DSP1), high mobility group box 1 (HMGB1), heterogeneous nuclear ribonucleoprotein (HNR), stress-induced protein 1 (SIP1), heat shock protein 70 B2 (HSP70), x-box-binding protein 1 (XBP1), death-associated inhibitor of apoptosis 2 (A2I), heat shock protein 20 (HSP20), and heat shock protein 90 (HSP90) — chosen for qPCR validation at each timepoint during the experiment. Hierarchical clustering was performed for genes (rows) using Euclidean distance and complete linkage. A colour gradient from blue (low) to red (high) represents Log₂FC values 59

Figure 2.3 Heat map of relative expression ($2^{\Delta Cq}$) for the five genes of interest (GOIs)—death-associated inhibitor of apoptosis 2 (A2I), heat shock protein 90 (HSP90), high mobility group box 1 (HMGB1), peptidyl-prolyl cis-trans isomerase (PPCTI), and high mobility group protein DSP1 (DSP1) — that showed significant ($p < 0.05$) changes under single-gene response assessment. Hierarchical clustering was performed for both genes (columns) and temperatures (rows) using Euclidean distance and complete linkage. A colour gradient from blue (low) to red (high) represents z-transformed relative expression values. Relative expression is similar at higher temperatures, as indicated by clustering of darker green rows 60

Figure 2.4 Mean relative expression ($2^{\Delta Cq}$) and standard error ($n = 12$) for high mobility group protein DSP1 (DSP1) on day 0 (T0, 16°C), day 2 (T1, 18°C), day 4 (T2, 20°C), day 6 (T3, 22°C), day 8 (T4, 24°C), and day 10 (T5, 26°C) of the simulated heatwave compared to the control (16°C). Relative expression normalized to actin where $\Delta Cq = (Cq_{actin} - Cq_{DSP1})$. Capital

letters in the legend show significant ($p < 0.05$) differences identified for the treatment effect via two-way ANOVA, while lower-case letters above the bars show significant ($p < 0.05$) differences between treatments and timepoints identified by a post-hoc Student-Newman-Keuls (SNK) test

..... 61

Figure 2.5 Mean relative expression ($2^{\Delta Cq}$) and standard error ($n = 12$) for high mobility group box 1 (HMGB1) on day 0 (T0, 16°C), day 2 (T1, 18°C), day 4 (T2, 20°C), day 6 (T3, 22°C), day 8 (T4, 24°C), and day 10 (T5, 26°C) of the simulated heatwave compared to the control (16°C). Relative expression normalized to actin where $\Delta Cq = (Cq_{actin} - Cq_{HMGB1})$. Capital letters in the legend show significant ($p < 0.05$) differences identified for the treatment effect via two-way ANOVA, while lower-case letters above the bars show significant ($p < 0.05$) differences between timepoints identified by a post-hoc Student-Newman-Keuls (SNK) test 62

Figure 2.6 Mean relative expression ($2^{\Delta Cq}$) and standard error ($n = 12$) for peptidyl-prolyl cis-trans isomerase (PPCTI) on day 0 (T0, 16°C), day 2 (T1, 18°C), day 4 (T2, 20°C), day 6 (T3, 22°C), day 8 (T4, 24°C), and day 10 (T5, 26°C) of the simulated heatwave compared to the control (16°C). Relative expression normalized to actin where $\Delta Cq = (Cq_{actin} - Cq_{PPCTI})$. Capital letters in the legend show significant ($p < 0.05$) differences identified for the treatment effect via two-way ANOVA, while lower-case letters above the bars show significant ($p < 0.05$) differences between timepoints identified by a post-hoc Student-Newman-Keuls (SNK) test 63

Figure 2.7 Mean relative expression ($2^{\Delta Cq}$) and standard error ($n = 12$) for death-associated inhibitor of apoptosis 2 (A2I) on day 0 (T0, 16°C), day 2 (T1, 18°C), day 4 (T2, 20°C), day 6 (T3, 22°C), day 8 (T4, 24°C), and day 10 (T5, 26°C) of the simulated heatwave compared to the control (16°C). Relative expression normalized to actin where $\Delta Cq = (Cq_{actin} - Cq_{A2I})$. Capital letters in the legend show significant ($p < 0.05$) differences identified for the treatment effect via two-way ANOVA, while lower-case letters above the bars show significant ($p < 0.05$) differences between timepoints identified by a post-hoc Student-Newman-Keuls (SNK) test 64

Figure 2.8 Mean relative expression ($2^{\Delta Cq}$) and standard error ($n = 12$) for heat shock protein 90 (HSP90) on day 0 (T0, 16°C), day 2 (T1, 18°C), day 4 (T2, 20°C), day 6 (T3, 22°C), day 8 (T4,

24°C), and day 10 (T5, 26°C) of the simulated heatwave compared to the control (16°C). Relative expression normalized to actin where $\Delta Cq = (Cq_{actin} - Cq_{HSP90})$. Capital letters in the legend show significant ($p < 0.05$) differences identified for the treatment effect via two-way ANOVA, while lower-case letters above the bars show significant ($p < 0.05$) differences between treatments and timepoints identified by a post-hoc Student-Newman-Keuls (SNK) test 65

Figure 2.9 Mean relative expression ($2^{\Delta Cq}$) and standard error ($n = 12$) for heat shock protein 20 (HSP20) on day 0 (T0, 16°C), day 2 (T1, 18°C), day 4 (T2, 20°C), day 6 (T3, 22°C), day 8 (T4, 24°C), and day 10 (T5, 26°C) of the simulated heatwave compared to the control (16°C). Relative expression normalized to actin where $\Delta Cq = (Cq_{actin} - Cq_{HSP20})$. Capital letters in the legend show significant ($p < 0.05$) differences identified for the treatment effect via two-way ANOVA, while lower-case letters above the bars show significant ($p < 0.05$) differences between timepoints identified by a post-hoc Student-Newman-Keuls (SNK) test 66

Figure 2.10 Mean relative expression ($2^{\Delta Cq}$) and standard error ($n = 12$) for heat shock protein 70 B2 (HSP70) on day 0 (T0, 16°C), day 2 (T1, 18°C), day 4 (T2, 20°C), day 6 (T3, 22°C), day 8 (T4, 24°C), and day 10 (T5, 26°C) of the simulated heatwave compared to the control (16°C). Relative expression normalized to actin where $\Delta Cq = (Cq_{actin} - Cq_{HSP70})$. Capital letters in the legend show significant ($p < 0.05$) differences identified for the treatment effect via two-way ANOVA, while lower-case letters above the bars show significant ($p < 0.05$) differences between timepoints identified by a post-hoc Student-Newman-Keuls (SNK) test 67

Figure 2.11 Principal Component Analysis (PCA) of relative expression for the five genes of interest (GOIs)—death-associated inhibitor of apoptosis 2 (A2I), heat shock protein 90 (HSP90), high mobility group box 1 (HMGB1), peptidyl-prolyl cis-trans isomerase (PPCTI), and high mobility group protein DSP1 (DSP1)—that showed significant ($p < 0.05$) changes under single-gene response assessment. The first two principal components (PC1 and PC2) are plotted, explaining 43.98% and 39.12% of the total variance, respectively. Samples are colored according to treatment group (control = blue, heatwave = red) and ellipses represent 95% confidence intervals for each group. PCA reveals some cluster separation between control and heatwave, especially along PC1..... 68

Figure 2.12 Biplot showing the results of Principal Component Analysis (PCA) on relative expression for the five genes of interest (GOIs)—death-associated inhibitor of apoptosis 2 (A2I), heat shock protein 90 (HSP90), high mobility group box 1 (HMGB1), peptidyl-prolyl cis-trans isomerase (PPCTI), and high mobility group protein DSP1 (DSP1)—that showed significant ($p < 0.05$) changes under single-gene response assessment. Samples are colored according to treatment group (control = blue, heatwave = red) and arrows represent the loadings of individual genes, with longer arrows indicating stronger contributions to the corresponding principal components. HSP90 is strongly associated with PC1, while HMGB1, PPCTI, and DSP1 are associated with PC2 69

Figure 3.1 Heat map of changes in gene expression (Log2FC) during the simulated heatwave for the 45 differently expressed genes detected by RNAseq at the height of the heatwave (T5, 26°C) in the heatwave treatment at each timepoint during the experiment. Hierarchical clustering was performed for genes (rows) using Euclidean distance and complete linkage. A colour gradient from blue (low) to red (high) represents Log2FC values 110

Figure 3.2 Heat map of changes in gene expression (Log2FC) during the simulated heatwave for the 133 differently expressed genes detected by RNAseq at the height of the heatwave (T5, 26°C) in the heatwave + hypoxia treatment at each timepoint during the experiment. Hierarchical clustering was performed for genes (rows) using Euclidean distance and complete linkage. A colour gradient from blue (low) to red (high) represents Log2FC values 111

Figure 3.3 Heat map of changes in gene expression (Log2 fold change) detected by RNAseq for the 10 genes of interest— peptidyl-prolyl cis-trans isomerase (PPCTI), x-box-binding protein 1 (XBP1), death-associated inhibitor of apoptosis 2 (A2I), high mobility group protein DSP1 (DSP1), high mobility group box 1 (HMGB1), heat shock protein 20 (HSP20), heat shock protein 70 B2 (HSP70), heat shock protein 90 (HSP90), stress-induced protein 1 (SIP1), and heterogeneous nuclear ribonucleoprotein (HNR)—chosen for qPCR validation across all five timepoints for the heatwave treatment. Hierarchical clustering was performed for genes (rows)

using Euclidean distance and complete linkage. A colour gradient from blue (low) to red (high) represents Log2FC values 112

Figure 3.4 Heat map of changes in gene expression (Log2 fold change) detected by RNAseq for the 10 genes of interest— x-box-binding protein 1 (XBP1), death-associated inhibitor of apoptosis 2 (A2I), heterogeneous nuclear ribonucleoprotein (HNR), heat shock protein 90 (HSP90), heat shock protein 20 (HSP20), heat shock protein 70 B2 (HSP70), stress-induced protein 1 (SIP1), peptidyl-prolyl cis-trans isomerase (PPCTI), high mobility group protein DSP1 (DSP1), and high mobility group box 1 (HMGB1)—chosen for qPCR validation across all five timepoints for the heatwave + hypoxia treatment. Hierarchical clustering was performed for genes (rows) using Euclidean distance and complete linkage. A colour gradient from blue (low) to red (high) represents Log2FC values 113

Figure 3.5 Heat map of relative expression ($2^{\Delta Cq}$) for the five genes of interest—heat shock protein 90 (HSP90), death-associated inhibitor of apoptosis 2 (A2I), high mobility group box 1 (HMGB1), peptidyl-prolyl cis-trans isomerase (PPCTI), and high mobility group protein DSP1 (DSP1)—that showed significant ($p < 0.05$) changes under single-gene response assessment. Hierarchical clustering was performed for both genes (columns) and temperatures (rows) using Euclidean distance and complete linkage. A colour gradient from blue (low) to red (high) represents z-transformed relative expression values. Relative expression is similar at higher temperatures, as indicated by clustering of darker green rows 114

Figure 3.6 Mean relative expression ($2^{\Delta Cq}$) and standard error ($n = 6$) for high mobility group protein DSP1 (DSP1) on day 0 (T0, 16°C), day 2 (T1, 18°C), day 4 (T2, 20°C), day 6 (T3, 22°C), day 8 (T4, 24°C), and day 10 (T5, 26°C) of the simulated heatwave compared to the control (16°C). Relative expression normalized to actin where $\Delta Cq = (Cq_{actin} - Cq_{DSP1})$. Letters show significant ($p < 0.05$) differences identified via post-hoc Student-Newman-Keuls (SNK) test 115

Figure 3.7 Mean relative expression ($2^{\Delta Cq}$) and standard error ($n = 6$) for high mobility group box 1 (HMGB1) on day 0 (T0, 16°C), day 2 (T1, 18°C), day 4 (T2, 20°C), day 6 (T3, 22°C), day

8 (T4, 24°C), and day 10 (T5, 26°C) of the simulated heatwave compared to the control (16°C). Relative expression normalized to actin where $\Delta Cq = (Cq_{actin} - Cq_{HMGB1})$. Letters show significant ($p < 0.05$) differences identified via post-hoc Student-Newman-Keuls (SNK) test.

..... 116

Figure 3.8 Mean relative expression ($2^{\Delta Cq}$) and standard error ($n = 6$) for peptidyl-prolyl cis-trans isomerase (PPCTI) on day 0 (T0, 16°C), day 2 (T1, 18°C), day 4 (T2, 20°C), day 6 (T3, 22°C), day 8 (T4, 24°C), and day 10 (T5, 26°C) of the simulated heatwave compared to the control (16°C). Relative expression normalized to actin where $\Delta Cq = (Cq_{actin} - Cq_{PPCTI})$. Letters show significant ($p < 0.05$) differences identified via post-hoc Student-Newman-Keuls (SNK) test 117

Figure 3.9 Mean relative expression ($2^{\Delta Cq}$) and standard error ($n = 6$) for death-associated inhibitor of apoptosis 2 (A2I) on day 0 (T0, 16°C), day 2 (T1, 18°C), day 4 (T2, 20°C), day 6 (T3, 22°C), day 8 (T4, 24°C), and day 10 (T5, 26°C) of the simulated heatwave compared to the control (16°C). Relative expression normalized to actin where $\Delta Cq = (Cq_{actin} - Cq_{A2I})$. Capital letters in the legend show significant ($p < 0.05$) differences identified for the treatment effect via post-hoc Student-Newman-Keuls (SNK) test, while lower-case letters above the bars show significant ($p < 0.05$) differences between timepoints identified by an additional SNK test 118

Figure 3.10 Mean relative expression ($2^{\Delta Cq}$) and standard error ($n = 6$) for heat shock protein 90 (HSP90) on day 0 (T0, 16°C), day 2 (T1, 18°C), day 4 (T2, 20°C), day 6 (T3, 22°C), day 8 (T4, 24°C), and day 10 (T5, 26°C) of the simulated heatwave compared to the control (16°C). Relative expression normalized to actin where $\Delta Cq = (Cq_{actin} - Cq_{HSP90})$. Letters show significant ($p < 0.05$) differences identified via post-hoc Student-Newman-Keuls (SNK) test.

..... 119

Figure 3.11 Mean relative expression ($2^{\Delta Cq}$) and standard error ($n = 6$) for heat shock protein 20 (HSP20) on day 0 (T0, 16°C), day 2 (T1, 18°C), day 4 (T2, 20°C), day 6 (T3, 22°C), day 8 (T4, 24°C), and day 10 (T5, 26°C) of the simulated heatwave compared to the control (16°C). Relative expression normalized to actin where $\Delta Cq = (Cq_{actin} - Cq_{HSP20})$. Capital letters in the

legend show significant ($p < 0.05$) differences identified for the treatment effect via post-hoc Student-Newman-Keuls (SNK) test, while lower-case letters above the bars show significant ($p < 0.05$) differences between timepoints identified by an additional SNK test 120

Figure 3.12 Mean relative expression ($2^{\Delta Cq}$) and standard error ($n = 6$) for heat shock protein 70 B2 (HSP70) on day 0 (T0, 16°C), day 2 (T1, 18°C), day 4 (T2, 20°C), day 6 (T3, 22°C), day 8 (T4, 24°C), and day 10 (T5, 26°C) of the simulated heatwave compared to the control (16°C). Relative expression normalized to actin where $\Delta Cq = (Cq_{actin} - Cq_{HSP70})$. Capital letters in the legend show significant ($p < 0.05$) differences identified for the treatment effect via post-hoc Student-Newman-Keuls (SNK) test, while lower-case letters above the bars show significant ($p < 0.05$) differences between timepoints identified by an additional SNK test 121

Figure 3.13 Principal Component Analysis (PCA) of relative expression for the five genes of interest—death-associated inhibitor of apoptosis 2 (A2I), high mobility group box 1 (HMGB1), high mobility group protein DSP1 (DSP1), heat shock protein 90 (HSP90), and peptidyl-prolyl cis-trans isomerase (PPCTI)— that showed significant ($p < 0.05$) changes under single-gene response assessment. The first two principal components (PC1 and PC2) are plotted, explaining 43.98% and 39.12% of the total variance, respectively. Samples are colored according to treatment group (control = blue, heatwave = red, heatwave + hypoxia = purple) and ellipses represent 95% confidence intervals for each group. PCA reveals some cluster separation between control and heatwave treatments, especially along PC1 122

Figure 3.14 Biplot showing the results of Principal Component Analysis (PCA) on relative expression for the five genes of interest—death-associated inhibitor of apoptosis 2 (A2I), high mobility group box 1 (HMGB1), high mobility group protein DSP1 (DSP1), heat shock protein 90 (HSP90), and peptidyl-prolyl cis-trans isomerase (PPCTI)—that showed significant ($p < 0.05$) changes under single-gene response assessment. Samples are colored according to treatment group (control = blue, heatwave = red, heatwave + hypoxia = purple) and arrows represent the loadings of individual genes, with longer arrows indicating stronger contributions to the corresponding principal components. HSP90 is strongly associated with PC1, while PPCTI, HMGB1, and DSP1 are associated with PC2 123

Figure 4.1 Hypothesized mechanisms by which marine heatwaves affect oyster physiology and pathogenic bacteria, contributing to Pacific oyster summer mortality, along with the proposed mitigating effects of artificial aeration. Arrows represent interactions between factors: red arrows indicate relationships established in previous studies, while blue arrows indicate potential interactions suggested by findings from this thesis. Increases and decreases in individual factors are indicated by (+) and (-), respectively..... 132

Acknowledgements

I would like to thank the members of my supervisory committee, Dr. Christopher Pearce, Dr. Amanda Bates, and Dr. Timothy Green for their continuous support, and guidance throughout this project. I would also like to thank the Fisheries and Oceans Canada Sustainable Invertebrate Aquaculture Program team at Pacific Biological Station in Nanaimo, without whom this research would not have been possible. Specifically, I would like to thank Dr. Clara Mackenzie for working closely with me in all aspects of this project and for supporting this work with enthusiasm. I would also like to thank Chen Walker, who trained me in all the genetics laboratory techniques that were essential to this work, and Sierra Gray, whose encouragement and spirit convinced me to take on this MSc. In addition, this work would not have been possible without the financial support provided by a Competitive Science Research Fund through Fisheries and Oceans Canada. I am very grateful to my friends and family who have supported me through this work. While many deserve mention, a special thank you to Carter Burtlake, Mara Bohm, Kiarra Kattler, Gena Desjardin, Tristyn Erwood, Austin Neetz and Rachel Morris. Lastly, thank you to my parents, my biggest supporters.

Chapter 1. Introduction

1.1 Climate change

Climate change is perhaps the most significant global challenge of the 21st century. The Intergovernmental Panel on Climate Change (IPCC) has recently concluded that the anthropogenic release of greenhouse gases (GHGs), particularly carbon dioxide (CO₂) and methane (CH₄), into the atmosphere has unequivocally led to the observed 1.1°C of warming of the planet compared to pre-industrial levels (1850–1900) (Calvin et al., 2023). Since the industrial revolution (1750), average atmospheric CO₂ has increased from around 280 parts per million (ppm) to 410 ppm, a level which has not been observed for at least 2 million years (IPCC, 2023). This increase in emissions has given rise to the greenhouse effect, whereby these GHGs trap heat in the Earth's atmosphere by absorbing and re-emitting infrared radiation that would otherwise escape into space (Arrhenius, 1897), leading to warming of the planet. In the past 50 years, mean global surface temperatures have increased faster than during any other period over the last 2000 years (Calvin et al., 2023) and each of the last four decades has been successively warmer than any preceding decade since 1850 (IPCC, 2023). Rising temperatures have disrupted global weather patterns leading to more frequent and extreme hurricanes, heatwaves, droughts, forest fires, and heavy rainfall (Calvin et al., 2023). Damage to infrastructure, disruption of ecosystem services, and impacts to agriculture are all well documented, with implications for human health, food security, and economic stability (Calvin et al., 2023; United Nations Department of Economic and Social Affairs, 2023). Thus, in the era of climate change, there is an immediate need for research across numerous disciplines to inform effective responses to the expanding reach of climate impacts.

The oceans make up over 70% of the Earth's surface and serve a vital role in regulating the global climate by absorbing and redistributing heat, sequestering carbon, and influencing weather patterns (IPCC, 2022). As such, marine climate change research is of particular significance. Many of these regulating processes are disrupted by ocean warming, further exacerbating the impacts of climate change (IPCC, 2022). For example, as the upper layers of the ocean absorb excess heat, the capacity for seawater to absorb CO₂ decreases, leaving more CO₂ in the atmosphere and creating a positive feedback loop that magnifies the greenhouse effect (Sabine et al., 2004). Other impacts include ocean acidification, where CO₂ absorbed by surface waters reacts to form carbonic acid, which lowers the pH of seawater (Doney et al., 2009). Since 1980, ocean surface pH has declined by a rate of approximately 0.017–0.027 pH units per decade (IPCC, 2022). Warmer oceans also hold less dissolved oxygen (DO) and become increasingly stratified, thus DO in the upper 1000 m of the open ocean has decreased between 0.5 and 3.3% since the 1970s, and oxygen minimum zones have expanded between 3 and 8% (IPCC, 2022). Global mean sea level has also risen approximately 0.16 m since 1902, driven by ice loss from the Greenland and Antarctic ice sheets, but exacerbated as seawater expands at higher temperatures (IPCC, 2022). These trends are forecast to continue with virtual certainty, thus the world's oceans are projected to undergo unprecedented physical change over the next century (IPCC, 2022).

As a result of these changes, marine ecosystems are transforming rapidly. For example, ocean warming has been driving species range shifts to higher latitudes (García Molinos et al., 2022; Pecl et al., 2017). Many tropical species of fish and invertebrates have expanded their native ranges to temperate regions as ocean waters warm, often displacing native species and disrupting local ecosystems (Vergés et al., 2016; Zarzyczny et al., 2024). Arctic and Antarctic

species have also experienced a narrowing of habitable ranges due to warming (Deb & Bailey, 2023; Ingels et al., 2012), and loss of sea ice in these regions has disrupted local food webs through impacts to primary production and early stages of planktonic invertebrates (Brandt et al., 2023; Clarke et al., 2007). Warming and acidification have also driven declines in populations of important foundational species globally (Wernberg et al., 2024). In tropical regions, warmer waters have resulted in outbreaks of coral bleaching (Baker et al., 2008), where elevated temperatures trigger the expulsion of algal symbionts from the coral, resulting in a loss of pigment and often death (Cunning & Baker, 2013). Ocean acidification exacerbates this effect, as lower pH hinders the accumulation of calcium carbonate in corals, increasing their susceptibility to bleaching (Anthony et al., 2008). Coral reefs support at least 25% of all known marine species (Fisher et al., 2015) and thus coral bleaching is one of the most illustrative examples of the cascading effect of climate change on marine ecosystems (Hoegh-Guldberg et al., 2017). Temperate regions are also under threat as ocean warming is driving declines in kelp forests (Smale, 2020), highly diverse and productive ecosystems that support thousands of marine species (Teagle et al., 2017). These examples represent only a small subset of an immense and growing list of climate-change-related impacts to marine life. These rapid and unprecedented changes threaten biodiversity in the ocean and, as a result, marine ecosystems are becoming increasingly unstable (Doney et al., 2012).

This instability has direct implications for the services that are supported by marine ecosystems (Doney et al., 2012). For example, global fisheries have already been severely impacted by the effects of climate change (Lam et al., 2016; C. Moore et al., 2021). Range shifts for commercially important species in the Northern hemisphere, such as Atlantic cod (*Gadus morhua*), have resulted in declining stocks at lower latitudes (Engelhard et al., 2014; Rouyer et

al., 2014). Tropical fisheries are losing stocks at even higher rates as these populations expand their range towards the poles (Serpetti et al., 2017; Townhill et al., 2021). Additionally, the loss of ecosystems supported by foundational species like coral reefs and kelp forests has decreased nursery habitat for commercially important fish species (Hamilton et al., 2022; James & Whitfield, 2023; Lefcheck et al., 2019; Piñeiro-Corbeira et al., 2022). A trend of declining global stocks has coincided with vast overfishing to meet demand, exacerbating the vulnerability of these populations (Hilborn et al., 2020). Billions of people depend on fisheries for a sustainable source of dietary protein (Beveridge et al., 2013; Boyd et al., 2022) and for their livelihoods, especially in coastal communities in the global South (Tigchelaar et al., 2022). This problem disproportionately affects small-scale sustenance and indigenous fisheries, as they have fewer resources to adapt to climate change (Galappaththi et al., 2021; Villasante et al., 2022). Threats to global fisheries represent one example, but other industries such as aquaculture, ecotourism, and biotechnology are all supported by marine ecosystems and are thus threatened by the impacts of climate change (IPCC, 2022). Therefore, action to address the effects of climate change on marine ecosystems is critical to ensure food security for developing nations, to safeguard socioeconomic stability, and to support coastal economies (United Nations Department of Economic and Social Affairs, 2023).

If current levels of GHG emissions persist, the IPCC forecasts an additional 3°C of warming over the next century, the consequences of which are predicted to be catastrophic (Calvin et al., 2023). As such, many governments have made commitments to the transition away from fossil fuels to more sustainable energy sources, with broad targets for net-zero emissions by 2050 (Kikstra et al., 2022). Unfortunately, the combined pledges of the Paris Agreement will likely decrease GHG emissions by only 0.3% (compared to 2019 levels) by 2030, falling well

short of the 43% reduction called for by the IPCC (United Nations Department of Economic and Social Affairs, 2023). Even under the most optimistic predictions of the IPCC, warming of at least 1.5°C over the next century is virtually certain with 2°C presented as the most likely scenario (Calvin et al., 2023; Möller et al., 2024). The effects of climate change are not only inevitable, but ongoing and well documented. As such, there is a marked need for world governments, industries, and regulatory bodies to not only mitigate, but adapt to the effects of climate change (IPCC, 2023). Accordingly, research to inform and support social adaptation efforts is of the utmost importance, especially in the context of preserving ecosystem services upheld by the marine environment and maintaining food production through capture fisheries and aquaculture.

1.2 Marine heatwaves

While ocean climate change research has historically prioritized understanding how marine ecosystems will respond to gradual trends of warming and acidification over the next century, it is now understood that acute climactic events can have severe impacts on marine ecosystems (Oliver et al., 2019; White et al., 2023). Of particular concern are marine heatwaves (MHWs), characterized by anomalously warm sea surface temperatures, which are typically defined as periods where the daily sea surface temperature exceeds the local 90th percentile (Hobday et al., 2016). These events, which can occur on the scale of days to months, are increasing in both duration and frequency in conjunction with gradual warming under climate change (IPCC, 2022). MHWs have doubled in frequency since 1982, and approximately 90% that occurred between 2006 and 2015 are directly attributable to anthropogenic climate change (IPCC, 2022). The average duration of MHWs has increased by 17% over the last century, and

average heatwave intensity has increased in over 65% of the global ocean during the same time period (Oliver et al., 2018). Furthermore, eight of the 10 most extreme MHWs ever recorded occurred in the last decade (Oliver et al., 2019). MHWs are predicted to increase in frequency, duration, spatial extent, and intensity over the next century (IPCC, 2022), with potentially disastrous implications for marine life.

The catastrophic effects of MHWs on marine ecosystems are well documented. In fact, the term ‘marine heatwave’ was popularized in the early 2010s specifically to characterize these emerging events that triggered devastating impacts on marine ecosystems in an alarmingly short amount of time. In 2011, following a record-breaking heatwave along the Australian coastline, the term ‘marine heatwave’ was first coined to explain the unprecedented changes to the local ecosystem (Wernberg et al., 2013). Temperature anomalies of 2–4°C drove mass mortalities of habitat forming kelp, resulting in complete tropicalization of fish communities in a traditionally temperate region in a matter of weeks (Wernberg et al., 2013). Other notable examples include the Northeast Pacific Ocean MHW (nicknamed ‘the Blob’), which persisted from 2013 to 2016 and stretched from the Gulf of Alaska to Baja California (Gentemann et al., 2017). Temperature anomalies reached 6.2°C above average, resulting in range shifts, strandings of marine mammals, mass mortalities of marine life, and outbreaks of harmful algal blooms (Scripps Institution of Oceanography et al., 2016). More recently, a July 2021 heatwave in the Northeast Pacific Ocean broke the Canadian national temperature record by 4.6°C, resulting in surface temperatures in the intertidal exceeding 50°C (White et al., 2023). This event resulted in severe losses to marine life, with mortalities of invertebrate communities reaching 70% and total deaths estimated in the billions (White et al., 2023). Countless other MHWs have been linked to mass mortalities of invertebrates, fish, seabirds, and marine mammals (Gammelsrød et al., 1998; Garrabou et al.,

2019; Jones et al., 2018; Piatt et al., 2020), and have been reliably demonstrated to negatively impact a range of taxa and ecological functions (Smith et al., 2023).

The impacts of MHWs extend to ecosystem services supported by these marine systems. Commercial fisheries have been impacted by population decline and closures due to harmful algal blooms, both driven by MHWs (Barbeaux et al., 2020; Caputi et al., 2019; S. K. Moore et al., 2019). Similarly, global aquaculture has seen devastating losses due to MHWs, also due to increased mortality and harmful algal blooms (Kajtar et al., 2024; Trainer et al., 2020). Ecotourism has also been affected, as MHWs have driven bleaching and mass mortalities of coral reefs, once popular tourist destinations (Curnock et al., 2019; Doshi et al., 2012). In all, financial losses attributed to MHWs are estimated in the billions USD, with direct implications for coastal economies, food security, human health, and the livelihoods of millions (Smith et al., 2021). Thus, the need for these industries supported by marine systems to adapt to and mitigate the impacts of MHWs is imperative (IPCC, 2022). These actions will likely include improved climatological forecasting, proactive resource management practices, and developing enhanced resilience (Smith et al., 2021). Thus, while research into the effects of MHWs is still vital, there is an urgent need for research that prioritizes informing these actions to respond to the growing impacts of MHWs (Oliver et al., 2019).

1.3 Coastal hypoxic events

While the impacts of MHWs have gained particular notoriety over the past 15 years, they are not the only acute climactic event that warrants attention. In particular, coastal hypoxic events are predicted to become more frequent in tandem with MHWs (Bakun et al., 2015). Climate change has resulted in a gradual decline in average DO over the past century as well as

an expansion of oxygen minimum zones (IPCC, 2022). Underlying these gradual trends, the incidence of acute events, where oxygen levels in coastal waters drop to critically low levels (typically $< 2 \text{ mg O}_2 \text{ L}^{-1}$) (Vaquer-Sunyer & Duarte, 2008), has also increased (Whitney, 2022). These events can be driven by natural processes, such as wind-driven coastal upwelling causing a seasonal cycling of oxygen-poor water to the surface (Connolly et al., 2010; De La Maza & Farías, 2023). Increasingly, however, these events are driven by anthropogenic nutrient input causing eutrophication (Levin et al., 2009). Excess nitrogen and phosphorus from agricultural runoff, wastewater, and industrial waste can enter coastal waters, fueling rapid growth of phytoplankton (Michael Beman et al., 2005). The decomposition of this phytoplankton then depletes DO, leading to zones of hypoxic conditions (Diaz, 2001). As anthropogenic nutrient-input-driven eutrophication has increased, so too have coastal hypoxic events. These hypoxic events can have widespread effects on marine ecosystems, the impacts of which may even surpass those of ocean warming (Sampaio et al., 2021). DO below $2 \text{ mg O}_2 \text{ L}^{-1}$ has been implicated in outbreaks of mortality of many sessile invertebrates, such as bivalves (J. Song et al., 2024) and corals (Doyle et al., 2022; Johnson et al., 2021), and is one of the most common drivers of fish kills (La & Cooke, 2011; Walsh et al., 2004). Mortality often affects habitat-forming foundational species such as coral reefs (Johnson et al., 2021), seagrass meadows (Rasmusson et al., 2020), and oyster beds (Coffin et al., 2021), resulting in biodiversity decline from habitat loss (Wernberg et al., 2013). However, negative sublethal effects are also well documented, with downstream impacts on ecosystem function. Even moderate hypoxia ($\sim 4 \text{ mg O}_2 \text{ L}^{-1}$) can impair respiration, feeding, and reproduction in a range of taxa (Sampaio et al., 2021). In addition, mobile species often detect and avoid hypoxic areas, escaping to regions with more favourable levels of DO (Yu et al., 2023). This, in turn, affects food-web dynamics by

increasing competition in oxygen-rich areas and shifting abundance of both predator and prey species (Vaquer-Sunyer & Duarte, 2008). Naturally, these effects cascade to impact ecosystem services, and financial losses for commercial fisheries (Huang et al., 2010), aquaculture (Lee et al., 2017) and ecotourism (Curnock et al., 2019) have all been documented. While the effects of coastal hypoxic events are becoming increasingly apparent, they remain understudied compared to other acute climactic stressors (Sampaio et al., 2021).

There is a growing understanding that hypoxia may pose a unique threat to marine ecosystems when coinciding with other acute stressors (Carrier-Belleau et al., 2021; Krishna et al., 2025). For example, the effects of hypoxia are compounded in the presence of elevated temperatures. In general, elevated water temperatures increase metabolic rate in ectotherms, increasing the demand for already limited DO (Sampaio et al., 2021). This increased demand for oxygen lowers thermal tolerance in a range of taxa, increasing vulnerability to heat stress (H.-O. Pörtner et al., 2017). A variety of studies have demonstrated that a combination of these stressors amplifies negative effects due to the conflicting energy demand of metabolism and stress response (Del Rio et al., 2019; Earhart et al., 2022; Frakes et al., 2021; Krishna et al., 2025; Roman et al., 2019). Other levels of biological function are also negatively impacted under hypoxia and thermal stress. For example, both stressors generally weaken immune response in fish and invertebrates (Levin et al., 2009), while pathogenic bacteria thrive under the same conditions, increasing the likelihood of disease outbreaks (Nydahl et al., 2013). Negative effects on reproduction and growth have also been documented for many species of mollusks, crustaceans, and fish (Sampaio et al., 2021). As coastal hypoxic events are predicted to increase in frequency along with MHWs, these acute stressor events are projected to overlap with

increasing frequency over the next century (IPCC, 2022), potentially exacerbating their individual negative effects.

In addition to the risk of coinciding MHWs and hypoxic events driven by eutrophication, thermal and hypoxia stress are all but certain to coincide as oxygen limitation is inexorably linked to elevated water temperatures. MHWs can directly drive hypoxic events by reducing the capacity for seawater to retain DO as temperature increases (C. Li et al., 2024; Shunk et al., 2024). In addition, MHWs intensify stratification, preventing oxygen from mixing between surface and deeper waters and creating localized hypoxic zones (Breitburg et al., 2018). MHWs driving reductions in DO has been linked to severe ecosystem impacts in many field case studies globally (Kawai et al., 2025; C. Li et al., 2024; Safonova et al., 2024; Shunk et al., 2024). Despite the link between these stressors, the impacts of coinciding thermal and hypoxia stress on marine ecosystems remains relatively understudied (Earhart et al., 2022). Therefore, research to inform a comprehensive response to the effects of climate change on marine ecosystems and their associated services must account for these combined, and potentially amplified, impacts.

1.4 Aquaculture

Global aquaculture is one of the largest and fastest growing industries supported by marine ecosystems. In 2022, aquaculture surpassed capture fisheries in aquatic animal production for the first time, yielding 94.4 million tonnes and accounting for 57 percent of the seafood for human consumption (*The State of World Fisheries and Aquaculture 2024*, 2024). Today, the industry is valued at 312.8 billion USD, providing livelihoods for an estimated 61.8 million people, especially in lower income countries in Africa, Asia, and South America (*The State of World Fisheries and Aquaculture 2024*, 2024). The expansion of aquaculture largely

aligns with the United Nations (UN) Sustainable Development Goals, specifically Sustainable Development Goal 14 (SDG 14), to sustainably use marine resources (United Nations Department of Economic and Social Affairs, 2023). Global aquaculture is largely sustainable in terms of economic, ecological, and social sustainability, though areas for improvement exist (Garlock et al., 2024; Tigchelaar et al., 2022). Aquaculture has been identified as a critical factor in combating food insecurity and malnutrition in developing nations (Beveridge et al., 2013; Golden et al., 2021; Murshed-e-Jahan et al., 2010; Tigchelaar et al., 2022) as well as supporting the food sovereignty of Indigenous populations (Chung-Do et al., 2024; Joyce & Satterfield, 2010). Thus, future expansion of aquaculture is consistent with a global food system that prioritizes sustainability, benefits human health, and supports vulnerable communities (Golden et al., 2021).

Molluscs largely outperform all other aquaculture species in terms of environmental sustainability (Garlock et al., 2024). Farming of filter-feeding shellfish is particularly sustainable because it can be integrated within marine ecosystems, requires no input of manufactured feeds (Naylor et al., 2009), and can even enhance certain ecosystem services (Shumway et al., 2003). Accordingly, the cultivation of shellfish, particularly bivalves, has a low carbon footprint compared to other forms of animal farming and may even act as a carbon sink (Le et al., 2023; W. Li et al., 2024). Farmed bivalves remove and sequester particulate organic carbon (POC) and dissolved inorganic carbon (DIC) through filter feeding and shell formation, respectively (Tang et al., 2011). The filtration of particulate matter from the water column by cultivated bivalves has also been demonstrated to improve water quality and to regulate the growth of phytoplankton during blooms (Coen et al., 2007; Shumway et al., 2003). Shellfish farming also usually involves the use of lines or cages that can create artificial reefs that promote biodiversity through

increased structural complexity (Coen et al., 2007; Lemasson et al., 2017). In all, the economic value of ecosystem services generated by bivalve aquaculture has been estimated to be at least \$6.5 billion USD per year globally (Van Der Schatte Olivier et al., 2020). Thus, shellfish aquaculture is a key component in the development of an environmentally-sustainable global food-production system (Golden et al., 2021).

Unfortunately, environmental instability brought on by climate change represents a major obstacle in the expansion of shellfish aquaculture, with potential consequences for human well-being (*The State of World Fisheries and Aquaculture 2024*, 2024). Molluscan shellfish culture is particularly vulnerable to the impacts of climate change compared to other sectors (Stewart-Sinclair et al., 2020). In fact, shellfish farming is currently one of the least sustainable forms of aquaculture in terms of economic stability, specifically because of its susceptibility to environmental stresses (Garlock et al., 2024). Both MWHs and coastal hypoxic events due to climate change have resulted in major financial losses, especially through increased incidence of mass mortality (Coffin et al., 2021; Kajtar et al., 2024; Smith et al., 2021; J. Song et al., 2024; Trainer et al., 2020). If current levels of GHG emissions persist, major declines in mollusk production in the next decade are forecast for many nations with an industry sustainability ‘tipping point’ identified for 2060 (Stewart-Sinclair et al., 2020). Therefore, the impacts of these acute climactic stressors directly interfere with SDG 14 and will have indirect effects on the Sustainable Development Goals to achieve zero hunger (SDG 2) and decent work and economic growth (SDG 8) (United Nations Department of Economic and Social Affairs, 2023). The development of adaptation and mitigation strategies has been identified as the primary route to improving the economic sustainability of aquaculture under climate change (Maulu et al., 2021). Research to inform these strategies is therefore critical to support many aspects of human well-

being identified by the UN, and to fulfil the promise of a healthy, thriving planet (United Nations Department of Economic and Social Affairs, 2023).

1.5 Pacific oyster summer mortality

Oysters are the most highly cultivated shellfish in global aquaculture, and the Pacific oyster (*Crassostrea gigas*) makes up the majority of this production (*The State of World Fisheries and Aquaculture 2024*, 2024). While endemic to the Western Pacific Ocean (Quayle, 1988), Pacific oysters have been introduced globally to 64 countries from both deliberate and accidental introductions (Martínez-García et al., 2022) and are currently established in 32 countries for aquaculture production (Martínez-García et al., 2022). The success of this species in aquaculture is largely due to physiological characteristics that permit recruitment in many regions and high yield (Quayle, 1988). Pacific oysters can tolerate a relatively broad range of temperatures and salinities (Quayle, 1988), are highly fecund and genetically diverse (Troost, 2010; Wendling & Wegner, 2015), and have a favourably rapid growth rate compared to other commercial bivalve species (Miossec et al., 2009). However, these characteristics have also made them highly successful invasive species (Troost, 2010). As such, wild populations of Pacific oysters have established in many countries through accidental introduction, often displacing native species with deleterious effects on coastal ecosystems (Martínez-García et al., 2022; Troost, 2010; Wendling & Wegner, 2015). Despite potential ecological risks of Pacific oyster introduction, many benefits exist as well. Oyster farming offers many ecosystem services (Coen et al., 2007; Shumway et al., 2003), is culturally important to many Indigenous communities (Joyce & Satterfield, 2010; Reeder-Myers et al., 2022), and contributes to the growth of coastal economies (Martínez-García et al., 2022). Thus, continued growth of Pacific

oyster aquaculture has the potential to increase many aspects of human well-being, so long as concerns of ecological sustainability are considered (Garlock et al., 2024).

Unfortunately, Pacific oysters are highly vulnerable to mass mortality associated with elevated water temperature, typically during the summer (Petton et al., 2021). Pacific oyster summer mortality related to environmental stressors was first described in the 1940s in Japan, and continues to threaten the economic sustainability of the industry (EFSA Panel on Animal Health and Welfare (AHAW), 2015). Mortality events (20–100%) resulting in major financial losses have been observed in nearly every region where Pacific oysters are farmed, including North America, Europe, Asia, and Australia (Cowan et al., 2023; Dégremont et al., 2010; Go et al., 2017; King et al., 2019; Malham et al., 2009; B. Yang et al., 2021; X. Zhang et al., 2023). Under climate change, an increasing number of mortality outbreaks has been observed in the last 15 years (Oliver et al., 2018; Petton et al., 2021). In British Columbia, Canada, a region with historically low levels of oyster mortality (Quayle, 1988), an emerging problem of summer mortality has been observed (Cowan et al., 2024; Mackenzie et al., 2024). British Columbia oyster production was 15,079 tonnes valued at \$16.1 million CAD in 2023, representing nearly half of all Canadian oyster production in terms of biomass (Department of Fisheries and Oceans Canada, 2023). Thus, research to address the growing challenge of Pacific oyster summer mortality is critical to safeguard the sustainable development of this important sector of shellfish aquaculture.

Climate change is likely to exacerbate Pacific oyster summer mortality due to the increased incidence of acute climatic stressors, particularly MHWs. Mortality typically occurs during periods of elevated seawater temperatures ($>20^{\circ}\text{C}$) (Garnier et al., 2007; Green et al., 2019) and is driven by both environmental stressors and opportunistic pathogens (Cowan et al.,

2023; Garnier et al., 2007; Go et al., 2017; Wendling & Wegner, 2013). Specifically, elevated temperatures induce energetically costly physiological processes like gametogenesis, spawning, and increases in metabolism (Delaporte et al., 2006; Y. Li et al., 2007, 2009; Wendling & Wegner, 2013). This shift in energy allocation impairs immune response, leaving oysters more susceptible to pathogenic infection in environmental conditions that also enhance the growth and virulence of bacteria (Kimes et al., 2012; Vezzulli et al., 2012). As such, there is a growing understanding that MHWs contribute significantly to Pacific oyster summer mortality (Green et al., 2019; Siboni et al., 2024). They have been implicated in recent Pacific oyster mortality events in both Australia and Asia (Heo et al., 2023; Whittington et al., 2024), and simulated heatwaves leave oysters susceptible to pathogenic infection (Green et al., 2019; Siboni et al., 2024). The increased incidence of summer mortality has coincided with more frequent heatwaves (Oliver et al., 2018; Petton et al., 2021). As MHWs will increase in frequency, duration, and intensity over the next century (IPCC, 2022), understanding their role in summer mortality is of critical importance.

Oxygen limitation also likely contributes to summer mortality (Cowan et al., 2023; Sussarellu et al., 2010), especially given the link between elevated water temperatures and reductions in DO (C. Li et al., 2024). Hypoxic conditions weaken immune response in oysters independent of heatwaves (Barnett et al., 2020; David et al., 2005) and may also lower thermal tolerance (Bruhns et al., 2023), exacerbating negative effects. DO limitation has also been directly implicated in a number of cases of Pacific oyster mortality (Coffin et al., 2021; Soletchnik et al., 2007; Whittington et al., 2024). Despite the growing research on the role of MHWs in Pacific oyster summer mortality, the contribution of oxygen limitation to mortality events remains unclear. Given the potential for combined MHW and hypoxia stress to amplify

negative effects on metabolism and stress response in other species (Del Rio et al., 2019; Earhart et al., 2022; Frakes et al., 2021; Krishna et al., 2025; Roman et al., 2019), coinciding MHW and coastal hypoxic events have the potential to exacerbate mortality events. However, the combined effects of heatwaves and hypoxia on summer mortality are not well understood. Filling these knowledge gaps is therefore critical to inform responses to the growing problem of Pacific oyster summer mortality and to adapt to the impacts of climate change.

1.6 Mortality monitoring and mitigation

Developing adaptation and mitigation strategies under climate change is the primary route to improving the economic sustainability of shellfish aquaculture, including Pacific oyster farming (IPCC, 2022; Maulu et al., 2021). The development of these tools is of critical importance to maintaining a sustainable food system, supporting human well-being, and working towards a thriving planet (Kikstra et al., 2022; United Nations Department of Economic and Social Affairs, 2023). Therefore, research into Pacific oyster summer mortality should prioritize informing methods to monitor oyster health and mitigate the potential impacts of mortality under the increasing instability of climate change. This is especially true given that reliable monitoring and mitigation strategies for Pacific oyster summer mortality are currently limited (Mackenzie et al., 2024).

Genetic biomarkers are a widely used tool in environmental monitoring and may have utility in monitoring Pacific oyster health and predicting outbreaks of summer mortality (Chaney & Gracey, 2011; Evans & Hofmann, 2012; Hoffmann & Daborn, 2007a; Mukhopadhyay et al., 2003). Currently, many oyster health monitoring techniques involve whole-organism metrics such as an assessment of shell gaping behaviour or changes in condition indices based on ratios

of soft tissue to shell mass (McMahon, 1988; Rainier & Mann, 1992; Oh et al., 2021). However, monitoring methods involving molecular responses have the potential to detect changes in organism health that whole-organism responses cannot (Evans & Hofmann, 2012; Hoffmann & Daborn, 2007a). In particular, genetic biomarkers offer highly granular and specific insights into cellular processes within an organism. In many cases, this can act as an ‘early warning signal’ of stress, such that intervention to improve organism health can take place before the onset of irreversible negative effects (Hoffmann & Daborn, 2007a). For this reason, genetic biomarkers of stress, such as heat shock protein 70 (HSP70) and hypoxia inducible factor (HIF), are routinely used in environmental monitoring (Fu et al., 2023; Mukhopadhyay et al., 2003; Patterson et al., 2014). In addition, many stress marker genes have shown utility in monitoring the effects of MHWs and hypoxia on similar species (Dimitriadis et al., 2012; Dondero et al., 2006; Patterson et al., 2014; Y. Xu et al., 2022a). However, few studies have explored the development of genetic biomarkers in the specific context of monitoring Pacific oyster summer mortality (Chaney & Gracey, 2011). Given the complex nature of these mortality outbreaks, direct investigation is needed to advance the available tools to reliably monitor summer mortality of Pacific oysters.

Unfortunately, effective mitigation strategies for summer mortality that could take advantage of reliable monitoring remain deficient. Current mitigation approaches are largely preventative, limited to altering farming practises to increase resilience to mortality. Such practices include the management of stocking density affecting food availability (Cowan et al., 2024), as well as culture in the intertidal rather than deep-water during the initial year of a two-year growth period, which may confer some resilience to summer mortality (Mackenzie et al., 2024). Selective breeding for strains of heat-tolerant and disease-resistant oysters also continues to be a promising approach to reduce the extent of summer mortality (Liu et al., 2022; Sae-Lim

et al., 2017). While preventative measures are important, farmers have few options to take advantage of early detection by biomarkers (Evans & Hofmann, 2012). Alternative site transplantation and the use of shading structures over oyster beds are the current extent of intervention options (Evans & Hofmann, 2012). However, thermal and hypoxia stress mitigation strategies exist for other aquaculture species that may be effective in the context of Pacific oyster summer mortality. Specifically, artificial aeration is an existing intervention for finfish aquaculture, utilized in periods of low DO, harmful algal blooms, and/or high temperature to increase thermal tolerance and improve water circulation (Berillis et al., 2016). This practice shows promise for shellfish aquaculture (H.O. Pörtner et al., 2006), but has not been directly investigated in the context of Pacific oyster summer mortality. Therefore, research to inform the development of summer mortality mitigation strategies that align with monitoring practices is critically needed.

1.7 Objectives

The overall goal of this thesis was to examine the effects of acute stressor events (heatwaves and hypoxia) on Pacific oysters and to contribute to the development of genetically-based monitoring tools and novel mitigation strategies for summer mortality. To that end, the primary objectives of this thesis were as follows:

1. Examine the impacts of heatwaves and hypoxia on stress gene expression, condition index, and survival in the Pacific oyster.
2. Identify candidate genes that show altered expression under conditions that lead to mortality and develop genetically based mortality monitoring tools.

3. Use differences in candidate gene expression to infer molecular responses to heatwaves and hypoxia and speculate on the role of oxygen limitation in heatwave-driven mortality.
4. Assess the potential for artificial aeration to act as a mitigation strategy for Pacific oyster summer mortality.

To address these objectives, I performed two laboratory experiments (Chapter 2 and 3) subjecting farmed Pacific oysters to a combination of simulated heatwave and hypoxic events. The findings of this thesis will directly contribute to Pacific oyster summer mortality monitoring and mitigation strategies, supporting the adaptation of shellfish aquaculture to the impacts of climate change and the continued development of a sustainable global food system.

Chapter 2. Simulated marine heatwave alters gene expression in the Pacific oyster (*Crassostrea gigas*): potential monitoring tools for summer mortality

2.1 Introduction

The Pacific oyster (*Crassostrea gigas*) is the most widely cultivated oyster species in the world (The State of World Fisheries and Aquaculture 2024, 2024). In part, the physiological resilience and adaptability of this species has contributed to its successful global introduction. Pacific oysters can tolerate a relatively broad range of temperatures and salinities (Quayle, 1988), and are highly fecund and genetically diverse, allowing for high phenotypic plasticity in populations that must adapt to new and changing environments (Troost, 2010; Wendling & Wegner, 2015). However, despite this resilience, cultured Pacific oysters have suffered from mass mortality associated with elevated temperature during summer (Petton et al., 2021), typically when elevated seawater temperatures exceed 20°C (Garnier et al., 2007; Green et al., 2019; Whittington et al., 2024). Pacific oyster summer mortality is a ubiquitous and recurrent challenge for shellfish aquaculture, resulting in major financial losses that threaten the sustainability of the industry (EFSA Panel on Animal Health and Welfare (AHAW), 2015). Mortality events have been observed in nearly every region where Pacific oysters are farmed including North America, Europe, Asia, and Australia (Cowan et al., 2023; Dégremont et al., 2010; Go et al., 2017; King et al., 2019; Malham et al., 2009; B. Yang et al., 2021; X. Zhang et al., 2023). Despite this challenge, shellfish farming continues to be one of the fastest growing sectors in global aquaculture (The State of World Fisheries and Aquaculture 2024, 2024). Thus, research to support both oyster health monitoring and mortality mitigation is essential for sustaining coastal economies and ensuring global food security.

There is a growing understanding that marine heatwaves, characterized by anomalously warm water conditions, contribute significantly to Pacific oyster summer mortality (Green et al., 2019; Siboni et al., 2024). The impacts of marine heatwaves on shellfish aquaculture are well documented and severe, including mass mortalities and harvest closures due to harmful algal blooms and disease (Smith et al., 2021). While elevated water temperatures have been associated with Pacific oyster mortality for decades, more frequent marine heatwaves have coincided with increased mortality events in the last 15 years (Oliver et al., 2018; Petton et al., 2021). For example, shellfish growers in British Columbia (BC), Canada have reported an emerging problem of Pacific oyster summer mortality (Cowan et al., 2024; Mackenzie et al., 2024), despite historically low mortality reported in the region (Quayle, 1988). Concurrently, severe marine heatwaves have caused mass die-offs of wild shellfish populations along the coast of BC (White et al., 2023). Marine heatwaves have also been implicated in recent Pacific oyster mortality events in both Australia and Asia (Heo et al., 2023; Whittington et al., 2024). As marine heatwaves are forecast to increase in both frequency and intensity over the next century (Intergovernmental Panel On Climate Change (IPCC), 2022; Oliver et al., 2019), understanding the role of these acute thermal stressors in Pacific oyster mortality is of utmost importance to mitigating the effects of climate change on shellfish aquaculture.

In particular, characterizing the molecular responses of Pacific oysters to heatwaves is critical, as these insights inform the selection of resilient oyster strains and reveal sensitive molecular biomarkers essential for monitoring stress. As sessile invertebrates adapted to the highly variable intertidal, oysters have many molecular adaptations to contend with daily fluctuations in temperature and exposure to air. The genome of the Pacific oyster contains an increased number of genes associated with stress response compared to other species (G. Zhang

et al., 2012). Most notably, genes encoding heat shock proteins (HSPs), a group of molecular chaperones involved in stress response, are abundant and highly expressed in the Pacific oyster (G. Zhang et al., 2016). For example, heat shock protein 70 (HSP70), the most highly conserved and well-studied family of these genes, is overrepresented in the Pacific oyster compared to other invertebrates. In a recent analysis of the updated Pacific oyster genome, 113 HSP70 gene family members were identified, compared to just 15 in the Japanese sea cucumber (*Apostichopus japonicus*) (Lu et al., 2024). Sensitive and highly detectable upregulation of HSP70 during acute heat stress (30–50°C) is well documented in Pacific oysters (Farcy et al., 2009; Kim et al., 2017; Lim et al., 2016; C. Yang et al., 2017; C.-Y. Yang et al., 2016), as in countless other animal groups (Bahrndorff et al., 2009; Bastaki et al., 2023; Garner et al., 2020; Harada & Goto, 2017; Jeyachandran et al., 2023). For this reason, HSP70 is routinely used as a biomarker in environmental monitoring (Mukhopadhyay et al., 2003; Sørensen et al., 2003) and in research evaluating responses to thermal stress for oysters (Y. Xu, et al., 2022a). HSP70 polymorphism is also implicated in improved thermal tolerance (Hamdoun et al., 2003; Valenzuela Castillo et al., 2019) and is of interest for genetic intervention in molluscan aquaculture (Liu et al., 2022). Related gene families such as HSP20 and HSP90 are also biomarkers for thermal stress in marine species and have been used to monitor responses to marine heatwaves (Masanja et al., 2022; Y. Xu, et al., 2022b). However, it may be the case that these thermal stress biomarkers have limited applicability to monitoring Pacific oyster summer mortality.

While the adverse effects of elevated water temperatures on Pacific oysters are well documented, it is widely understood that Pacific oyster summer mortality is not only a direct result of thermal stress but linked to a complex interaction of environmental stressors and opportunistic pathogens (Cowan et al., 2023; Garnier et al., 2007; Go et al., 2017; Wendling &

Wegner, 2013). The role of pathogenic infection may, in part, explain why the extent of mortality has been difficult to replicate in laboratory studies with simulated heatwaves alone (Chaney & Gracey, 2011; De Lorgeril et al., 2011). Summer mortality is usually observed at temperatures exceeding 20°C, yet the thermal tolerance of Pacific oysters is well above this threshold and oysters routinely survive acute thermal stress conditions above 40°C (Hamdoun et al., 2003; Lim et al., 2016). Negative effects on filtration rate and metabolic demand due to physiological stress have been observed above 20°C and may contribute to the onset of summer mortality (Bougrier et al., 1995; Ren et al., 2000). However, elevated water temperatures do trigger physiological responses that increase vulnerability to pathogenic infection (Malham et al., 2009). In particular, gametogenesis and spawning induced by elevated temperature are energetically costly, diverting resources away from immunity (Delaporte et al., 2006; Y. Li et al., 2007, 2009; Wendling & Wegner, 2013) and likely contributing to summer mortality. In turn, the growth and virulence of pathogenic bacteria also increase under high temperatures (Kimes et al., 2012; Vezzulli et al., 2012), creating ideal conditions for outbreaks of disease. Infection with pathogenetic bacteria in the *Vibrio* genus, such as *Vibrio aestuarianus*, have been linked to mass mortalities of Pacific oysters in many regions around the world, almost always coinciding with periods of high temperature (Cowan et al., 2024; Siboni et al., 2024; Wendling & Wegner, 2013; B. Yang et al., 2021). This relationship has been supported by several laboratory studies, which have demonstrated that simulated heatwaves both alter pathogen abundance in oysters and exacerbate mortality of infected individuals (Green et al., 2019; Siboni et al., 2024). As such, monitoring approaches that take only thermal stress into account may be incomplete.

Since our understanding of how marine heatwaves affect oyster physiology and contribute to the onset of summer mortality is limited, appropriate monitoring tools remain

largely non-existent. Ideally, genetic biomarkers for monitoring Pacific oyster summer mortality would show detectably altered expression under specific environmental conditions that permit outbreaks of mortality (Evans & Hofmann, 2012). This is challenging given the current lack of direct investigation into the genetic responses of Pacific oyster to marine heatwaves. While responses to thermal stress for Pacific oyster have been extensively studied, these laboratory experiments typically select higher temperatures and shorter heat exposure durations compared to observed marine heatwaves implicated in summer mortality (Farcy et al., 2009; Lim et al., 2016; C. Yang et al., 2017; C.-Y. Yang et al., 2016). To date, few studies have examined the transcriptomic response of Pacific oysters to thermal stress that is environmentally relevant to the onset of summer mortality. Furthermore, altered expression of ideal biomarkers should be replicable and their molecular products characterized. Unfortunately, the Pacific oyster genome is highly polymorphic and annotation is incomplete (G. Zhang et al., 2012), further complicating access to reliable biomarkers. Thus, there is an immediate need for a comprehensive understanding of transcriptomic response of Pacific oysters to heatwaves that provoke summer mortality outbreak.

To address these gaps, farmed Pacific oysters were subjected to a simulated marine heatwave similar in duration and intensity to a 2021 heatwave that co-occurred with summer mortalities of shellfish in the Baynes Sound region in BC (Mackenzie et al., 2024). Changes in gene expression in the gill tissue of oysters were assessed using RNAseq at several timepoints during the heatwave, identifying genes that were differently expressed compared to a control. To identify potential biomarkers for summer mortality, a subset of candidate genes whose expression changed with heatwave intensity were then selected for verification. Whole-organism metrics of health, e.g. condition index (Rainier & Mann, 1992), were also examined to

confirm whether candidate gene expression detected changes that traditional monitoring methods could not. Finally, mortality during the simulated heatwave was tracked to evaluate the utility of those candidate genes in predicting outbreaks of summer mortality. The findings will provide further physiological insights into the effect of marine heatwaves on Pacific oyster summer mortality and contribute to the development of genetically-based monitoring tools. The project results will inform comprehensive vulnerability assessments for Pacific oysters and support the adaptation of shellfish aquaculture to the impacts of climate change.

2.2 Materials and methods

2.2.1 Oyster collection and acclimation

Adult Pacific oysters (*Crassostrea gigas*) (N = 300) were collected from a commercial oyster farmer located in Baynes Sound, BC on January 31, 2023. They were transported dry in coolers to the Pacific Biological Station (PBS) in Nanaimo, BC, which took approximately 1 h. All individuals were cleaned of biofouling using a shucking knife and rinsed with ambient seawater, 240 of them being haphazardly chosen for experimentation. Ten individuals were haphazardly placed in each of 24 black-plastic mesh baskets (diameter: 30 cm, height: 8 cm) suspended within plastic buckets (volume: 20 L, diameter: 30 cm, height: 24 cm) with ~20 L of static cartridge-filtered (20 µM) seawater. Those buckets were arranged in four blocks of six within four shallow fibreglass tanks (length x width x height: 122 x 91 x 30 cm) filled with circulating filtered (20 µM) seawater. Water temperatures in those tanks were achieved and maintained via in-tank heaters, chilling coils, and pumps for circulation. Dissolved oxygen levels were maintained via individual air stones to each bucket. Oysters were then maintained for a

two-week pre-experimental acclimation period, during which water temperatures in the tanks and buckets were raised from collection site temperature (~4–6°C) to experimental control levels (16°C) by 2°C per day. To acclimate the oysters to simulated summer conditions, all animals were then held under experimental control conditions for an additional 8 d prior to the start of the experiment. Oysters were fed daily with a mixture of cultured phytoplankton (60% *Tisochrysis lutea* and 40% *Chaetoceros mulleri*, by cell number) at a concentration of ~4–8 million cells mL⁻¹, and daily water changes (~50% volume change) were performed for all buckets using cartridge-filtered (20 µM) seawater heated to 16°C.

2.2.2 Experimental conditions

Following the acclimation period, feeding was ceased to avoid potential interference of metabolic changes on genomic stress response (C.-Y. Yang et al., 2016) and a 10-d heatwave event was simulated. Seawater temperature in 12 buckets was incrementally raised from 16 to 26°C by 1°C per day, with the other 12 buckets kept at a control temperature of 16°C. The former conditions, including rate of temperature change, duration, and maximum temperature are consistent with those measured during a July 2021 heatwave in BC. Commercial oyster float bags in Baynes Sound showed increases in sea surface temperature (SST) from 16 to 28°C over a 7-d period, during which time several shellfish mortality events were recorded (Mackenzie et al., 2024). Simulated experimental conditions were therefore environmentally relevant to actual summer heatwaves in the region that have previously induced mortality events for Pacific oysters. Tanks in the control treatment were subjected to continuous temperatures of 16°C, which is consistent with recorded values for average summer seawater temperature in the Baynes Sound region (Mackenzie et al., 2024). As during the acclimation period, seawater temperatures

were achieved and maintained via in-tank heaters, chilling coils, and pumps for circulation and dissolved oxygen levels were maintained via individual air stones to each bucket. Daily water changes of the buckets were performed as described for the acclimation period.

2.2.3 Experimental monitoring

Seawater temperatures in tanks were monitored using temperature loggers (HOBO TidbiT, Onset Computer Corporation, Bourne, Massachusetts, USA) recording at 10-min intervals. In addition, temperature, salinity, dissolved oxygen, and pH in each bucket were recorded twice daily, before and after water changes, using a YSI multi-probe (YSI Incorporated, Yellow Springs, Ohio, USA). Oysters were monitored daily for physical signs of stress and mortality (i.e. lack of startle response, gaping shell, absence of response to touch). Mortality and any apparent signs of physical stress were recorded and individuals that were deceased before the experiment began were removed.

2.2.4 Oyster sampling

Before the heatwave started (T₀), one oyster was haphazardly sampled from 12 haphazardly chosen buckets (N = 12). Once the heatwave began, one haphazardly chosen oyster from each bucket was sampled (N = 24; n = 12 per treatment) at five timepoints (days 2, 4, 6, 8, and 10 (T₁–T₅)), which corresponded to temperatures of 18, 20, 22, 24, and 26°C for the heatwave group. Wet weight and shell height were measured for all sampled individuals using digital calipers and a digital balance, respectively. Oysters were then opened using a sterile shucking knife and ~0.03 g of gill tissue excised using sterile dissection scissors. The tissue samples were placed individually in labelled 2-mL tubes and stored at -80°C. At T₀, one oyster

was haphazardly sampled from 6 haphazardly chosen buckets ($N = 6$) for baseline measurement of condition index (see Section 2.2.5). Then, at two timepoints during the heatwave (T2 and T4), six additional oysters were haphazardly sampled from both heatwave and control treatments ($N = 12$, $n = 6$ per treatment). All sampled individuals were immediately frozen at -80°C for subsequent processing.

2.2.5 Condition index

Oysters sampled for condition index were thawed at room temperature and opened using a sterile shucking knife. The shell and soft tissues were then dried at 60°C for 7 d, until constant weight. Soft-tissue dry weight and shell dry weight were measured for all sampled individuals using a digital balance, and condition index was calculated as: $\text{CI} = (\text{P1} \times 100)/\text{P2}$, where P1 equals the dry weight (g) of soft tissues and P2 equals the dry weight (g) of the shell (Rainier & Mann, 1992). To assess differences in CI between heatwave and control (16°C) conditions, a one-way analysis of variance (ANOVA) was performed with CI as the response variable and treatment as the factor. The data were assessed for normality using a Shapiro-Wilk test and for homogeneity of variance using Levene's test. Outliers were identified using the Z-score method and removed if more than 3 standard deviations from the mean.

2.2.6 RNA extraction and purification

Total RNA was extracted from each gill tissue sample for gene expression analysis using an RNeasy[®] Mini Kit (QIAGEN, Hilden, Germany). First, gill tissue samples were placed in lysing matrix tubes (MPbio, Santa Ana, California, USA) with 600 μL of RLT lysis buffer containing guanidine isothiocyanate and β -mercaptoethanol (β -ME) and homogenised using a

TissueLyser II bead mill homogenizer (QIAGEN) at 25.0 Hz for 2 min. The resulting homogenate was then centrifuged at $\geq 10,000 \times g$ for 3 min before extracting total RNA according to the QIAGEN RNeasy[®] Mini Kit instructions. For each sample, the supernatant was transferred into a 2-mL tube, mixed with 600 μL of 70% ethanol and transferred to a RNeasy[®] spin column before centrifuging for 15 s at 8000 $\times g$. The resulting precipitant was run through a series of washes with RNeasy[®] Mini Kit buffers RW1 and RPE (QIAGEN) to remove contaminants such as proteins, salts, and other impurities from the nucleic acids. After those washes, the RNeasy spin column placed in a new 2-mL collection tube and centrifuged at $\geq 10,000 \times g$ for 1 min to dry the sample and remove any carryover buffer. Finally, the RNeasy spin column was placed in a new 2-mL tube and 50 μL of RNase-free dH_2O were added directly to the spin column membrane. This was then centrifuged for 1 min at 8000 $\times g$ to elute the RNA. The preliminary amount and quality of RNA were recorded before purification using a Nanodrop spectrophotometer.

A TURBO DNA-free Kit (Thermo Fisher Scientific, Waltham, Massachusetts, USA) was then used to purify the resulting RNA. According to kit instructions, the procedure for DNA decontamination was dependent on the concentration of nucleic acid in the sample. For all samples $\leq 400 \text{ ng mL}^{-1}$, 5 μL 10X TURBO DNase buffer and 1 μL of TURBO DNase Enzyme were added to the RNA. For any samples $\geq 400 \text{ ng mL}^{-1}$, half of the RNA elution was added into a new 2-mL tube and 2.5 μL of 10X TURBO DNase buffer and 2 μL of TURBO DNase Enzyme were added. All samples were then incubated at 37°C for 30 min to remove DNA contamination from RNA samples. Following incubation, 6 μL of DNase inactivation reagent were added for 5 min at room temperature to stop the enzymatic activity of the TURBO DNase. The samples were then centrifuged for 2 min at 10,000 $\times g$ and the supernatant containing the purified RNA

transferred to 2-mL collection tubes. Following DNA decontamination, the final amount and quality of nucleic acid in each sample were recorded using a Nanodrop spectrophotometer and samples were stored at -80°C.

2.2.7 cDNA synthesis

Total RNA from the resulting samples was reverse transcribed using a Bio-Rad (Hercules, California, USA) iScript Select cDNA Synthesis Kit. First, all samples were diluted to 100 ng μL^{-1} using RNase-free dH₂O. Then, each diluted sample was combined with 5 μL of RNA template, 1.5 μL of RNase-free dH₂O, 2 μL of 5x iScript Select Reaction Mix, 0.5 μL of iScript Reverse Transcriptase, and 1 μL of random primer mix in the wells of a 12-well PCR strip. Those samples were incubated at 25°C for 5 min, 42°C for 30 min, 85°C for 5 min, and 12°C for 5 min according to kit instructions. The resulting cDNA was stored at -20°C in labelled 12-well PCR strips for future gene expression analysis.

2.2.8 RNA sequencing and analysis

cDNA from each treatment and timepoint in the experiment was pooled and sent to the Canadian Centre for Computational Genomics (C3G) at McGill University, where differently expressed genes (DEGs) were identified using next-generation sequencing. Procedures for RNA-Seq analysis were conducted according to the GenPipes workflow framework developed by C3G (Bourgey et al., 2019). First, FASTQ raw reads were obtained using paired-end sequencing on Illumina NovaSeq. R (Version 4.3.2) with RStudio (Version 2024.09.1) was then used to analyze the resulting data. Adaptor sequences and low-quality base calls (Phred score < 30) were trimmed from the reads using Trimmomatic (Bolger et al., 2014). The resulting reads were

mapped to the reference genome of *C. gigas* (Peñaloza et al., 2021) using STAR (Dobin et al., 2013) and read counts were obtained using HTSeq (Anders et al., 2015). Counts generated by HTSeq were analyzed using the DESeq2 package (Love et al., 2014) to identify differences in expression levels across timepoints and treatments using negative binomial GLM fitting and Wald statistics. Then, the ashR package (Stephens, 2016) was used to shrink Log2FoldChange (Log2FC) values in the gene expression data. Since samples were pooled for each timepoint, significance was established by modeling the relationship between mean expression and dispersion across all genes, not by using group variability based on replicates. Thus, Log2FC values in the present study represent solely exploratory indicators for further qPCR investigation. Tidyverse (Wickham et al., 2019) and pheatmap (Raivo Kolde, 2010) packages were used for data manipulation and visualization.

2.2.9 Candidate gene selection

A subset of genes that showed differential expression in the RNAseq analysis was chosen for further investigation via qPCR verification. Considering that the objective of this study was to investigate physiological responses to a simulated heatwave and reveal potential biomarkers for summer mortality, a number of criteria were considered when selecting genes to investigate further. First, genes that were significantly differentially expressed at multiple points during the simulated heatwave (especially after the 20°C threshold, which typically results in summer mortality) were prioritized. That decision was made to emphasize genes whose expression was most likely to be correlated with heatwave intensity upon more thorough investigation. Genes with known products or those whose products could be speculated upon with high confidence were also prioritized. In particular, genes with products that have been documented as

biomarkers for stress but were not necessarily significantly differentially expressed at multiple points during the simulated heatwave, were examined. This was done to assess the utility of those genes as biomarkers for summer mortality and to provide insight into the physiological state of oysters subjected to a simulated marine heatwave.

Given those criteria, 10 genes of interest (GOIs) were deemed appropriate for further investigation through qPCR verification, including five with known products and five with products that could be inferred via shared homology. Gene products were identified using the Ensembl Metazoa and UniProt Knowledgebase (UniProtKB) databases, as well as the National Center for Biotechnology Information Basic Local Alignment Search Tool (NCBI BLAST) program. Using the Ensembl Metazoa transcript IDs associated with each gene, orthologues were reviewed and FASTA sequences for the Ensembl canonical transcript were generated. The canonical transcript indicates a single transcript chosen by Ensembl Metazoa to be most representative for a gene and is represented in both NCBI and UniProtKB. This is typically the orthologue that is most conserved, most highly expressed, and has the longest coding sequence. The UniProtKB/TrEMBL database, which derives protein sequences from the computational translation of coding sequences, was then used to determine the likely protein product associated with each gene. Genes with associated proteins whose existence was supported by evidence at a transcript level, such as previously published cDNA(s), RT-PCR, or Northern blots, were said to have known function. Those genes were high mobility group protein DSP1 (DSP1), heat shock protein 20 (HSP20), heat shock protein 70 B2 (HSP70), and heat shock protein 90 (HSP90) and high mobility group box 1 (HMGB1). For genes with associated proteins whose existence was inferred from homology with orthologues in closely related species, or predicted based on computational annotation, FASTA sequences were cross referenced with the NCBI BLAST

program to determine the most likely protein product based on the results of both queries. Sequences belonging to *C. gigas* with higher query coverage, higher percent identity, and E-values of 0, whose description matched the results of the UniProtKB prediction, were chosen as the most likely gene product. Genes that fell into this category were said to have inferred function. Those genes were death-associated inhibitor of apoptosis 2 (A2I), heterogeneous nuclear ribonucleoprotein (HNR), peptidyl-prolyl cis-trans isomerase (PPCTI), stress-induced protein 1 (SIP1), and x-box-binding protein 1 (XBP1).

2.2.10 Primer design

Once the function of each gene product could be determined or inferred, primers for qPCR verification of differential expression were designed. First, FASTA sequences for the cDNA of each GOI from Ensembl Metazoa were obtained using sequences for the Ensembl canonical transcript. Those sequences were then inputted into the NCBI Primer Blast tool to design primer pairs for each GOI. Primer sequences for the reference genes actin (Farcy et al., 2007) and elongation factor 1-alpha (EF1- α) (De Lorgeril et al., 2011) were obtained from previous studies (Farcy et al., 2009; Green & Montagnani, 2013). All primers were between 18 and 21 nucleotides long, had melting temperatures between 58 and 62°C with no more than 3°C difference between the pair, had GC content between 40 and 60%, and total self-complementarity ≤ 4 and 3' self-complementarity ≤ 2 . All amplicon sizes were between 80 and 150 base pairs. Primer sequences and their associated gene IDs are provided in Table 2.1. Generated primer sequences were sent to Integrated DNA Technologies (IDT, Coralville, Iowa, USA), who manufactured custom 100-nm DNA oligos purified according to standard desalting. Those primers were delivered dry and made up to a 100 μ M working solution using Invitrogen

UltraPure distilled water (Thermo Fisher Scientific). RNAase-free dH₂O was then used to dilute the working solution to 10 µM. A standard curve method was used to test the efficacy of those primers. First, 20 cDNA samples were haphazardly chosen and 20 µL from each were pooled to a total of 400 µL. A range of dilutions (1–1/1000 x volume) were then prepared using RNase-free dH₂O and the quantification cycle (C_q) as a function of the log starting RNA concentration was plotted. Primer pairs that showed efficiency levels between 90 and 110% for each of the four orders of magnitude were accepted.

2.2.11 qPCR verification

All qPCR reactions were performed in a Bio-Rad CFX Opus 96 Real-Time PCR System using Bio-Rad CFX Maestro 2.3 version 5.3.022.1030 software. Subsequent reactions were conducted in 96-well PCR plates with loaded reactions in duplicate to ensure quality reading for each sample. Total reaction volume for each well was 10 µL, containing 5 µL of SsoAdvanced Universal SYBR[®] Green Supermix (Bio-Rad), 0.5 µL of forward primer, 0.5 µL of reverse primer, and 4 µL of cDNA template. Amplification conditions were 1 cycle of 2 min at 95°C, 39 cycles of 10 s at 95°C, and 1 cycle of 30 s at 60°C. This was followed by a melting curve analysis, raising the temperature from 65 to 95°C in 0.5°C increments at 2–5 s per step. C_q values were calculated from fluorescence readings as the cycle where a signal above the defined background fluorescence could be detected. C_q value is dependent on the starting amount of cDNA and thus can be used to quantify the amount of reverse transcribed mRNA for each target in each sample to calculate relative expression. As two reactions were conducted for each target sequence and cDNA sample, the mean C_q value between both reactions was calculated for all samples and those values were used for all further analysis. The relative expression of each GOI

was then calculated by normalizing C_q values to expression of a reference gene. C_q values were calculated for two reference genes, actin and EF1- α , and the stabilities of both genes were evaluated using the RefFinder tool (Xie et al., 2023). Actin was determined to be the more stable reference gene between the two and therefore its expression was utilized for all further calculations. Relative expression for each target and sample was calculated using the ΔC_q method, where relative expression = $2^{\Delta C_q}$ and $\Delta C_q = (C_{q \text{ actin}} - C_{q \text{ target}})$. That formula converts the difference in C_q values into a fold change measure of relative expression by assuming each reaction cycle doubles qPCR product.

2.2.12 qPCR statistical analysis

All statistical analyses and visualizations of relative expression data were performed using R (Version 4.4.2) and RStudio (Version 2024.12.0). Key packages included tidyverse (Wickham et al., 2019) and pheatmap (Raivo Kolde, 2010) for data manipulation and visualization. For single-gene responses, a two-way analysis of variance (ANOVA) for each GOI was performed, with relative expression as the response variable and treatment, timepoint, and their interaction as factors. The data were assessed for normality using a Shapiro-Wilk test and for homogeneity of variance using a Levene's test. A post-hoc Student-Newman-Keuls (SNK) test was performed for each ANOVA to determine which timepoints during the heatwave showed significant differences in relative expression, including the control (16°C) at each timepoint. Additionally, separate linear models (LM) were run to examine the effect of temperature on relative expression of each GOI.

To assess the effect of the simulated heatwave on relative expression of all 10 selected GOIs, a permutational multivariate analysis of variance (PERMANOVA) was conducted using

the *vegan* package (Oksanen et al., 2001). Bray-Curtis dissimilarity indices were calculated using the *vegdist* function, and the resulting distance matrix was analyzed using the *adonis2* function to assess the effects of treatment, temperature, and their interaction on relative expression (Oksanen et al., 2001). The assumption of homogeneity of multivariate dispersion was tested using the *betadisper* function to calculate dispersions, followed by the *aov* function for comparison across groups. A Bonferroni-corrected post-hoc pairwise PERMANOVA was then conducted using the *pairwise.adonis* function in the *pairwiseAdonis* package (Oksanen et al., 2001). This was done to determine which timepoints during the heatwave showed significant differences in relative expression, including to the control 16°C.

Further multivariate analyses were conducted for only the GOIs that showed significant responses in the single-gene response models. An additional PERMANOVA was conducted on this subset of GOIs to assess multivariate differences, as described above. Similarly, a post-hoc pairwise PERMANOVA test (Bonferroni-corrected for multiple comparisons?) was conducted to compare differences in relative expression at each timepoint during the heatwave for this subset of genes. A SIMPER (Similarity Percentage Analysis) analysis was then conducted to identify which genes were the primary contributors to relative expression differences between the simulated heatwave and control (16°C) and at each timepoint during the simulated heatwave. Finally, a principal component analysis (PCA) was performed on this subset of GOIs using the *prcomp* function. This was done to visualize clustering of relative expression patterns and to identify GOIs that contribute most to differences in relative expression between treatments.

2.3 Results

2.3.1 Experimental monitoring

At the start of the simulated heatwave (T0; 16°C), mean water temperature was $15.6 \pm 0.1^\circ\text{C}$ and $15.6 \pm 0.1^\circ\text{C}$ for tanks in the heatwave and control groups, respectively. From days 2 to 10 of the simulated heatwave, mean water temperature for control tanks was $15.7 \pm 0.2^\circ\text{C}$. In the heatwave group, mean water temperatures were $18.0 \pm 0.5^\circ\text{C}$ on day 2 (T1; 18°C), $19.9 \pm 0.5^\circ\text{C}$ on day 4 (T2; 20°C), $21.9 \pm 0.4^\circ\text{C}$ on day 6 (T3; 22°C), $23.9 \pm 0.4^\circ\text{C}$ on day 8 (T4; 24°C), and $25.8 \pm 0.5^\circ\text{C}$ on day 10 (T5; 26°C). Over the 10-day experimental period, mean dissolved oxygen (DO) was $7.3 \pm 0.5 \text{ mg O}_2 \text{ L}^{-1}$ for the heatwave group and $8.4 \pm 0.6 \text{ mg O}_2 \text{ L}^{-1}$ for the control group. Over the same period, mean salinity and pH was $29.9 \pm 0.4 \text{ ppt}$ and 7.9 ± 0.2 for the former and $29.9 \pm 0.3 \text{ ppt}$ and 7.9 ± 0.2 for the latter. Only one mortality occurred, an individual in the heatwave group on day 8. No other physical signs of stress (lack of startle response, gaping shell, lack of response to touch) were noted.

2.3.2 Condition index

Mean baseline shell length, wet weight, and condition index (CI) for all sampled individuals was $65.8 \pm 4.7 \text{ mm}$, $34.2 \pm 7.4 \text{ g}$, and 58.8 ± 15.9 , respectively. On day 4 of the simulated heatwave, mean CI was 80.9 ± 15.3 in the control and 68.1 ± 5.1 in the heatwave treatment. On day 8, mean CI was 67.5 ± 6.0 in the control and 68.8 ± 16.1 in the heatwave treatment. Despite these differences, there was no significant effect (one-way ANOVA, $F_{(2,26)} = 2.536$, $p = 0.099$) of the heatwave treatment on CI. One outlier was identified in the heatwave group on day 8 and removed from the analysis.

2.3.3 RNA sequencing

Differently expressed genes (DEGs) were detected at all five timepoints during the simulated heatwave, where Log₂ fold change (Log₂FC) values in the heatwave treatment were significantly different ($p_{adj} < 0.05$) compared to the control. In addition, the number of DEGs increased at each timepoint as temperature increased (Table 2.2). At the height of the heatwave, we detected 246 DEGs comprised of 96 upregulated and 150 downregulated genes. Changes in expression (Log₂FC) of those 246 genes across all five timepoints are shown in Figure 2.1. Of those DEGs, 22 genes were differentially expressed on both days 8 and 10; 12 genes were differentially expressed on days 6, 8, and 10; and seven genes were differentially expressed on days 4, 6, 8, and 10. From this subset of genes that were differentially expressed at multiple timepoints during the simulated heatwave, 10 genes of interest (GOIs) were chosen for further investigation via real-time quantitative PCR (qPCR) verification. Those genes were A2I (death-associated inhibitor of apoptosis 2), DSP1 (high mobility group protein DSP1), HMGB1 (high mobility group box 1), HNR (heterogeneous nuclear ribonucleoprotein), HSP20 (heat shock protein 20), HSP70 (heat shock protein 70 B2), HSP90 (heat shock protein 90), PPCTI (peptidyl-prolyl cis-trans isomerase), SIP1 (stress-induced protein 1), and XBP1 (x-box-binding protein 1).

Changes in expression (Log₂FC) of those 10 genes across all five timepoints are shown in Figure 2.2. Six genes — A2I, HSP20, HSP70, HSP90, SIP1, and XBP1— were significantly upregulated compared to the control. A2I and XBP1 were significantly upregulated compared to the control on days 4, 6, 8, and 10; SIP1 was upregulated on days 6, 8, and 10; and HSP20, HSP70, and HSP90 were only upregulated on day 10. Four genes—DSP1, HMGB1, HNR, and PPCTI—were significantly downregulated compared to the control. DSP1 was significantly downregulated compared to the control at all five timepoints. HMGB1 and PPCTI were both

significantly downregulated on days 4, 6, 8, and 10, while HNR was downregulated on days 6, 8, and 10. Those patterns of differential expression were chosen for further investigation via qPCR.

2.3.4 qPCR single-gene responses

Single-gene responses were assessed, determining that five of the 10 GOIs showed relative expression ($2^{\Delta Cq}$) patterns under simulated heatwave conditions that were significantly different from the control (16°C). Those genes were A2I, DSP1, HMGB1, HSP90, and PPCTI (Figure 2.3). Three of them—DSP1, HMGB1, and PPCTI—were significantly downregulated during the simulated heatwave compared to the control. First, relative expression of DSP1 was significantly affected by treatment (two-way ANOVA, $F_{(1,119)} = 48.981$, $p < 0.001$), timepoint ($F_{(5,119)} = 3.953$, $p = 0.002$), and their interaction ($F_{(5,119)} = 3.302$, $p = 0.008$) and was significantly lower than the control on days 6, 8, and 10 (Figure 2.4). Temperature also had a significant effect on the relative expression of DSP1 (LM, $\beta = -0.007$, SE = 0.001, $t_{(129)} = -7.26$, $p < 0.001$), explaining approximately 29% of the variance ($R^2 = 0.29$). Second, relative expression of HMGB1 was significantly affected by treatment (two-way ANOVA, $F_{(1,119)} = 17.908$, $p < 0.001$) and timepoint ($F_{(5,119)} = 9.782$, $p < 0.001$), but not by their interaction ($F_{(5,119)} = 1.296$, $p = 0.270$). Its expression was significantly lower in the heatwave than in the control and generally declined with increasing timepoint (Figure 2.5). Temperature also had a significant effect on relative expression of HMGB1 (LM, $\beta = -0.008$, SE = 0.0013, $t_{(129)} = -6.165$, $p < 0.001$), explaining approximately 23% of the variance ($R^2 = 0.23$). Third, relative expression of PPCTI was significantly affected by treatment (two-way ANOVA, $F_{(1,119)} = 70.217$, $p < 0.001$) and timepoint ($F_{(5,119)} = 3.106$, $p = 0.011$), but not by their interaction ($F_{(5,119)} = 1.248$, $p = 0.291$). As with HMGB1, PPCTI expression was significantly lower in the heatwave than in the control and

generally declined with increasing timepoint (Figure 2.6). Temperature also had a significant effect on relative expression of PPCTI (LM, $\beta = -0.008$, SE = 0.0009, $t_{(129)} = -9.306$, $p < 0.001$), explaining approximately 40% of the variance ($R^2 = 0.40$).

Two genes, A2I and HSP90, were significantly upregulated during the simulated heatwave compared to the control. First, relative expression of A2I was significantly affected by treatment (two-way ANOVA, $F_{(1,119)} = 31.792$, $p < 0.001$) and timepoint ($F_{(5,119)} = 6.743$, $p < 0.001$), but not by their interaction ($F_{(5,119)} = 2.176$, $p = 0.061$). Relative expression of A2I was significantly higher in the heatwave treatment than in the control and increased from days 0 to day 6 and then declined (Figure 2.7). In addition, relative expression of A2I was significantly affected by temperature (LM, $\beta = 0.002$, SE = 0.0002, $t_{(129)} = 6.700$, $p < 0.001$), with temperature explaining approximately 26% of the variance ($R^2 = 0.26$). Second, the relative expression of HSP90 was significantly affected by treatment (two-way ANOVA, $F_{(1,119)} = 7.132$, $p = 0.009$), timepoint ($F_{(5,119)} = 4.404$, $p = 0.001$), and the interaction of treatment and timepoint ($F_{(5,119)} = 2.464$, $p = 0.037$). HSP90 expression was upregulated in comparison to the control at days 6, 8, and 10, significantly so at days 6 and 10, its expression remaining relatively constant from days 0 to 8, after which it significantly increased in the heatwave treatment (Figure 2.8). HSP90 expression was also significantly affected by temperature (LM, $\beta = 0.008$, SE = 0.0018, $t_{(129)} = -4.927$, $p < 0.001$) with temperature explaining approximately 16% of the variance in HSP90 relative expression ($R^2 = 0.16$). A third gene, XBP1, was also significantly upregulated, but a post-hoc Student-Newman-Keuls (SNK) test revealed that relative expression of XBP1 was not significantly different from the control at any timepoint during the simulated heatwave. Relative expression of XBP1 was significantly affected by treatment (two-way ANOVA, $F_{(1,119)} = 18.297$, $p < 0.001$) and timepoint ($F_{(5,119)} = 4.719$, $p < 0.001$), but not by their interaction ($F_{(5,119)} = 0.557$,

$p = 0.733$). Additionally, temperature had a significant effect on XBP1 relative expression (LM, $\beta = 0.001$, $SE = 0.0002$, $t_{(129)} = -4.370$, $p < 0.001$), explaining approximately 13% of the variance ($R^2 = 0.13$).

The remaining four genes—HNR, HSP20, HSP70, and SIP1—did not show any significant differences in relative expression compared to the control. Relative expression of HNR was not significantly affected by treatment (two-way ANOVA, $F_{(1,119)} = 0.579$, $p = 0.448$), timepoint ($F_{(5,119)} = 2.188$, $p = 0.060$), or their interaction ($F_{(5,119)} = 2.122$, $p = 0.068$). In addition, temperature did not have a significant effect on HNR relative expression (LM, $\beta = -0.0002$, $SE = 0.0002$, $t_{(129)} = -1.680$, $p = 0.096$). In contrast, relative expression of HSP20 was significantly affected by timepoint (two-way ANOVA, $F_{(5,119)} = 5.025$, $p < 0.001$), but not by treatment ($F_{(1,119)} = 1.685$, $p = 0.197$) or their interaction ($F_{(5,119)} = 0.562$, $p = 0.729$). Despite the significant main effect of timepoint in the ANOVA, SNK analysis could not show any significant differences among timepoints (Figure 2.9). Temperature did have a significant effect on relative expression of HSP20 (LM, $\beta = 0.019$, $SE = 0.006$, $t_{(129)} = 2.958$, $p = 0.004$), but only explained approximately 6% of the variance ($R^2 = 0.06$). Similarly, relative expression of HSP70 was significantly affected by timepoint two-way ANOVA, ($F_{(5,119)} = 2.937$, $p = 0.016$), but not by treatment ($F_{(1,119)} = 1.703$, $p = 0.194$) or their interaction ($F_{(5,119)} = 0.117$, $p = 0.988$). Again, despite the significant main effect in the ANOVA, SNK analysis failed to show any significant timepoint differences, although there is suggestion of possible HSP70 upregulation at day 6 (Figure 2.10). There was no significant effect of temperature on HSP70 relative expression (LM, $\beta = 0.0003$, $SE = 0.0002$, $t_{(129)} = 1.788$, $p = 0.076$). Finally, relative expression of SIP1 was not significantly affected by treatment (two-way ANOVA, $F_{(1,119)} = 2.760$, $p = 0.099$), timepoint ($F_{(5,119)} = 1.391$, $p = 0.232$), or their interaction ($F_{(5,119)} = 0.752$, $p = 0.586$). However, there was

a significant effect of temperature on SIP1 relative expression (LM, $\beta = 0.003$, SE = 0.001, $t_{(129)} = 3.079$, $p = 0.003$).

2.3.5 qPCR multivariate response

A PERMANOVA test (Bray-Curtis dissimilarity, 999 permutations) demonstrated that relative expressions of the 10 GOIs in the study were significantly affected by treatment ($F_{(1,125)} = 13.641$, $R^2 = 0.086$, $p = 0.001$), timepoint ($F_{(1,125)} = 24.737$, $R^2 = 0.161$, $p = 0.001$), and their interaction ($F_{(1,125)} = 3.712$, $R^2 = 0.023$, $p = 0.015$). A post-hoc pairwise PERMANOVA test (Bonferroni-corrected) showed that relative expression of the 10 GOIs in the heatwave treatment was significantly different from that in the control on days 6, 8, and 10. An additional PERMANOVA test (Bray-Curtis dissimilarity, 999 permutations) was run to assess the relative expression of the five GOIs that showed significant differences in the single-gene response models (A2I, DSP1, HMGB1, HSP90, and PPCTI). The results of that analysis indicated that relative expression of those genes was significantly affected by treatment ($F_{(1,127)} = 30.507$, $R^2 = 0.165$, $p = 0.001$), timepoint ($F_{(1,127)} = 14.918$, $R^2 = 0.081$, $p = 0.001$), and their interaction ($F_{(1,127)} = 11.493$, $R^2 = 0.062$, $p = 0.001$). A post-hoc pairwise PERMANOVA test (Bonferroni-corrected) showed that relative expression of those GOIs in the heatwave treatment was significantly different from that of the control on days 4, 6, 8, and 10.

DSP1, HMGB1, HSP90, and PPCTI are the primary contributors to relative expression differences between the simulated heatwave and control (SIMPER analysis). In a comparison of the heatwave and control groups, differences in HMGB1 relative expression accounted for the largest contribution, explaining 26.1% of the dissimilarity between treatments ($p = 0.001$). Differences in PPCTI and DSP1 relative expression accounted for 22.5% ($p = 0.001$) and 19.4%

($p = 0.001$) of the dissimilarity, respectively. HSP90 relative expression also contributed significantly to the dissimilarity (25.6%), but this contribution was not statistically significant ($p = 0.809$). An additional SIMPER analysis comparing each timepoint revealed that those contributions changed over the course of the heatwave. Differences in DSP1, HMGB1, and PPCTI contributed most to dissimilarity between treatments earlier in the heatwave, but differences in HSP90 contributed most to dissimilarity later in the heatwave. From day 0 to day 6, no contributions to dissimilarity between the heatwave and control groups were statistically significant. On day 8, HMGB1, PPCTI, and DSP1 accounted for 27.9% ($p = 0.001$), 24.5% ($p = 0.001$), and 21.7% ($p = 0.001$) of the observed dissimilarity, respectively, while the contribution from HSP90 was not statistically significant ($p = 0.623$). However, by day 10, HSP90 accounted for the largest contribution, explaining 35.8% of the dissimilarity between treatments ($p = 0.001$), with PPCTI also accounting for 21.5% ($p = 0.001$) of the observed dissimilarity. Differences in HMGB1 and DSP1 contributed 21.5% ($p = 0.279$) and 16.3% ($p = 0.087$) to dissimilarity, respectively, but these contributions were not statistically significant.

A PCA was performed to visualize clustering of relative expression patterns and to identify GOs that contribute most to those differences between treatments. The first and second principal components (PC1 and PC2) accounted for 43.98% and 39.12% of the total variance, respectively. Cumulative variance explained by the first two components was 83.10%, suggesting that most of the meaningful variability in the data was captured by PC1 and PC2. A PCA score plot revealed partial separation of clustering between heatwave and control, especially along PC1 (Figure 2.11). Relative expression of HSP90 had the highest loading for PC1 (0.983), suggesting it is a major driver of variation along this axis. Additionally, relative expression of HMGB1 (0.741), PPCTI (0.482), and DSP1 (0.445) contributed strongly to the

variation along PC2, suggesting that differences in relative expression of those four genes contributed the most to the variance between heatwave and control groups (Figure 2.12).

2.4 Discussion

2.4.1 Identification of candidate genes for summer mortality monitoring

The project findings suggest that the expression of five candidate genes—HSP90, HMGB1, DSP1, PPCTI, A2I—demonstrate potential utility in monitoring heatwave-driven mortality for the Pacific oyster. We detected hundreds of DEGs via RNAseq, but only a small subset of those genes were differently expressed at multiple timepoints during the simulated heatwave. This lack of consistency is expected given the extent of polymorphism in the Pacific oyster genome (G. Zhang et al., 2012), and likely lends further credibility to selecting genes that were consistently differently expressed. Verification by qPCR demonstrated that the relative expressions of the 10 GOIs were significantly different under heatwave exposure compared to the control. However, differences in single-gene relative expression responses were only detected for five of these, HSP90, HMGB1, PPCTI, DSP1, and A2I. In addition, differences in relative expression of HSP90, HMGB1, PPCTI, and DSP1 consistently accounted for the majority of variation between treatments, and thus we expect their expressions are the most relevant in terms of monitoring heatwave-driven mortality.

Notably, differences in relative expression of those candidate genes were detectable while a whole-organism response was not—there was no significant difference between heatwave and control treatments in CI. This whole-organism metric is an established method of monitoring

oyster health (He et al., 2022; Rainier & Mann, 1992) and has been recently utilized in the context of monitoring Pacific oysters during heatwaves (De Marco et al., 2023). However, reductions in soft tissue mass driving differences in CI seem to only occur for prolonged heatwaves in excess of 30 d, and a naturally occurring 10-d heatwave also did not alter CI (De Marco et al., 2023). In addition, changes in CI have not been reliably demonstrated to correlate with susceptibility mass mortality (Chávez-Villalba et al., 2007; Mackenzie et al., 2024; Pace et al., 2020) or with the expression of stress response genes (Encomio & Chu, 2005). Thus, our findings are consistent with the previous state of knowledge concerning CI and summer mortality. We also saw no notable physical signs of stress during the simulated heatwave. In particular, we monitored for shell gaping behaviour during the heatwave, as this has been established as a whole-organism metric for stress monitoring in bivalves (McMahon, 1988; Oh et al., 2021). However, we did not see any notable differences in shell gaping between the heatwave and control treatments during the experiment. The results therefore provide further evidence that genetically based monitoring tools for summer mortality may detect changes in Pacific oyster health that whole-organism metrics, such as CI and shell gaping, cannot.

Like other studies (Chaney & Gracey, 2011; De Lorgeril et al., 2011), the experiment was unsuccessful in replicating the extent of summer mortality using a laboratory-simulated heatwave. We recorded only a single mortality in the heatwave group on day 8 (T4) of the simulated heatwave, which corresponded to 24°C. The result is consistent with the hypothesized role of pathogenic bacteria in summer mortality (Cowan et al., 2023; Garnier et al., 2007; Go et al., 2017; Wendling & Wegner, 2013), as the only study to date to successfully replicate summer mortality in the laboratory did so by deliberately selecting oysters with microbiomes consistent with a population undergoing naturally-occurring mortality outbreaks (Green et al., 2019). The

present study did not account for seasonal changes in oyster microbiome. Oysters for the experiment were collected in January (winter for the Northern hemisphere) and therefore it is unlikely that the bacterial communities of oysters in this study were consistent with those during incidents of summer mortality (Conceição et al., 2021; Garnier et al., 2007; Saulnier et al., 2010). Nevertheless, we did detect differences in expression of these four candidate genes with simulated heatwave conditions similar to those in the study that successfully triggered mortality (Green et al., 2019). Therefore, it remains possible that differences in expression would still be detectable and precede mortality in oysters with seasonally accurate bacterial communities. To preserve the seasonal bacterial community and validate the utility of these potential monitoring genes, future laboratory experiments should simulate heatwaves during summer and collect oysters prior to a heatwave as performed by Green et al. (2019). Because we did not successfully replicate a heatwave-driven mortality event in this experiment, it should be noted that the predictive power of these candidate genes remains unclear.

A potential limitation of this study is the seasonal variation in gene expression for Pacific oysters that has been established in previous studies. Summer mortality is a seasonal phenomenon, and while we simulate summer temperatures relevant to mortality, other aspects of seasonality that contribute to mortality are not accounted for. Seasonal variations in bacterial community have already been noted, but changes to reproductive effort in summer also contribute to mortality and may alter patterns of gene expression (Farcy et al., 2007). Seasonal patterns of reproductive effort can be induced in the laboratory with elevated temperature outside the normal spawning season (Vasquez et al., 2013), so it may be that the effect of this discrepancy is negligible. However, the expression of stress marker genes such as HSP70 and HSP90 vary seasonally in oysters, independent of seasonal changes in temperature (Encomio &

Chu, 2005; Farcy et al., 2007). Previous studies have demonstrated that relative expression of HSP70 and HSP90 in response to acute thermal stress is much higher in summer than in winter (Farcy et al., 2009). Therefore, it is possible that the present study, undertaken in winter, actually undervalued HSP70/HSP90 expression in a summer mortality context. It should be noted that Farcy et al. (2009) showed seasonal differences in expression of stress marker genes for a 1-h exposure to 37°C, so it may be the case that these differences are not relevant to the simulated heatwave in the present study. In addition, seasonal variation in expression of stress response genes is not well understood (Encomio & Chu, 2005) and other studies have shown higher relative expression levels of HSP70 and HSP90 in winter compared to summer (Farcy et al., 2007). In the context of monitoring summer mortality, relative expression of stress marker genes during summer is most relevant. Therefore, future studies should simulate heatwaves for oysters collected during summer to minimize uncertainty related to seasonality and confirm the efficacy of these candidate genes in monitoring summer mortality.

2.4.2 Genes involved in stress response

Changes in relative expression of four genes associated with stress response were assessed in this study and only HSP90 showed significant differences under heatwave conditions compared to the control. The GOIs that did not show detectable differences in relative expression under heatwave conditions were HSP70, HSP20, and SIP1. In the present study, differences in relative expression of HSP90 were significant only on the day 10 of the heatwave (T5: 26°C) and contributed most to dissimilarity at higher temperatures. This is consistent with previous studies that have shown reliable upregulation of HSP90 under acute thermal stress for oysters. The majority of those studies detected differences in relative expression for seawater temperatures

between 32 and 37°C (Farcy et al., 2009; Kim et al., 2017; Lim et al., 2016; Y. Xu et al., 2022b), and to our knowledge this is the first study to demonstrate upregulation of HSP90 under heatwave conditions that are relevant to Pacific oyster summer mortality in a temperate region. The present findings are therefore consistent with previous insights that have supported HSP90 as a molecular biomarker to predict heatwave-driven mortality for other oyster species (Masanja et al., 2022; Y. Xu et al., 2022b). As previously noted, genomic response to acute thermal stress has the potential to vary seasonally in Pacific oysters (Farcy et al., 2009). Therefore, future studies should investigate HSP90 relative expression under simulated heatwaves and field studies in summer to confirm its potential applicability as a monitoring tool for Pacific oyster summer mortality.

Despite their ubiquitous use as thermal stress biomarkers in environmental monitoring (Gupta et al., 2010; Hoffmann & Daborn, 2007b; Mukhopadhyay et al., 2003), the present study did not detect any significant differences in relative expression of HSP20 or HSP70 under simulated heatwave conditions. No significant differences in relative expression of SIP1, an orthologue of HSP20 (G. Zhang et al., 2012), were detected either. Those results align with our hypothesis that the use of traditional stress biomarkers may not be applicable to monitoring summer mortality due to realistic temperatures. Detectable upregulation of HSP70 and HSP20 in response to acute thermal stress usually occurs at temperatures between 32 and 38°C in oysters (Farcy et al., 2009; Lim et al., 2016; Liu et al., 2022; Y. Xu, et al., 2022a; C. Yang et al., 2017; Y. Zhang et al., 2015), well above the maximum temperature of the simulated heatwave in the present study. While the heatwave conditions simulated in the present study did not induce upregulation of HSP20 or HSP70, similar temperature conditions do trigger outbreaks of mortality in the field (Garnier et al., 2007; Mackenzie et al., 2024; Whittington et al., 2024) and

in appropriate laboratory settings (Green et al., 2019). Therefore, these results provide evidence that novel molecular biomarkers, other than HSP20 and HSP70, are needed to effectively monitor and predict Pacific oyster summer mortality.

2.4.3 Genes involved in regulation of transcription

While upregulation of HSP70 was not induced in the present experiment, significant downregulation of a proposed negative regulator of HSP70 was detected. Relative expression of DSP1 was significantly negatively affected by simulated heatwave conditions. Notably, DSP1 was downregulated relatively early in the heatwave in seawater temperatures that were only slightly elevated (T3; 22°C) compared to the control (16°C). Summer mortality is usually triggered by similar temperatures (Garnier et al., 2007; Green et al., 2019) and thus DSP1 may be an especially appropriate choice for monitoring summer mortality. In the Hong Kong oyster (*Crassostrea hongkongensis*), a closely related estuarine species (Zhao et al., 2014), DSP1 is a recently discovered negative regulator of HSP70 (Miao et al., 2016). To date, there is only one study on this regulatory mechanism in oysters, but current evidence suggests DSP1 suppresses HSP70 transcription through direct binding to its promoter region (Miao et al., 2016).

Coordinated expression of HSP70 and DSP1 has been observed for *C. hongkongensis* exposed to heat stress, as upregulation of DSP1 occurred in tandem with downregulation of HSP70 during recovery from 37°C heat shock (Miao et al., 2016). This is consistent with the RNAseq results of the present work, as early downregulation of DSP1 followed by upregulation of HSP70 at the height of the heatwave was observed, indicating a shift away from heat-shock suppression as temperature increased. We therefore provide the first indirect evidence of this HSP70 regulation

mechanism in *C.gigas*, although future studies should investigate this system directly to confirm its role in HSP70 expression in the Pacific oyster.

Early detection of DSP1 downregulation before the onset of HSP70 response may provide an early warning signal of stress that can lead to mortality. While it is unlikely that HSP70 would act as a reliable biomarker for summer mortality based on the results of the present study, we do provide evidence that certain genes associated with HSP70 regulation, specifically DSP1, may have the potential to act as biomarkers for summer mortality. This is consistent with previous studies that have identified regulators of HSP70 expression such as HIF-1 α as biomarkers for early stress detection in Pacific oysters (Fu et al., 2023; Patterson et al., 2014; Wang et al., 2016). If those regulatory mechanisms become activated under environmental conditions that permit summer mortality, then altered expression of those genes may allow detection of vulnerability to mortality where traditional stress biomarkers would not. The present study indicates that this is the case with expression of DSP1 and further investigation into its predictive power for Pacific oyster mortality is recommended.

2.4.4 Genes involved in immune function

Changes in relative expression of three genes associated with immune function—A2I, HMGB1, and PPCTI—were examined in the current study, all of which showed significant differences under heatwave conditions compared to the control. Relative expression of A2I in the heatwave treatment was significantly higher than in the control. A2I is an inhibitor of apoptosis (IAP) and a member of a family of genes involved in cell survival that are upregulated during heat and low-salinity stress (G. Zhang et al., 2012). The Pacific oyster genome contains an increased number of IAPs compared to other species, indicating a robust cell death defense

system likely evolved to contend with exposure to air in the intertidal (Witkop et al., 2022; G. Zhang et al., 2012). IAPs are also involved in innate immunity for oysters, as they function to maintain cell stability in the late stages of infection (Cai et al., 2022; Witkop et al., 2022). While the role of apoptosis regulation in immune response is complex, in general, upregulation of IAPs is associated with increased susceptibility to bacterial and viral infection in oysters (Goedken et al., 2005; Segarra et al., 2014; Witkop et al., 2022). In the early stages of infection, apoptosis of infected cells is a defense mechanism to limit the spread of pathogens (Goedken et al., 2005; Martenot et al., 2017; Segarra et al., 2014). Inhibition of apoptosis can interrupt this process increasing the likelihood of infection. As such, many pathogens have evolved mechanisms to inhibit host apoptosis and increase their survival (Barber, 2001; Cuff & Ruby, 1996). Therefore, upregulation of A2I in the present study may not only indicate cellular stress but also increased susceptibility to pathogenic infection. However, expression of IAP genes is also associated with enhanced survival for oysters during heatwaves (Kim et al., 2017; Scanes et al., 2020) and their potential role in disease resistance for Pacific oysters is still being explored (Cai et al., 2022; Martenot et al., 2017; Witkop et al., 2022). Therefore, further research is needed to elucidate the role of IAP expression and apoptosis regulation in Pacific oyster summer mortality.

Significant downregulation of HMGB1 in comparison to the control was also observed. The HMGB1 protein is a highly conserved DNA-binding protein involved in regulation of transcription, inflammation, and immune response in eukaryotes (J. Li et al., 2003; Štros, 2010). HMGB1 in *C. gigas* was first described by J. Li et al. (2013) and has since been demonstrated to function in innate immunity for oysters (J. Li et al., 2013; T. Xu et al., 2012). HMGB1 is highly expressed in the hemocytes, the primary immune cells in oysters, and is significantly upregulated in the presence of pathogenic bacteria such as *Vibrio alginolyticus* and *V. splendidus* (J. Li et al.,

2013; Lv et al., 2022). HMGB1 acts synergistically with the cytokine Rel to regulate the expression of Nuclear Factor- κ B (NF- κ B) (J. Li et al., 2013), a proinflammatory molecule and reporter gene often used to assess activation of immune responses (Skjæveland et al., 2009). Activation of the NF- κ B pathway by HMGB1 induces the expression of the immune signalling genes IL17 and TNF as well as the antimicrobial peptide DefH (J. Li et al., 2013; Lv et al., 2022). In the absence of bacterial challenge, HMGB1 expression is constitutive in a range of tissues including the gills (J. Li et al., 2013). Thus, downregulation of HMGB1 in this study may suggest a shift away from innate immune function during heatwaves leaving oysters susceptible to bacterial infection.

In contrast, previous studies have observed upregulation of NF- κ B pathway genes both in simulated heatwave-driven mortality (Green et al., 2019) and in mortality events driven by naturally occurring marine heatwaves (Siboni et al., 2024), suggesting that heat-stressed *C. gigas* can still effectively activate immune response genes. For example, Green et al. (2019) found upregulation of the NF- κ B pathway genes IL17, TNF, and DefH under simulated heatwave conditions, all of which are induced by HMGB1 expression. In addition, negative impacts of elevated water temperature on haemocytes of *C. gigas* have primarily been observed above 40°C (Gagnaire et al., 2006; Wendling & Wegner, 2013), far exceeding the relevant threshold for Pacific oyster summer mortality. Those findings have led previous studies to conclude that heatwaves may not exacerbate mortality by compromising the immune response of *C. gigas* but instead drive such rapid proliferation of pathogenic bacteria that growth exceeds the capacity of the oyster immune system, ultimately leading to mortality (Green et al., 2019; Wendling & Wegner, 2013). However, upregulation of NF- κ B pathway genes usually occurs at the height of infection in parallel with mortality (Green et al., 2019; Siboni et al., 2024). Therefore, it remains

possible that heatwaves do drive reductions in innate immune function prior to infection, ultimately increasing vulnerability in the event that bacterial infection occurs. Indeed, more recent studies have demonstrated that under heat stress both IL17 and TNF are downregulated in the early stages of infection by *V. alginolyticus* and upregulated in later stages at the onset of mortality (X. Li et al., 2023). The present study provides the first evidence that elevated temperatures may impair HMGB1 activity in Pacific oyster, ultimately leading to reduced expression of immune signalling and antimicrobial genes. However, further investigation is needed to understand the exact role of HMGB1/Rel-induced NF- κ B pathway genes in Pacific oyster summer mortality.

Finally, significant downregulation of PPCTI was observed in comparison to the control. PPCTI describes a domain common to three superfamilies of genes involved in protein folding, usually referred to as PPIases (Takahashi et al., 1989). In molluscs, the most well described PPIases are cyclophilins (CyPs), which likely function in innate immunity similar to HMGB1. While the mechanism is not well understood, CyPs are generally upregulated in the presence of bacterial infection for bivalves (Chen et al., 2011; X. Song et al., 2009) and have been demonstrated to bind to immunosuppressive agents with high affinity (Marks, 1996), suggesting a possible regulatory role. In oysters, CyPs are constitutively expressed in a range of tissues, but most highly expressed in the haemocytes (T. Xu et al., 2016). CyPs are also upregulated in response to infections by *V. splendidus* (Huvet et al., 2004) and by a pathogenic rickettsia-like organism (T. Xu et al., 2016). Therefore, downregulation of PPCTI in the present study may also indicate a heatwave-driven shift away from innate immunity. That is consistent with previous work that has found reduced CyP expression is associated with increased susceptibility to

summer mortality following infection by *V. splendidus* (Huvet et al., 2004), suggesting that reductions in innate immunity driven by heatwaves may contribute to summer mortality.

Previous evidence challenged the hypothesis that heatwaves drive reductions in immune function in oysters, increasing susceptibility to summer mortality (Green et al., 2019; Wendling & Wegner, 2013), yet the present research provides evidence that at least three genes involved in immune function show altered relative expression under heatwave conditions. Therefore, the findings support previous work that has demonstrated the deleterious effect of heatwaves on Pacific oyster immunity and summer mortality (Delaporte et al., 2006; X. Li et al., 2023; Y. Li et al., 2007). However, relative expression of only one of these genes, PPCTI, has been corroborated by other studies on summer mortality (Huvet et al., 2004). Work has yet to investigate the relative expression of A2I and HMGB1 in the context of heatwave-driven mortality for Pacific oyster. Thus, further investigation is needed to understand the expression of Pacific oyster immune genes during heatwaves, especially in relation to summer mortality.

2.4.5 Conclusion

The present study examined the effect of a simulated heatwave on gene expression in the Pacific oyster to investigate the role of heatwaves in summer mortality and to identify candidate monitoring genes. Changes in relative expression of 10 genes of interest were assessed, five of them showing altered expression under heatwave conditions. Among traditional stress monitoring genes, HSP90 was upregulated under heat stress while HSP20 and HSP70 were not. Three immune genes—HMGB1, PPCTI, and A2I—showed altered expression during the heatwave, indicating possible impairment of innate immunity in response to elevated temperatures, which may contribute to mortality. The study provides the first indirect evidence

that DSP1 negatively regulates HSP70 in *C. gigas*, as its downregulation was observed at multiple points during the heatwave. Taken together, the results indicate that novel molecular biomarkers other than HSP70 and HSP20 are needed to effectively monitor Pacific oyster summer mortality, and that immune and regulatory genes may detect vulnerability to mortality where traditional stress biomarkers would not. The findings provide insights into the role of heatwaves in Pacific oyster summer mortality and will inform effective monitoring practices to support the adaptation of shellfish aquaculture to the growing impacts of climate change.

2.5 Tables and figures

Table 2.1 Primer sequences used in qPCR verification and associated gene IDs for cDNA sequences used in primer design.

Gene	EnsemblMetazoa gene ID	Forward primer	Reverse primer
Actin	G3054	5' GCCCTGGACTTCGAACAA 3'	5' CGTTGCCAATGGTGATGA 3'
Elongation factor 1- α	G4818	5' GAGCGTGAACGTGGTATCAC 3'	5' ACAGCACAGTCAGCCTGTGA 3'
Heat shock protein 70	G29360	5' TGACCAAGGCAACAGAACCA 3'	5' AATCAGACGGCCGGTATGTG 3'
Heat shock protein 20	G17983	5' CCGAAGGAAGAGACCAGGAGATG 3'	5' CGAACACCGACAGGTCTAAACTCTC 3'
Heat shock protein 90	G10994	5' TCACACAGGAGGAGTATGGC 3'	5' TGAGAAATGCTTCACAGCCAA 3'
High mobility group protein DSP1	G24596	5' CAGCCAAGAAAGCCAAACCTC 3'	5' ACAATGGTGCTTGCCGACT 3'
High mobility group box 1	G31074	5' TCCCACCCAAAACAAAGCCA 3'	5' ACTTCCCACTGTTACCCCT 3'
Peptidyl-prolyl cis-trans isomerase	G21557	5' CCGTTCGATGCTACCCAC 3'	5' ATGAACCAATCCTGGCACACA 3'
Death-associated inhibitor of apoptosis 2	G17932	5' AGGAACGGAAAACAATGACGA 3'	5' ACGTCCTTTGACATCCCGTG 3'
Stress-induced protein 1	G17984	5' AGCCTGACCACATTACCGTC 3'	5' GAACGAGACACCTTGACCCC 3'
Heterogeneous nuclear ribonucleoprotein	G1087	5' CCGGTGACTCCAAAACCATC 3'	5' ACTCACCTGATCGTATCCGT 3'
X-box-binding protein 1	G20574	5' AGTCTGCGGATTTAGCTGGAG 3'	5' GCCAATCACAGAAGCAGCAC 3'

Table 2.2. Numbers of differently expressed genes (DEGs) at each heatwave timepoint and corresponding temperature (in comparison to a control of 16°C), including both upregulated and downregulated DEGs.

Timepoint	Temperature (°C)	Number of upregulated genes	Number of downregulated genes	Total DEGs
T1	18	8	10	18
T2	20	26	38	64
T3	22	55	47	102
T4	24	62	61	123
T5	26	96	150	246

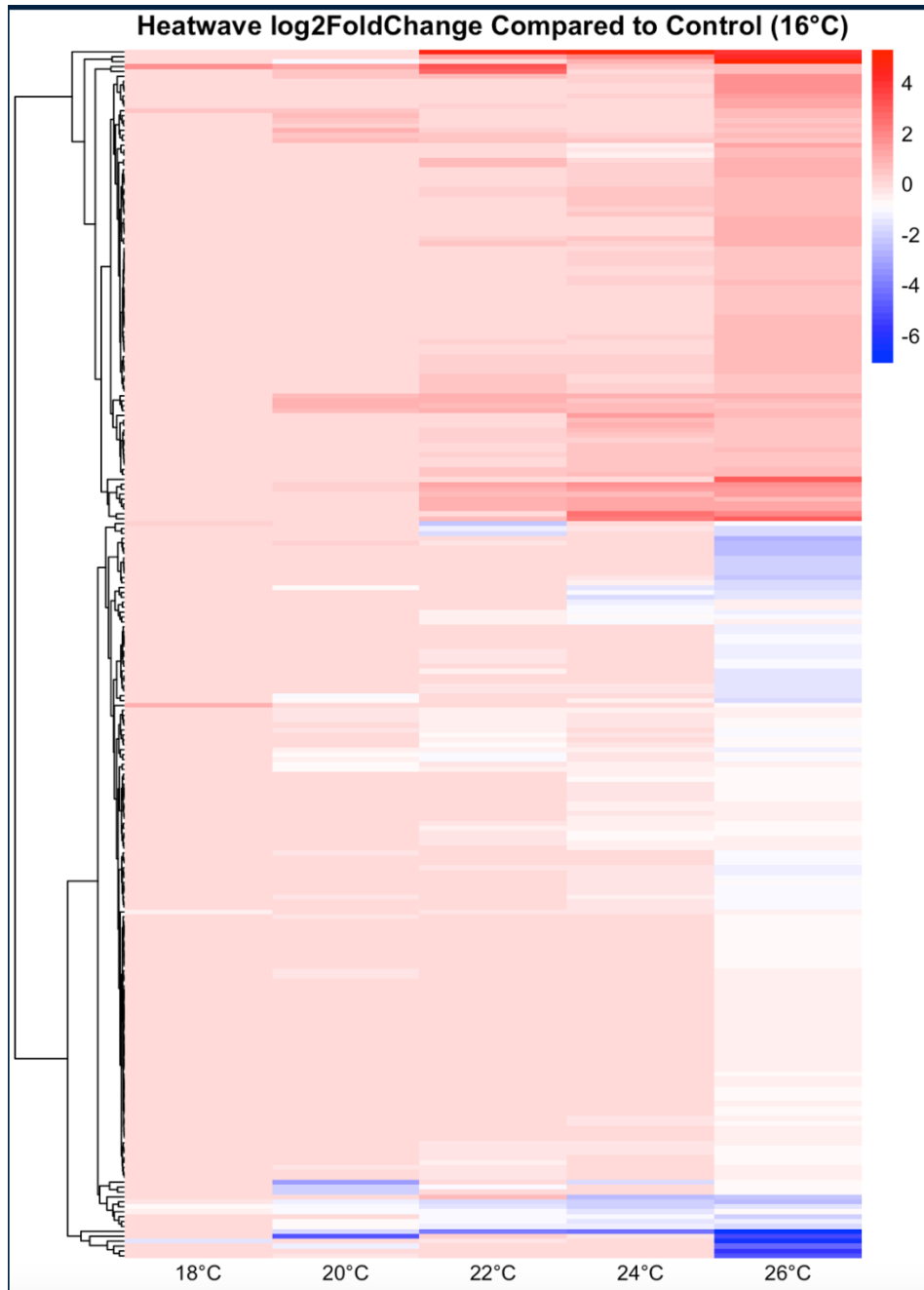


Figure 2.1. Heat map of changes in gene expression (Log2FC) for the 246 DEGs detected by RNAseq at the height of the heatwave (T5, 26°C) at each timepoint during the experiment. Hierarchical clustering was performed for genes (rows) using Euclidean distance and complete linkage. A colour gradient from blue (low) to red (high) represents Log2FC values.

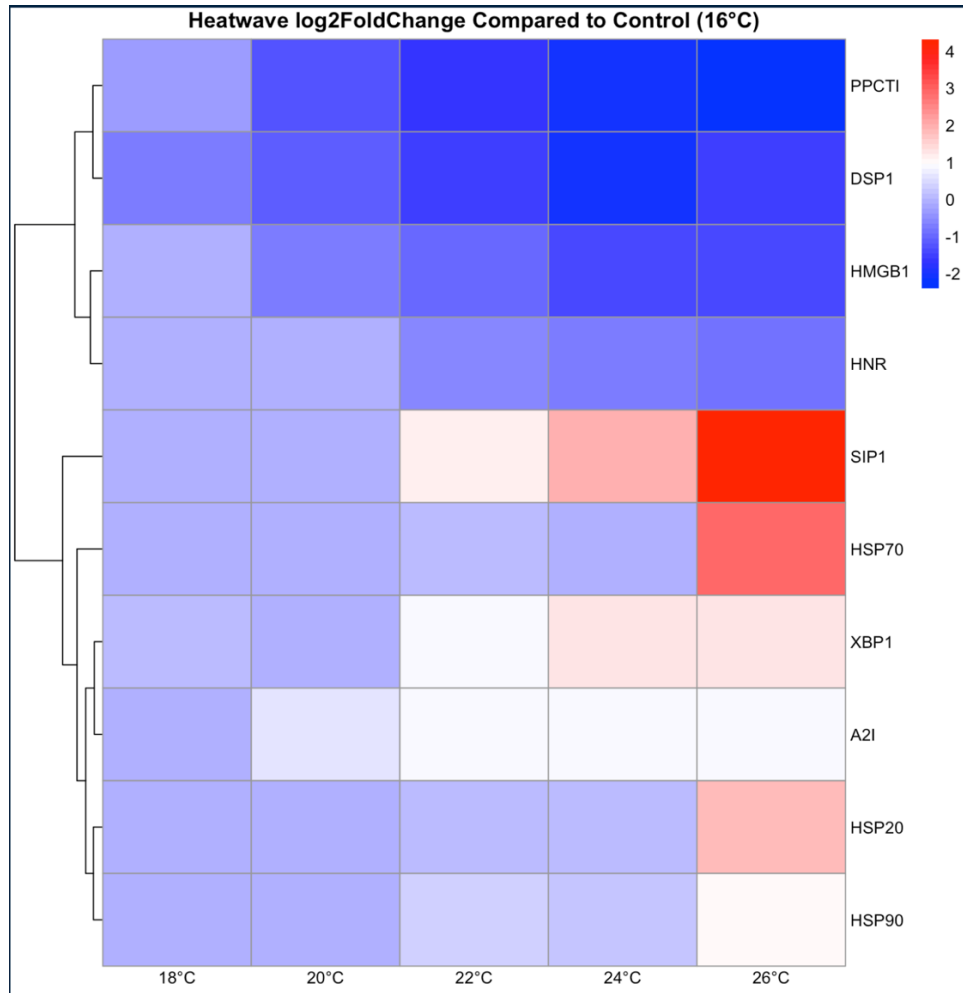


Figure 2.2. Heat map of changes in gene expression (Log2 fold change) detected by RNAseq for the 10 genes of interest (GOIs) — peptidyl-prolyl cis-trans isomerase (PPCTI), high mobility group protein DSP1 (DSP1), high mobility group box 1 (HMGB1), heterogeneous nuclear ribonucleoprotein (HNR), stress-induced protein 1 (SIP1), heat shock protein 70 B2 (HSP70), x-box-binding protein 1 (XBP1), death-associated inhibitor of apoptosis 2 (A2I), heat shock protein 20 (HSP20), and heat shock protein 90 (HSP90) — chosen for qPCR validation at each timepoint during the experiment. Hierarchical clustering was performed for genes (rows) using Euclidean distance and complete linkage. A colour gradient from blue (low) to red (high) represents Log2FC values.

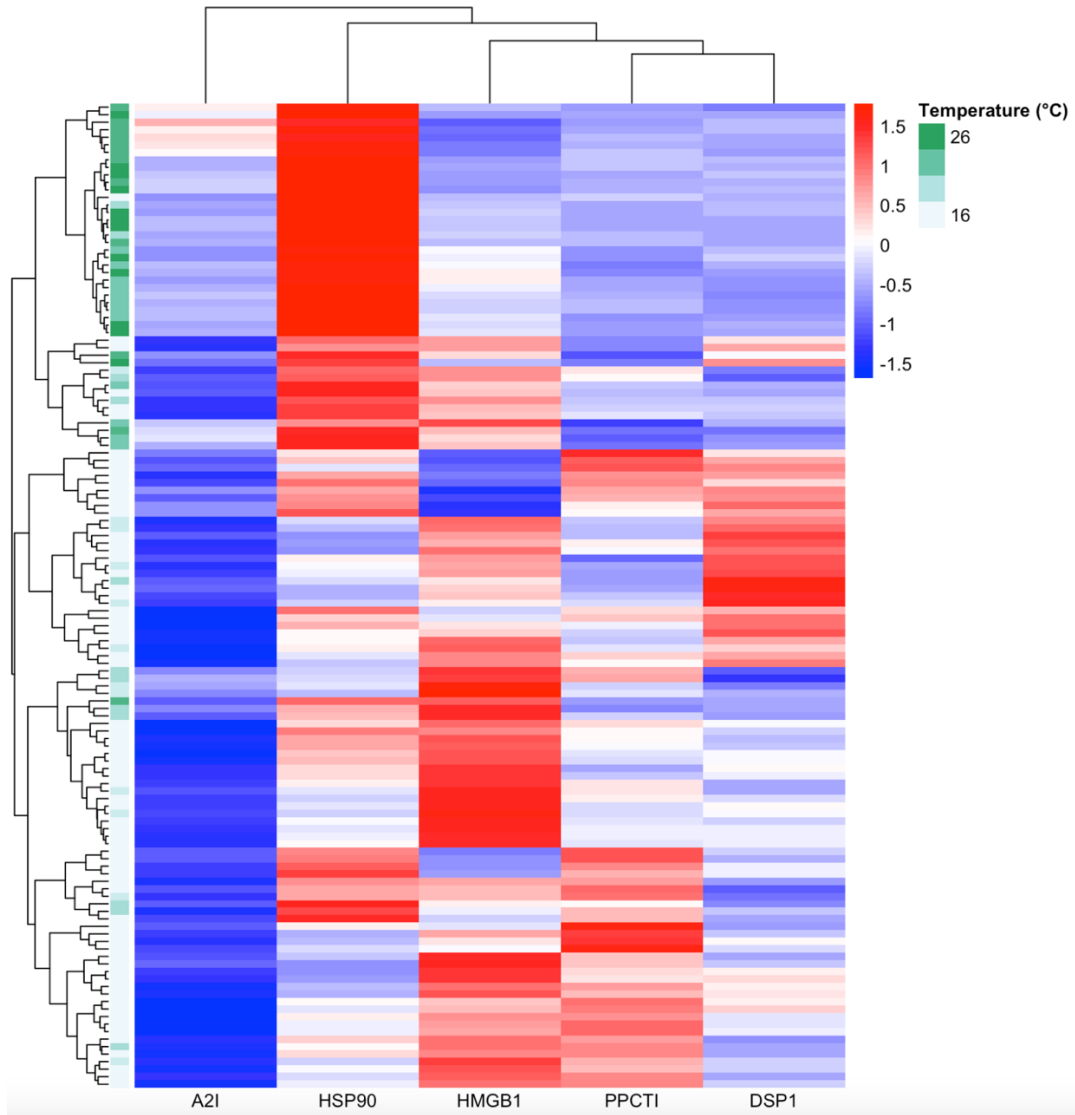


Figure 2.3. Heat map of relative expression ($2^{\Delta Cq}$) for the five genes of interest (GOIs)—death-associated inhibitor of apoptosis 2 (A2I), heat shock protein 90 (HSP90), high mobility group box 1 (HMGB1), peptidyl-prolyl cis-trans isomerase (PPCTI), and high mobility group protein DSP1 (DSP1) — that showed significant ($p < 0.05$) changes under single-gene response assessment. Hierarchical clustering was performed for both genes (columns) and temperatures (rows) using Euclidean distance and complete linkage. A colour gradient from blue (low) to red (high) represents z-transformed relative expression values. Relative expression is similar at higher temperatures, as indicated by clustering of darker green rows.

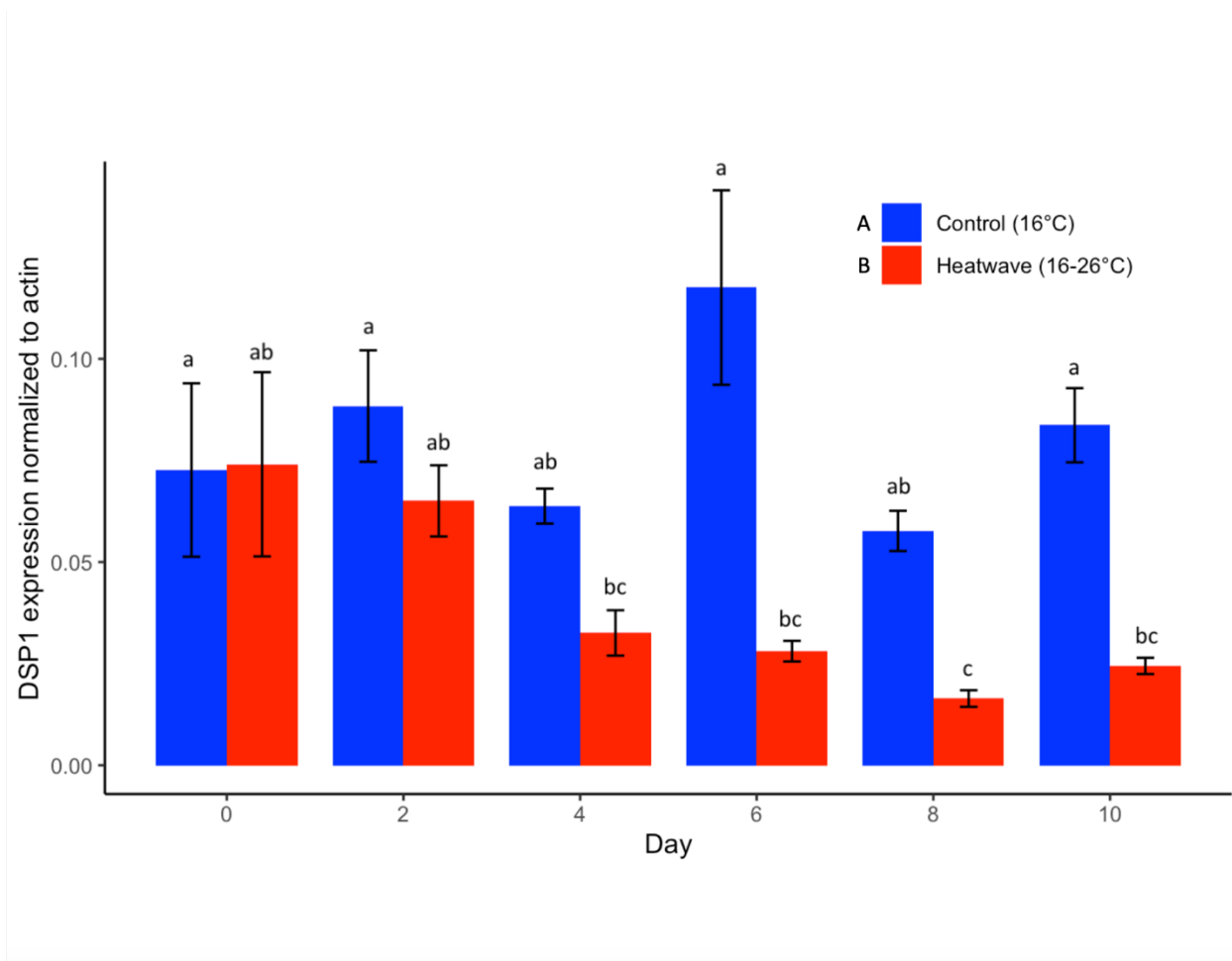


Figure 2.4. Mean relative expression ($2^{\Delta Cq}$) and standard error ($n = 12$) for high mobility group protein DSP1 (DSP1) on day 0 (T0, 16°C), day 2 (T1, 18°C), day 4 (T2, 20°C), day 6 (T3, 22°C), day 8 (T4, 24°C), and day 10 (T5, 26°C) of the simulated heatwave compared to the control (16°C). Relative expression normalized to actin where $\Delta Cq = (Cq_{actin} - Cq_{DSP1})$. Capital letters in the legend show significant ($p < 0.05$) differences identified for the treatment effect via two-way ANOVA, while lower-case letters above the bars show significant ($p < 0.05$) differences between treatments and timepoints identified by a post-hoc Student-Newman-Keuls (SNK) test.

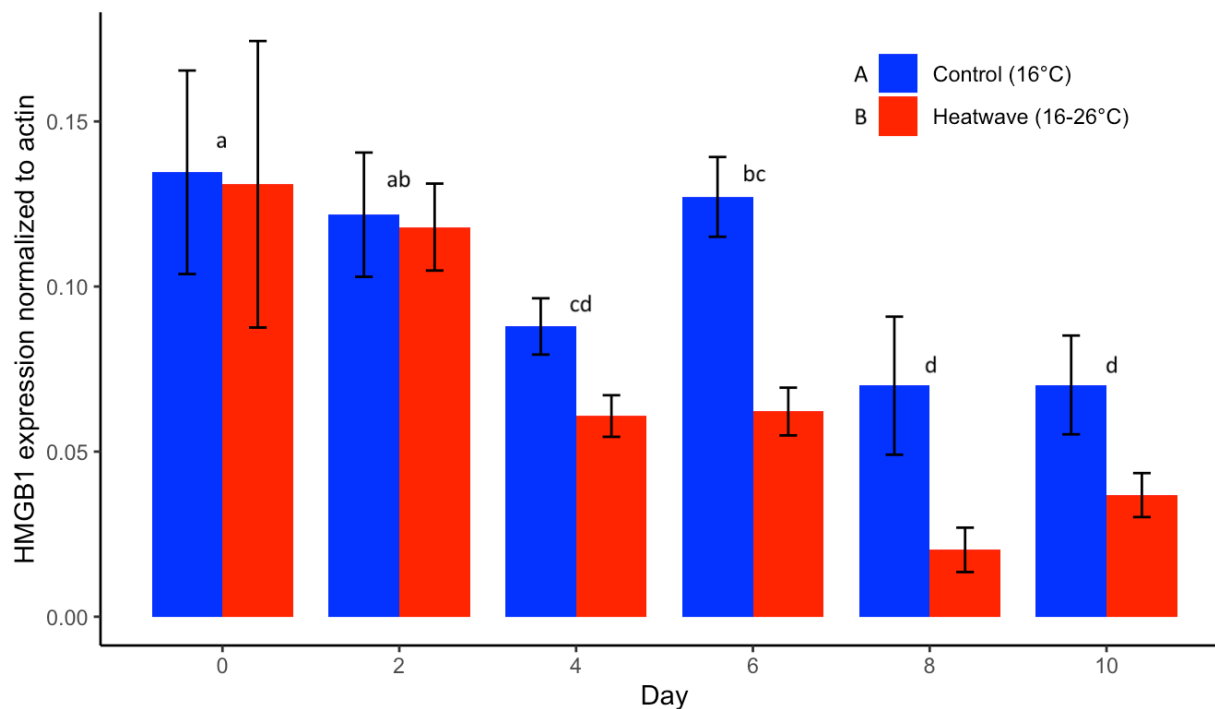


Figure 2.5. Mean relative expression ($2^{\Delta Cq}$) and standard error ($n = 12$) for high mobility group box 1 (HMGB1) on day 0 (T0, 16°C), day 2 (T1, 18°C), day 4 (T2, 20°C), day 6 (T3, 22°C), day 8 (T4, 24°C), and day 10 (T5, 26°C) of the simulated heatwave compared to the control (16°C). Relative expression normalized to actin where $\Delta Cq = (Cq_{actin} - Cq_{HMGB1})$. Capital letters in the legend show significant ($p < 0.05$) differences identified for the treatment effect via two-way ANOVA, while lower-case letters above the bars show significant ($p < 0.05$) differences between timepoints identified by a post-hoc Student-Newman-Keuls (SNK) test.

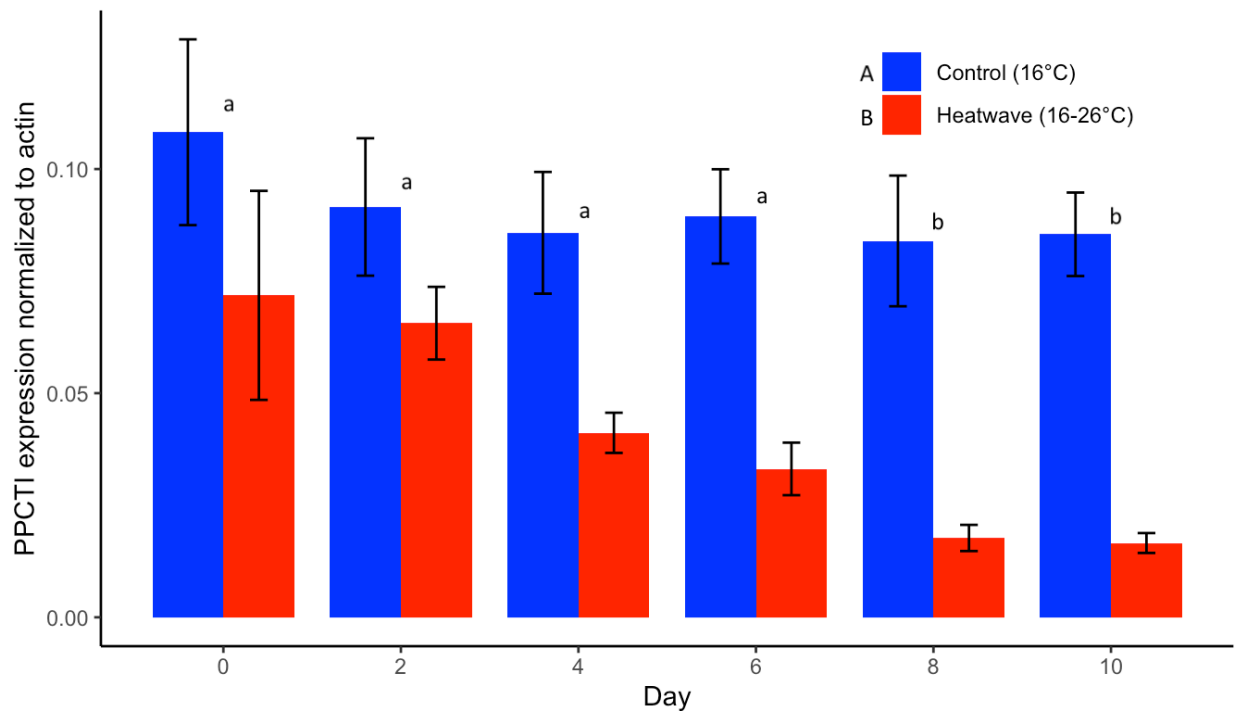


Figure 2.6. Mean relative expression ($2^{\Delta Cq}$) and standard error ($n = 12$) for peptidyl-prolyl cis-trans isomerase (PPCTI) on day 0 (T0, 16°C), day 2 (T1, 18°C), day 4 (T2, 20°C), day 6 (T3, 22°C), day 8 (T4, 24°C), and day 10 (T5, 26°C) of the simulated heatwave compared to the control (16°C). Relative expression normalized to actin where $\Delta Cq = (Cq_{actin} - Cq_{PPCTI})$. Capital letters in the legend show significant ($p < 0.05$) differences identified for the treatment effect via two-way ANOVA, while lower-case letters above the bars show significant ($p < 0.05$) differences between timepoints identified by a post-hoc Student-Newman-Keuls (SNK) test.

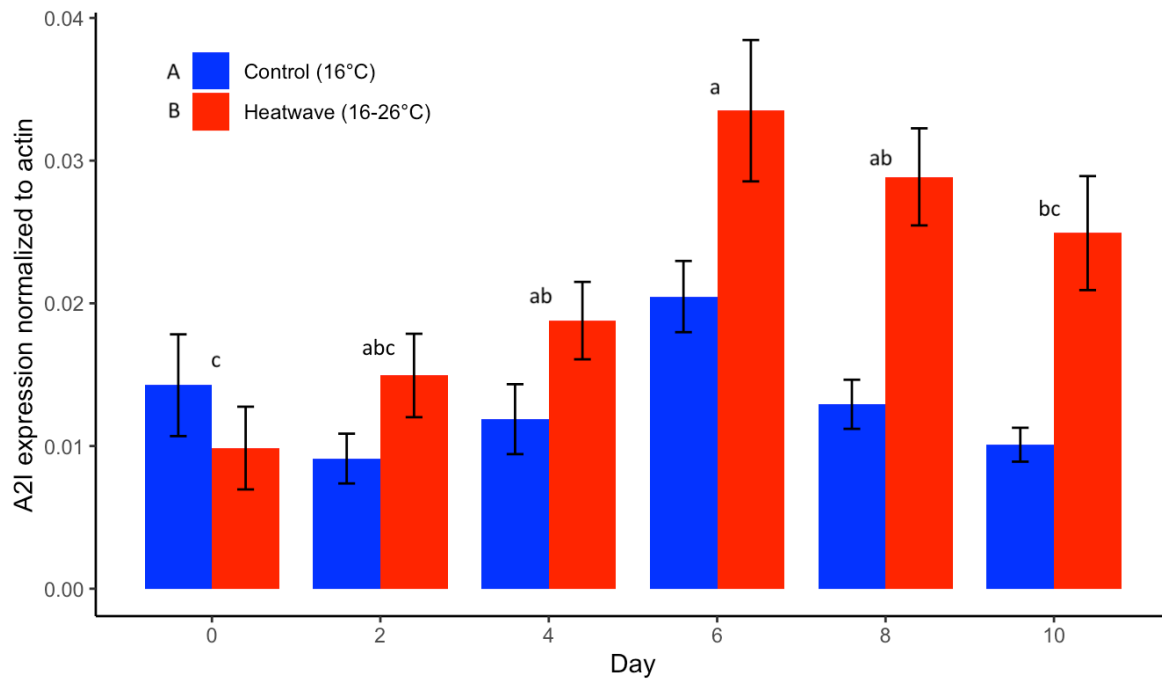


Figure 2.7. Mean relative expression ($2^{\Delta Cq}$) and standard error ($n = 12$) for death-associated inhibitor of apoptosis 2 (A2I) on day 0 (T0, 16°C), day 2 (T1, 18°C), day 4 (T2, 20°C), day 6 (T3, 22°C), day 8 (T4, 24°C), and day 10 (T5, 26°C) of the simulated heatwave compared to the control (16°C). Relative expression normalized to actin where $\Delta Cq = (Cq_{actin} - Cq_{A2I})$. Capital letters in the legend show significant ($p < 0.05$) differences identified for the treatment effect via two-way ANOVA, while lower-case letters above the bars show significant ($p < 0.05$) differences between timepoints identified by a post-hoc Student-Newman-Keuls (SNK) test.

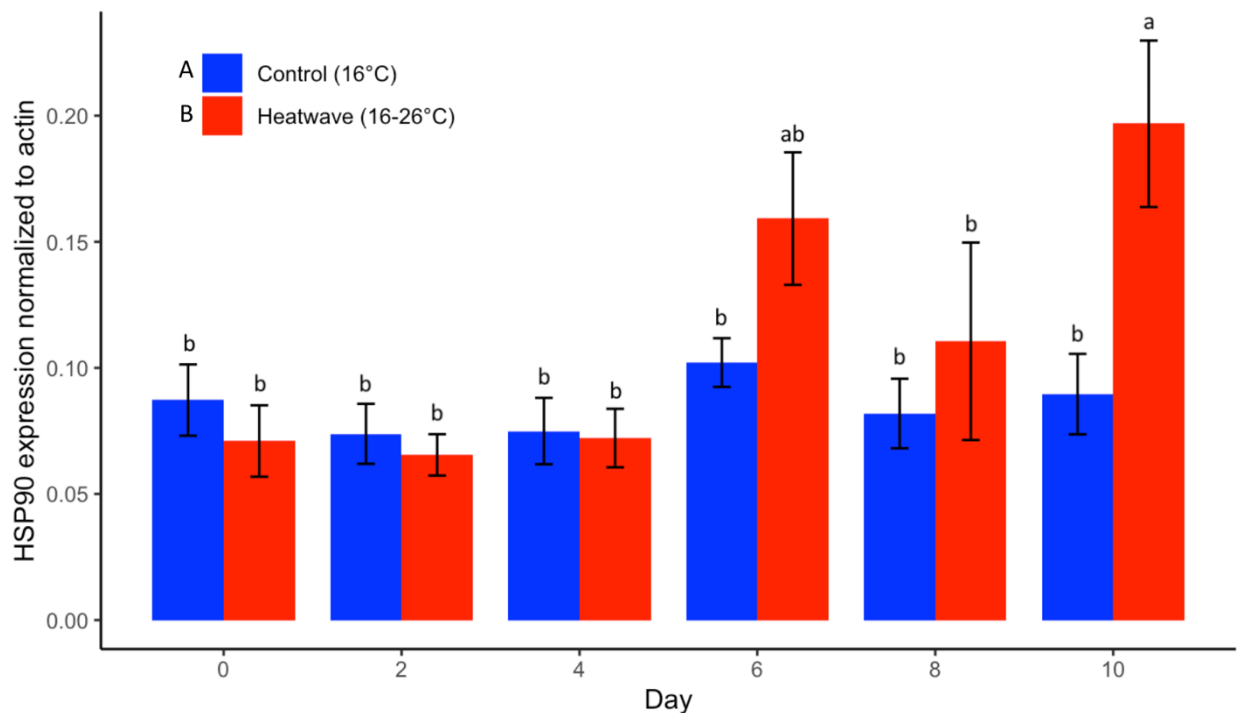


Figure 2.8. Mean relative expression ($2^{\Delta Cq}$) and standard error ($n = 12$) for heat shock protein 90 (HSP90) on day 0 (T0, 16°C), day 2 (T1, 18°C), day 4 (T2, 20°C), day 6 (T3, 22°C), day 8 (T4, 24°C), and day 10 (T5, 26°C) of the simulated heatwave compared to the control (16°C).

Relative expression normalized to actin where $\Delta Cq = (Cq_{actin} - Cq_{HSP90})$. Capital letters in the legend show significant ($p < 0.05$) differences identified for the treatment effect via two-way ANOVA, while lower-case letters above the bars show significant ($p < 0.05$) differences between treatments and timepoints identified by a post-hoc Student-Newman-Keuls (SNK) test.

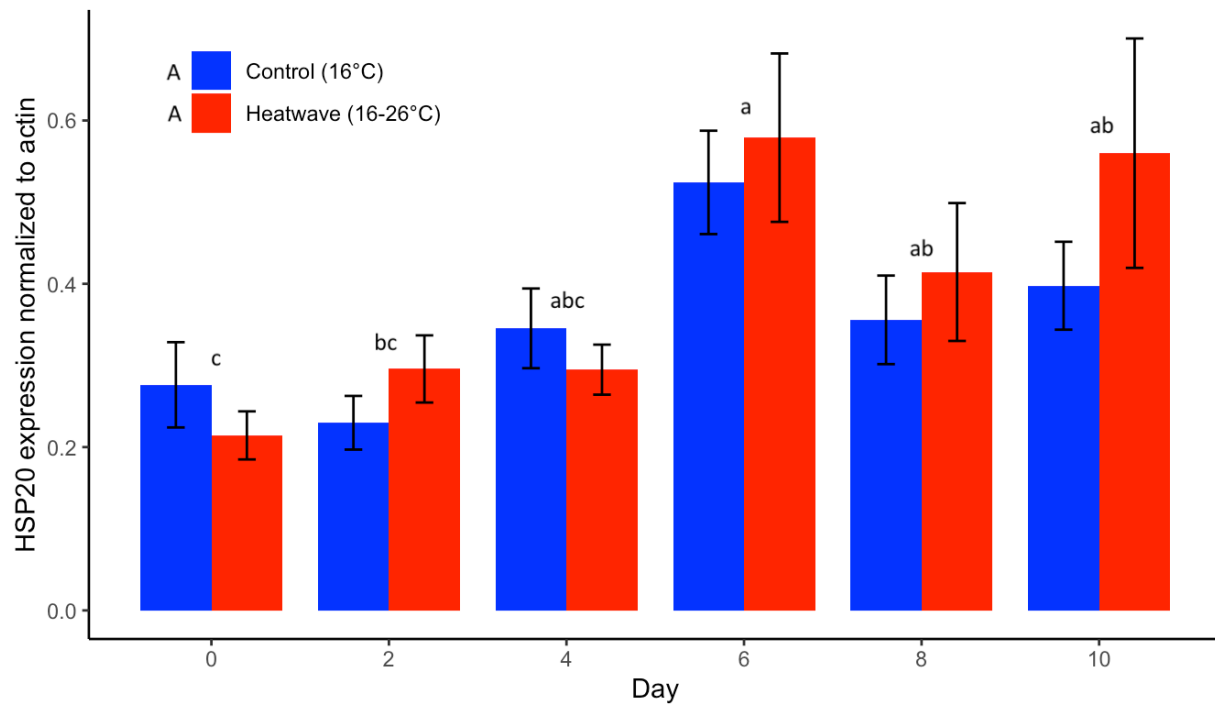


Figure 2.9. Mean relative expression ($2^{\Delta Cq}$) and standard error ($n = 12$) for heat shock protein 20 (HSP20) on day 0 (T0, 16°C), day 2 (T1, 18°C), day 4 (T2, 20°C), day 6 (T3, 22°C), day 8 (T4, 24°C), and day 10 (T5, 26°C) of the simulated heatwave compared to the control (16°C).

Relative expression normalized to actin where $\Delta Cq = (Cq_{actin} - Cq_{HSP20})$. Capital letters in the legend show significant ($p < 0.05$) differences identified for the treatment effect via two-way ANOVA, while lower-case letters above the bars show significant ($p < 0.05$) differences between timepoints identified by a post-hoc Student-Newman-Keuls (SNK) test.

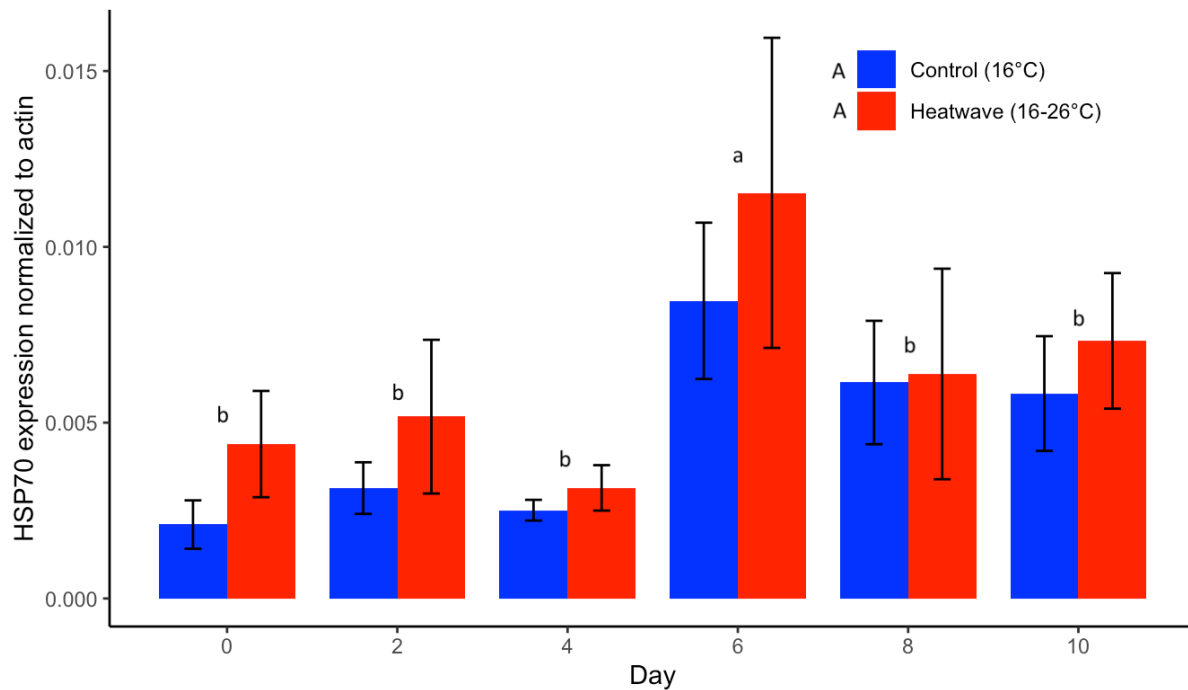


Figure 2.10. Mean relative expression ($2^{\Delta Cq}$) and standard error ($n = 12$) for heat shock protein 70 B2 (HSP70) on day 0 (T0, 16°C), day 2 (T1, 18°C), day 4 (T2, 20°C), day 6 (T3, 22°C), day 8 (T4, 24°C), and day 10 (T5, 26°C) of the simulated heatwave compared to the control (16°C). Relative expression normalized to actin where $\Delta Cq = (Cq_{actin} - Cq_{HSP70})$. Capital letters in the legend show significant ($p < 0.05$) differences identified for the treatment effect via two-way ANOVA, while lower-case letters above the bars show significant ($p < 0.05$) differences between timepoints identified by a post-hoc Student-Newman-Keuls (SNK) test.

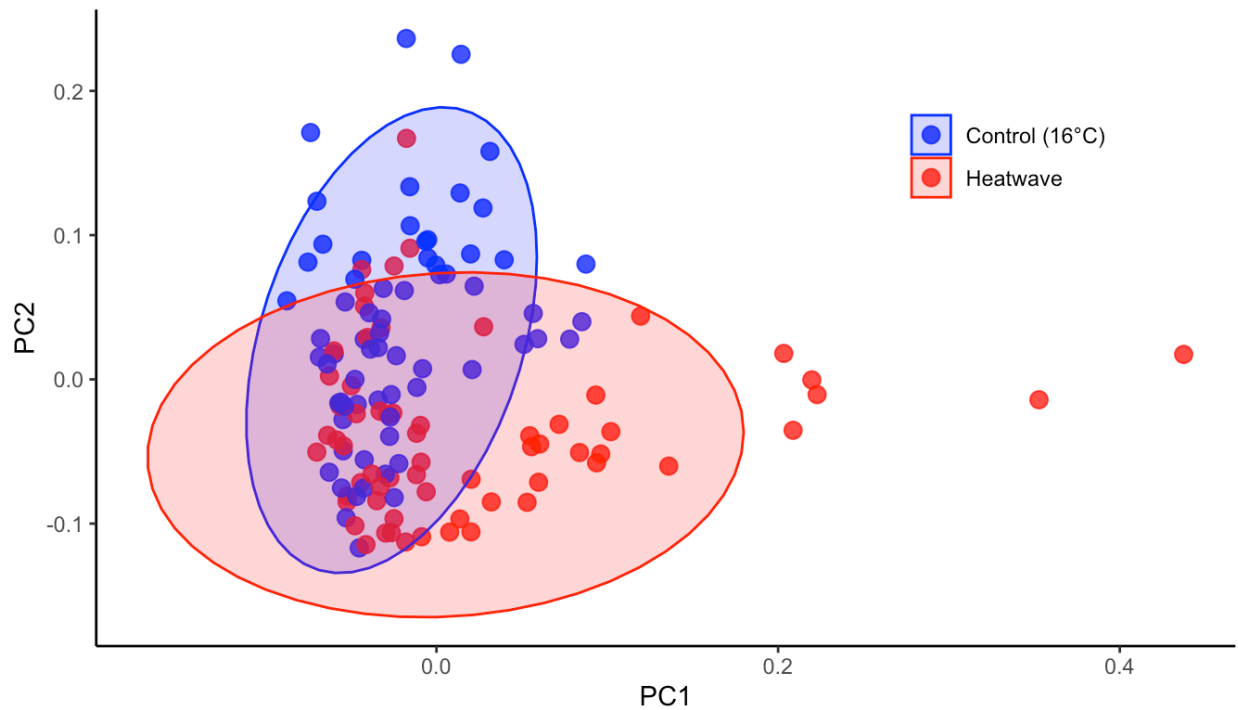


Figure 2.11. Principal Component Analysis (PCA) of relative expression for the five genes of interest (GOIs)—death-associated inhibitor of apoptosis 2 (A2I), heat shock protein 90 (HSP90), high mobility group box 1 (HMGB1), peptidyl-prolyl cis-trans isomerase (PPCTI), and high mobility group protein DSP1 (DSP1)—that showed significant ($p < 0.05$) changes under single-gene response assessment. The first two principal components (PC1 and PC2) are plotted, explaining 43.98% and 39.12% of the total variance, respectively. Samples are colored according to treatment group (control = blue, heatwave = red) and ellipses represent 95% confidence intervals for each group. PCA reveals some cluster separation between control and heatwave, especially along PC1.

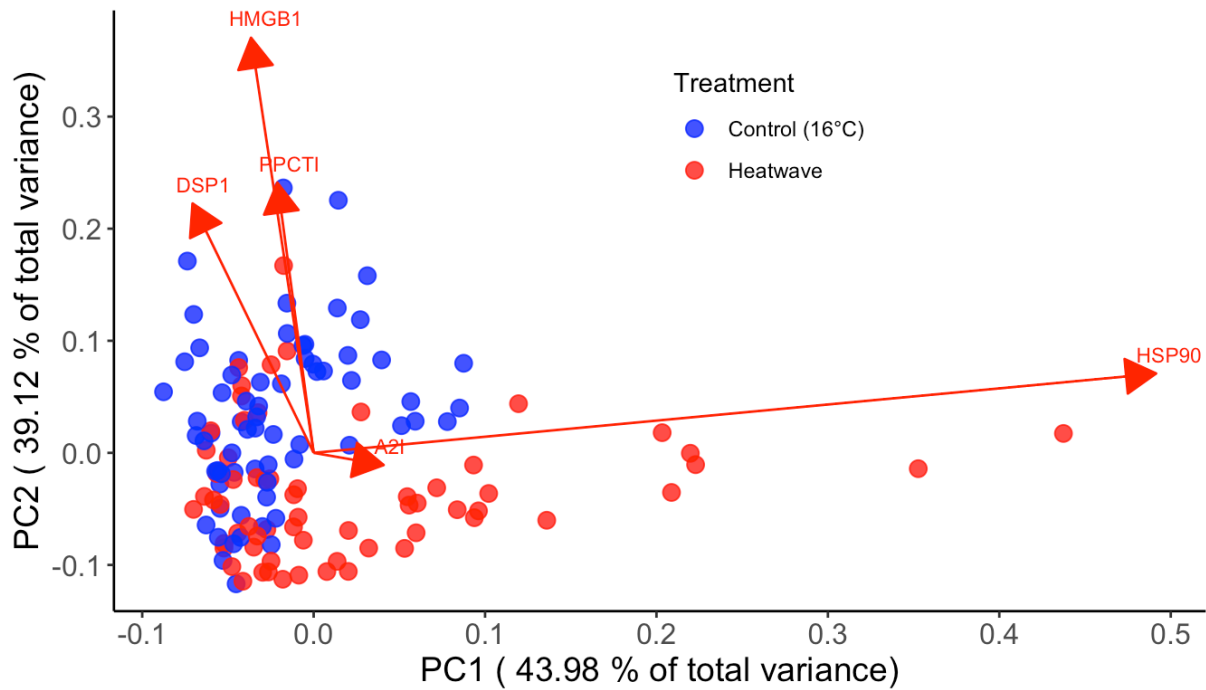


Figure 2.12. Biplot showing the results of Principal Component Analysis (PCA) on relative expression for the five genes of interest (GOIs)—death-associated inhibitor of apoptosis 2 (A2I), heat shock protein 90 (HSP90), high mobility group box 1 (HMGB1), peptidyl-prolyl cis-trans isomerase (PPCTI), and high mobility group protein DSP1 (DSP1)—that showed significant ($p < 0.05$) changes under single-gene response assessment. Samples are colored according to treatment group (control = blue, heatwave = red) and arrows represent the loadings of individual genes, with longer arrows indicating stronger contributions to the corresponding principal components. HSP90 is strongly associated with PC1, while HMGB1, PPCTI, and DSP1 are associated with PC2.

Chapter 3. Simulated heatwave and hypoxic event alter gene expression in the Pacific oyster (*Crassostrea gigas*): potential monitoring and mitigation strategies for summer mortality

3.1 Introduction

The world's oceans are rapidly transforming under climate change, threatening the stability of marine ecosystems and their associated services (Intergovernmental Panel On Climate Change (IPCC), 2022). While research has historically prioritized understanding long-term effects such as gradual warming and acidification, it is now understood that acute climatic events that occur on the scale of days to weeks can have significant impacts on marine organisms and ecosystems (Oliver et al., 2019; White et al., 2023). Extreme events such as marine heatwaves and coastal hypoxic events are increasing in both duration and frequency due to climate change (IPCC, 2022). Those acute stressors have led to a range of detrimental effects on marine ecosystem services, triggering downstream socioeconomic consequences (Smith et al., 2021). Most notably, global aquaculture has been severely affected by acute climate stressors causing a historic rise in incidents of mass mortality, especially for shellfish, resulting in major financial losses (The State of World Fisheries and Aquaculture 2024, 2024). For example, marine heatwaves have been implicated in mass mortalities of shellfish around the globe with subsequent economic losses estimated in the USD billions (Smith et al., 2021). Similarly, coastal hypoxic events caused by eutrophication and elevated temperatures have also driven mass mortalities in recent years (Maar et al., 2021; Sone et al., 2023). Despite industry challenges due to climate change, shellfish farming remains one of the fastest-growing sectors in global aquaculture, underscoring the urgent need for adaptation measures to combat climate impacts

(The State of World Fisheries and Aquaculture 2024, 2024). Consequently, research supporting thermal and hypoxia stress monitoring and mitigation strategies to reduce mass mortality are essential for sustaining coastal economies and ensuring global food security.

The Pacific oyster (*Crassostrea gigas*) is the most widely cultivated oyster species in the world and has been uniquely affected by summer mortality syndrome (Petton et al., 2021). Pacific oyster summer mortality has been an industry challenge for decades and has been observed in nearly every region where the species is farmed, including North America, Europe, Asia, and Australia (Cowan et al., 2023, 2024; Go et al., 2017; King et al., 2019; Malham et al., 2009; B. Yang et al., 2021; X. Zhang et al., 2023). Reported mortality rates at commercial farms can range from 20 to 100% (Cowan et al. 2023) and thus this phenomenon continues to threaten the stability of the oyster aquaculture industry. Summer mortality syndrome is typically driven by anomalously warm water conditions, especially those exceeding 20°C (Garnier et al., 2007; Green et al., 2019). As such, there is a growing understanding that marine heatwaves contribute significantly to Pacific oyster summer mortality (Cowan et al., 2024; Green et al., 2019; Siboni et al., 2024). Marine heatwaves have been implicated in Pacific oyster mortality events in both Australia and Asia (Heo et al., 2023; Whittington et al., 2024), as well as being identified as an emerging problem in British Columbia (BC), Canada (Cowan et al., 2023, 2024; Mackenzie et al., 2024), despite historically low mortality being reported in the region (Quayle, 1988). The increased frequency of marine heatwaves has also coincided with heightened mortality events in the last 15 years (Oliver et al., 2018; Petton et al., 2021). As marine heatwaves are projected to become more frequent and intense over the next century (IPCC, 2022; Oliver et al., 2019), understanding the role of those acute thermal stressors in Pacific oyster summer mortality is

critical to developing monitoring tools and mitigating the impact of climate change on shellfish aquaculture.

While marine heatwaves are clearly associated with increased Pacific oyster summer mortality, mortality events are likely not caused by thermal stress alone. Rather, a complex interaction of environmental stressors and opportunistic pathogens are hypothesized to drive mortality (Cowan et al., 2023; Garnier et al., 2007; Go et al., 2017; Wendling & Wegner, 2013). Summer mortality is usually observed at water temperatures exceeding 20°C, yet Pacific oysters routinely survive acute thermal stress conditions above 40°C (Hamdoun et al., 2003; Lim et al., 2016). However, water temperatures above 20°C do trigger physiological responses that increase vulnerability to pathogenic infection (Malham et al., 2009). In particular, gametogenesis, spawning, and increases in metabolism are all induced by elevated temperatures, energetically costly processes that divert resources away from immunity (Delaporte et al., 2006; Y. Li et al., 2007, 2009; Wendling & Wegner, 2013). In addition, both the growth and virulence of pathogenic bacteria increase under higher temperatures (Kimes et al., 2012; Vezzulli et al., 2012), creating ideal conditions for outbreaks of disease. Thus, mass mortalities of Pacific oysters driven by infection with pathogenetic bacteria almost always coincide with periods of high temperature (Cowan et al., 2024; Siboni et al., 2024; Wendling & Wegner, 2013; B. Yang et al., 2021). The relationship between heatwaves and disease outbreaks in Pacific oysters has been supported by several laboratory studies, which have demonstrated that elevated water temperatures alter both pathogen abundance and exacerbate mortality of infected individuals (Green et al., 2019; X. Li et al., 2023; Siboni et al., 2024). Accordingly, summer mortality syndrome has been difficult to replicate with laboratory-simulated heatwaves alone (Chaney & Gracey, 2011; De Lorgeril et al., 2011), likely because of the absence of pathogenic bacteria in

those settings (Green et al., 2019). Therefore, monitoring practices for summer mortality that only account for thermal stress may be incomplete.

In addition to thermal stress and bacterial infection, oxygen limitation likely contributes to the summer mortality phenomenon (Cowan et al., 2023; Sussarellu et al., 2010). As intertidal organisms, Pacific oysters are relatively adaptable to hypoxia, typically defined as $< 2 \text{ mg O}_2 \text{ L}^{-1}$ (Vaquer-Sunyer & Duarte, 2008), and can optimize metabolic rate in response to low oxygen (Sussarellu et al., 2013; G. Zhang et al., 2016). The oxygen critical point threshold, at which Pacific oysters switch to anaerobic metabolism, is $\sim 3 \text{ mg O}_2 \text{ L}^{-1}$ between 15 and 25°C (Le Moullac et al., 2007). Despite this, levels of dissolved oxygen (DO) of $\sim 4 \text{ mg O}_2 \text{ L}^{-1}$ have been demonstrated to coincide with summer mortality (Cowan et al., 2023). Oxygen limitation driven by harmful algal blooms (HABs) has also been directly implicated in a number of oyster mortality outbreaks (Coffin et al., 2021; Soletchnik et al., 2007; Whittington et al., 2024). As coastal hypoxic events are forecast to increase in frequency in tandem with marine heatwaves, the potential for those acute stressor events to coincide is likely to increase over the next century (IPCC, 2022). More notably however, marine heatwaves and hypoxic events are expected to coincide as hypoxia is inexorably linked to elevated water temperatures. Marine heatwaves can directly drive hypoxic events by reducing the capacity for seawater to retain DO as temperature increases (C. Li et al., 2024; Shunk et al., 2024). Marine heatwaves also intensify stratification, preventing oxygen from mixing between surface and deeper waters, creating localized hypoxic zones (Breitburg et al., 2018). Given the relationship between heatwaves and hypoxia, those coinciding stressors may have compounding effects that exacerbate outbreaks of mortality. For example, thermal stress and hypoxia induce metabolic shifts in Pacific oysters that may trigger physiological stress (Bruhns et al., 2023; Chaney & Gracey, 2011; Le Moullac et al., 2007).

Hypoxic conditions also weaken immune response in oysters (Barnett et al., 2020; David et al., 2005) and may lower thermal tolerance (Bruhns et al., 2023), exacerbating the effects of heatwaves and increasing vulnerability to pathogenic infections that drive mortality. However, it remains unclear to what extent oxygen limitation contributes to summer mortality events. Therefore, direct investigation is necessary to inform reliable monitoring and mitigation practises.

Characterizing molecular responses to heatwaves and hypoxia is crucial for identifying resilient oyster strains and developing molecular biomarkers for summer mortality monitoring. As sessile invertebrates, oysters are unable to avoid the fluctuations in temperature and air exposure characteristic of intertidal emersion phases. Thus, oysters have a multitude of molecular adaptations to contend with both thermal stress and oxygen limitation, many of which act as useful biomarkers. For example, heat shock protein 70 (HSP70), a molecular chaperone protein, is abundant and highly expressed in the Pacific oyster compared to other invertebrates (G. Zhang et al., 2016). Detectable upregulation of HSP70 during acute heat stress (30–50°C) is well documented in the species (Farcy et al., 2009; Kim et al., 2017; Lim et al., 2016; C. Yang et al., 2017; C.-Y. Yang et al., 2016), but its expression has been demonstrated to respond to a variety of stressors, including hypoxia (Liu et al., 2022; Patterson et al., 2014). For that reason, HSP70 is routinely used as a general biomarker in environmental monitoring (Mukhopadhyay et al., 2003; Sørensen et al., 2003) and has been of interest for genetic intervention to improve thermal tolerance (Hamdoun et al., 2003; Liu et al., 2022; Valenzuela Castillo et al., 2019). Similarly, hypoxia inducible factor (HIF), a transcription factor involved in responses to both low oxygen and thermal stress, has been proposed as a biomarker for hypoxia stress in the Pacific oyster (Fu et al., 2023; Kawabe & Yokoyama, 2012; Patterson et al., 2014). However, it

remains unclear whether these stress biomarkers may inform biomonitoring of Pacific oyster summer mortality, given that mortality occurs at relatively low temperatures and the role of hypoxia remains unclear. Therefore, there is an immediate need to identify biomarkers that show detectably altered expression under specific environmental conditions that permit summer mortality such that mortality events could be predicted and mitigation measures initiated.

Unfortunately, effective mitigation strategies for summer mortality in Pacific oysters remain limited. Current mitigation approaches involve preventative alterations in farming practises such as management of stocking density (Cowan et al., 2024), as well as intertidal growout prior to deep-water culture to confer some resilience to summer mortality (Mackenzie et al., 2024). Selective breeding for heat-tolerant and disease-resistant strains of oyster is also a promising measure to reduce the extent of summer mortality (Liu et al., 2022; Sae-Lim et al., 2017). Reactive interventions that could take advantage of early stress detection by biomarkers are currently limited to alternative site transplantation and the use of shading structures over oyster beds (Evans & Hofmann, 2012). However, further investigation into the effects of oxygen limitation on summer mortality may reveal a potential mitigation strategy in the form of artificial aeration. Artificial aeration systems are widely used in finfish aquaculture during low DO conditions (especially as a result of HABs) as they circulate surface waters, increasing contact at the air-water interface and thus, raising DO (Roy et al., 2021). In cage aquaculture, aeration also drives the upwelling of deep colder water to the surface, lowering temperatures and increasing DO solubility (Burke et al., 2022). Thus, aeration is currently used in finfish aquaculture as a loss mitigation strategy during periods of high temperature and limited oxygen driven primarily by HABs (Berillis et al., 2016; Lan et al., 2024; Lebel et al., 2016; Siddique et al., 2022). Given that hyperoxia has been demonstrated to expand thermal tolerance limits in bivalves (H. O. Pörtner et

al., 2006), artificial aeration of shellfish may similarly confer some resilience to outbreaks of mortality (Srisunont et al., 2022).

The overarching goals of this study are to contribute to the development of genetically-based mortality monitoring tools for Pacific oyster summer mortality and to assess the potential for artificial aeration to act as a mitigation strategy. We subjected farmed Pacific oysters to laboratory-simulated heatwave and hypoxic conditions, utilizing the presence or absence of artificial aeration to simulate different oxidic levels. We assessed changes in gene expression, condition index, and mortality, using differences in the expression of candidate genes to compare the effects of a simulated heatwave with and without hypoxia. Finally, we assessed the potential for artificial aeration to act as a mitigation strategy for Pacific oyster summer mortality, based on the effect of oxygen limitation on stress response. Those outputs will inform comprehensive vulnerability assessments for Pacific oysters and contribute to summer mortality mitigation strategies, supporting the adaptation of shellfish aquaculture to the impacts of climate change.

3.2 Materials and methods

3.2.1 Oyster collection and acclimation

Adult Pacific oysters (N = 300) were collected from a commercial oyster farm in Baynes Sound, BC, on February 28, 2023. They were transported dry in coolers to the Pacific Biological Station in Nanaimo, BC, a trip that took approximately 1 h. Upon arrival, all oysters were cleaned of biofouling using a shucking knife and rinsed with ambient seawater, after which 240 individuals were haphazardly selected for experimentation. Ten oysters were placed haphazardly into each of 24 black-plastic mesh (diameter: 30 cm, height: 8 cm) baskets, which were

suspended within plastic buckets (volume: 20 L, diameter: 30 cm, height: 24 cm) filled with ~20 L of static cartridge-filtered (20 μ M) seawater. The buckets were arranged in blocks of six within four shallow fiberglass tanks (length x width x height: 122 x 91 x 30 cm) containing circulating filtered (20 μ M) seawater. Temperatures in the water baths were regulated and maintained using in-tank heaters, chilling coils, and circulation pumps, while DO levels were sustained with individual air stones in each bucket. The oysters underwent a two-week pre-experimental acclimation period, during which water temperatures were gradually increased from the collection site temperature (~4–6°C) to the experimental control temperature (16°C) at a rate of 2°C per day. To simulate summer conditions, the oysters were then held at the experimental control temperature (16°C) for an additional 8 d before the experiment began. Throughout this period, oysters were fed daily with a cultured phytoplankton mixture (60% *Tisochrysis lutea* and 40% *Chaetoceros mulleri*, by cell volume) at a concentration of ~4–8 million cells mL⁻¹. Daily water changes (~50% volume) were performed for all buckets using cartridge-filtered (20 μ M) seawater heated to 16°C.

3.2.2 Experimental conditions

After the acclimation period, feeding was halted to prevent potential metabolic changes from interfering with the genomic stress response (C.-Y. Yang et al., 2016). A 10-d heatwave event was then simulated, with seawater temperatures in 12 buckets incrementally raised from 16 to 26°C at a rate of 1°C per day, while the remaining 12 buckets were maintained at a constant control temperature of 16°C. The rate of temperature increase, duration, and maximum temperature in the heatwave treatment was consistent with conditions observed during a July 2021 heatwave in BC, during which commercial oyster float bags in Baynes Sound experienced

sea surface temperature (SST) increases from 16 to 28°C over 7 d, coinciding with several recorded shellfish mortality events (Mackenzie et al., 2024). Therefore, experimental conditions were environmentally relevant to regional summer heatwaves that have previously induced Pacific oyster mortality. Temperature in the control tanks was consistent with the average summer seawater temperature recorded in Baynes Sound (Mackenzie et al., 2024). As during the acclimation period, water temperatures were regulated and maintained using in-tank heaters, chilling coils, and circulation pumps. Additionally, air stones were removed from 6 tanks in the heatwave treatment, and 6 tanks in the control to simulate hypoxic conditions and assess the effect of artificial aeration on heatwave-induced changes in gene expression. The removal of air stones replicated static water conditions and induced a mild reduction in DO to $\sim 4 \text{ mg O}_2 \text{ L}^{-1}$, consistent with environmental conditions associated with previous summer mortality events (Cowan et al., 2023). Simulated heatwave and hypoxic conditions were applied in a fully crossed design, resulting in four distinct treatment groups: control (16°C with an air stone), heatwave only, hypoxia only, and heatwave plus hypoxia. Daily water changes of the buckets were carried out as described during the acclimation period.

3.2.3 Experimental monitoring

Seawater temperatures in the tanks were monitored using temperature loggers (HOBO TidbiT, Onset Computer Corporation, Bourne, Massachusetts, USA) set to record every 10 min. Additionally, temperature, salinity, DO, and pH were measured in each bucket twice daily—once before and once after water changes—using a YSI multi-probe (YSI Incorporated, Yellow Springs, Ohio, USA). Oysters were observed daily for physical signs of stress, such as a lack of

startle response, gaping shells, or no reaction to touch. Instances of mortality and visible signs of stress were documented, and any deceased oysters were removed during the experiment.

3.2.4 Oyster sampling

Before the heatwave started (T0), one oyster was haphazardly sampled from 6 haphazardly chosen buckets for baseline measurement of gene expression. Once the heatwave began, one haphazardly chosen oyster from each bucket was sampled (N = 24; n = 6 per treatment) at five timepoints (days 2, 4, 6, 8, and 10 (T1–T5)), which corresponded to temperatures of 18, 20, 22, 24, and 26°C for the heatwave groups. Wet weight and shell height were measured for all sampled individuals using digital calipers and a digital balance, respectively. Oysters were then opened using a sterile shucking knife and ~0.03 g of gill tissue excised using sterile dissection scissors. The tissue samples were placed individually in labelled 2-mL tubes and stored at -80°C. At T0, six individuals were haphazardly sampled across all 24 buckets for baseline measurement of condition index (see Section 3.2.5). Then on day 8 of the experiment (T4), six oysters were haphazardly sampled from each bucket across the four treatments (N = 24; n = 6) to assess changes in condition index during the experiment. All sampled individuals were immediately frozen at -80°C for subsequent processing.

3.2.5 Condition index

Oysters sampled for condition index were thawed at room temperature and opened with a sterile shucking knife. The shell and soft tissues were then dried at 60°C for 7 d, until constant weight. The dry weight of both the soft tissue and the shell was measured for all sampled oysters using a digital balance, and condition index (CI) was calculated as: $CI = (P1 \times 100) / P2$, where

P1 is the dry weight (g) of the soft tissues and P2 is the dry weight (g) of the shell (Rainier & Mann, 1992). A one-way analysis of variance (ANOVA) was performed to evaluate differences in CI between treatment groups, with CI as the response variable and treatment as the factor. The data were tested for normality using the Shapiro-Wilk test and for homogeneity of variance using Levene's test. Outliers were identified using the Z-score method and removed if more than three standard deviations from the mean.

3.2.6 RNA extraction and purification

Total RNA was extracted from each gill tissue sample for gene expression analysis using an RNeasy[®] Mini Kit (QIAGEN, Hilden, Germany). First, gill tissue samples were placed in lysing matrix tubes (MPbio, Santa Ana, California, USA) with 600 μ L of RLT lysis buffer containing guanidine isothiocyanate and β -mercaptoethanol (β -ME) and homogenised using a TissueLyser II bead mill homogenizer (QIAGEN) at 25.0 Hz for 2 min. The resulting homogenate was then centrifuged at $\geq 10,000 \times g$ for 3 min before extracting total RNA according to the QIAGEN RNeasy[®] Mini Kit instructions. For each sample, the supernatant was transferred into a 2-mL tube, mixed with 600 μ L of 70% ethanol and transferred to a RNeasy[®] spin column before centrifuging for 15 s at 8000 $\times g$. The resulting precipitant was run through a series of washes with RNeasy[®] Mini Kit buffers RW1 and RPE (QIAGEN) to remove contaminants such as proteins, salts, and other impurities from the nucleic acids. After those washes, the RNeasy spin column was placed in a new 2-mL collection tube and centrifuged at $\geq 10,000 \times g$ for 1 min to dry the sample and remove any carryover buffer. Finally, the RNeasy spin column was placed in a new 2-mL tube and 50 μ L of RNase-free dH₂O were added directly to the spin column membrane. This was then centrifuged for 1 min at 8000 $\times g$ to elute the RNA.

The preliminary amount and quality of RNA were recorded before purification using a Nanodrop spectrophotometer.

A TURBO DNA-free Kit (Thermo Fisher Scientific, Waltham, Massachusetts, USA) was then used to purify the resulting RNA. According to kit instructions, the procedure for DNA decontamination was dependent on the concentration of nucleic acid in the sample. For all samples $\leq 400 \text{ ng mL}^{-1}$, 5 μL 10X TURBO DNase buffer and 1 μL of TURBO DNase Enzyme were added to the RNA. For any samples $\geq 400 \text{ ng mL}^{-1}$, half of the RNA elution was added into a new 2-mL tube and 2.5 μL of 10X TURBO DNase buffer and 2 μL of TURBO DNase Enzyme were added. All samples were then incubated at 37°C for 30 min to remove DNA contamination from RNA samples. Following incubation, 6 μL of DNase inactivation reagent were added for 5 min at room temperature to stop the enzymatic activity of the TURBO DNase. The samples were then centrifuged for 2 min at 10,000 x g and the supernatant containing the purified RNA transferred to 2-mL collection tubes. Following DNA decontamination, the final amount and quality of nucleic acid in each sample were recorded using a Nanodrop spectrophotometer and samples were stored at -80°C.

3.2.7 cDNA synthesis

Total RNA from the resulting samples was reverse transcribed using a Bio-Rad (Hercules, California, USA) iScript Select cDNA Synthesis Kit. First, all samples were diluted to 100 $\text{ng } \mu\text{L}^{-1}$ using RNase-free dH₂O. Then, each diluted sample was combined with 5 μL of RNA template, 1.5 μL of RNase-free dH₂O, 2 μL of 5x iScript Select Reaction Mix, 0.5 μL of iScript Reverse Transcriptase, and 1 μL of random primer mix in the wells of a 12-well PCR strip. Those samples were incubated at 25°C for 5 min, 42°C for 30 min, 85°C for 5 min, and 12°C for

5 min according to kit instructions. The resulting cDNA was stored at -20°C in labelled 12-well PCR strips for future gene expression analysis.

3.2.8 RNA sequencing and analysis

cDNA from each treatment and timepoint in the experiment was pooled and sent to the Canadian Centre for Computational Genomics (C3G) at McGill University, where differently expressed genes (DEGs) were identified using next-generation sequencing. Procedures for RNA-Seq analysis were conducted according to the GenPipes workflow framework developed by C3G (Bourgey et al., 2019). First, FASTQ raw reads were obtained using paired-end sequencing on Illumina NovaSeq. R (Version 4.3.2) with RStudio (Version 2024.09.1) was then used to analyze the resulting data. Adaptor sequences and low-quality base calls (Phred score < 30) were trimmed from the reads using Trimmomatic (Bolger et al., 2014). The resulting reads were mapped to the reference genome of *C. gigas* (Peñaloza et al., 2021) using STAR (Dobin et al., 2013) and read counts were obtained using HTSeq (Anders et al., 2015). Counts generated by HTSeq were analyzed using the DESeq2 package (Love et al., 2014) to identify differences in expression levels across timepoints and treatments using negative binomial GLM fitting and Wald statistics. Then, the ashR package (Stephens, 2016) was used to shrink Log2FoldChange (Log2FC) values in the gene expression data. Since samples were pooled for each timepoint, significance was established by modeling the relationship between mean expression and dispersion across all genes, not by using group variability based on replicates. Thus, Log2FC values in the present study represent solely exploratory indicators for further qPCR investigation. Tidyverse (Wickham et al., 2019) and pheatmap (Raivo Kolde, 2010) packages were used for data manipulation and visualization.

3.2.9 Candidate gene selection

A subset of genes showing differential expression in the RNAseq analysis was selected for further investigation via qPCR verification. Given that the major objectives of this study were to identify potential biomarkers for summer mortality and assess the potential for artificial aeration to alleviate heatwave-driven stress response, several criteria were considered when choosing genes for further investigation. First, genes that were significantly differentially expressed at multiple time points during the experiment, particularly after the 20°C threshold (which is typically associated with summer mortality), were prioritized. That approach was intended to focus on genes whose expression was most likely to be applicable to summer mortality monitoring upon more detailed analysis. Additionally, genes with known functional products or those whose products could be confidently inferred were given preference. Specifically, genes whose products have been established as biomarkers for stress, even if not significantly differentially expressed at multiple time points during the experiment, were also examined. This was done to evaluate the potential of these genes as biomarkers for summer mortality and to gain insight into the physiological state of oysters exposed to simulated heatwave and hypoxic conditions, potentially revealing differences in stress response under artificial aeration.

Based on those criteria, 10 genes of interest (GOIs) were selected for further investigation through qPCR verification. This included five with known products and five whose products could be inferred through shared homology. Gene products were identified using the Ensembl Metazoa and UniProt Knowledgebase (UniProtKB) databases, as well as the National Center for Biotechnology Information Basic Local Alignment Search Tool (NCBI BLAST) program. Using

the Ensembl Metazoa transcript IDs for each gene, orthologues were examined, and FASTA sequences for the Ensembl canonical transcript were generated. The canonical transcript is the one chosen by Ensembl Metazoa as the most representative for a gene, and it is also represented in both NCBI and UniProtKB. That transcript is typically the most conserved, highly expressed, and has the longest coding sequence. The UniProtKB/TrEMBL database, which derives protein sequences by computationally translating coding sequences, was then used to predict the likely protein product for each gene. Genes with associated proteins supported by transcript-level evidence, such as previously published cDNA(s), RT-PCR, or Northern blots, were considered to have known functions. Those genes included high mobility group box 1 (HMGB1), high mobility group protein DSP1 (DSP1), heat shock protein 20 (HSP20), heat shock protein 70 B2 (HSP70), and heat shock protein 90 (HSP90). For genes with associated proteins inferred from homology with orthologues in closely related species or predicted by computational annotation, FASTA sequences were cross-referenced with the NCBI BLAST program to determine the most likely protein product based on the results of both queries. Sequences from *C. gigas* with higher query coverage, higher percent identity, and E-values of 0, which matched the descriptions predicted by UniProtKB, were chosen as the most likely gene product. Those genes were considered to have inferred functions and included death-associated inhibitor of apoptosis 2 (A2I), heterogeneous nuclear ribonucleoprotein (HNR), peptidyl-prolyl cis-trans isomerase (PPCTI), stress-induced protein 1 (SIP1), and x-box-binding protein 1 (XBP1).

3.2.10 Primer design

Once the function of each gene product could be determined or inferred, primers for qPCR verification of differential expression were designed. First, FASTA sequences for the

cDNA of each GOI from Ensembl Metazoa were obtained using sequences for the Ensembl canonical transcript. Those sequences were then inputted into the NCBI Primer Blast tool to design primer pairs for each GOI. Primer sequences for the reference genes actin (Farcy et al., 2007) and elongation factor 1-alpha (EF1- α) (De Lorgeril et al., 2011) were obtained from previous studies (Farcy et al., 2009; Green & Montagnani, 2013). All primers were between 18 and 21 nucleotides long, had melting temperatures between 58 and 62°C with no more than 3°C difference between the pair, had GC content between 40 and 60%, and total self-complementarity ≤ 4 and 3' self-complementarity ≤ 2 . All amplicon sizes were between 80 and 150 base pairs. Primer sequences and their associated gene IDs are provided in Table 3.1. Generated primer sequences were sent to Integrated DNA Technologies (IDT, Coralville, Iowa, USA), who manufactured custom 100-nm DNA oligos purified according to standard desalting. Those primers were delivered dry and made up to a 100 μ M working solution using Invitrogen UltraPure distilled water (Thermo Fisher Scientific). RNAase-free dH₂O was then used to dilute the working solution to 10 μ M. A standard curve method was used to test the efficacy of those primers. First, 20 cDNA samples were haphazardly chosen and 20 μ L from each were pooled to a total of 400 μ L. A range of dilutions (1–1/1000 x volume) were then prepared using RNase-free dH₂O and the quantification cycle (Cq) as a function of the log starting RNA concentration was plotted. Primer pairs that showed efficiency levels between 90 and 110% for each of the four orders of magnitude were accepted.

3.2.11 qPCR verification

All qPCR reactions were performed in a Bio-Rad CFX Opus 96 Real-Time PCR System using Bio-Rad CFX Maestro 2.3 version 5.3.022.1030 software. All reactions were conducted in

96-well PCR plates with loaded reactions in duplicate to ensure quality reading for each sample. Total reaction volume for each well was 10 μ L containing 5 μ L of SsoAdvanced Universal SYBR[®] Green Supermix (Bio-Rad), 0.5 μ L of forward primer, 0.5 μ L of reverse primer, and 4 μ L of cDNA template. Amplification conditions were 1 cycle of 2 min at 95°C, 39 cycles of 10 s at 95°C, and 1 cycle of 30 s at 60°C. This was followed by a melting curve analysis, raising the temperature from 65 to 95°C in 0.5°C increments at 2–5 s per step. C_q values were calculated from fluorescence readings as the cycle where a signal above the defined background fluorescence could be detected. C_q value is dependent on the starting amount of cDNA and thus can be used to quantify the amount of reverse transcribed mRNA for each target in each sample to calculate relative expression. As two reactions were conducted for each target sequence and cDNA sample, the mean C_q value between both reactions was calculated for all samples and those values were used for all further analysis. The relative expression of each GOI was then calculated by normalizing C_q values to expression of a reference gene. C_q values were calculated for two reference genes, actin and EF1- α , and the stabilities of both genes were evaluated using the RefFinder tool (Xie et al., 2023). Actin was determined to be the more stable reference gene between the two and therefore its expression was utilized for all further calculations. Relative expression for each target and sample was calculated using the ΔC_q method, where relative expression = $2^{\Delta C_q}$ and $\Delta C_q = (C_{q \text{ actin}} - C_{q \text{ target}})$. That formula converts the difference in C_q values into a fold change measure of relative expression by assuming each reaction cycle doubles qPCR product.

3.2.12 qPCR statistical analysis

All statistical analyses and visualizations of relative expression data were performed using R (Version 4.4.2) and RStudio (Version 2024.12.0). Key packages included tidyverse (Wickham et al., 2019) and pheatmap (Raivo Kolde, 2010) for data manipulation and visualization. Based on the preliminary RNAseq analysis, very few DEGs were detected in the hypoxia only group. Therefore, we omitted these samples from the rest of the analysis and focussed exclusively on qPCR verification for the DEGs in the heatwave and heatwave + hypoxia treatments. Thus, for single-gene responses, a two-way analysis of variance (ANOVA) for each GOI was performed, with relative expression as the response variable and treatment (control, heatwave, or heatwave + hypoxia), timepoint, and their interaction as factors. The data were assessed for normality using a Shapiro-Wilk test and for homogeneity of variance using a Levene's test. A post-hoc Student-Newman-Keuls (SNK) test was performed for each ANOVA to determine which timepoints during the heatwave showed significant differences in relative expression, including the control (16°C). Additionally, separate linear models were run to examine the effect of temperature on relative expression of each GOI.

To assess the effect of the simulated heatwave and presence of aeration on relative expression of all 10 selected GOIs, a permutational multivariate analysis of variance (PERMANOVA) was conducted using the vegan package (Oksanen et al., 2001). Bray-Curtis dissimilarity indices were calculated using the vegdist function, and the resulting distance matrix was analyzed using the adonis2 function to assess the effects of treatment, temperature, and their interaction on relative expression. The assumption of homogeneity of multivariate dispersion was tested using the betadisper function to calculate dispersions, followed by the aov function for comparison across groups. A Bonferroni-corrected post-hoc pairwise PERMANOVA was then conducted using the pairwise.adonis function in the pairwiseAdonis package. This was done

to determine which timepoints during the heatwave showed significant differences in relative expression, including to the control (16°C).

Further multivariate analyses were conducted for only the GOIs that showed significant responses in the single-gene response models. An additional PERMANOVA was conducted on this subset of GOIs to assess multivariate differences, as described above. Similarly, a post-hoc pairwise PERMANOVA test (Bonferroni-corrected) was conducted to compare differences in relative expression at each timepoint during the heatwave for this subset of genes. A SIMPER (Similarity Percentage Analysis) analysis was then conducted to identify which genes were the primary contributors to relative expression differences between the simulated heatwave and control (16°C) and at each timepoint during the simulated heatwave. Finally, a principal component analysis (PCA) was performed on this subset of GOIs using the `prcomp` function. This was done to visualize clustering of relative expression patterns and to identify GOIs that contribute most to differences in relative expression between treatments.

3.3 Results

3.3.1 Experimental monitoring

At the start of the simulated heatwave (T0), mean water temperature was 15.3 ± 0.1 , 15.6 ± 0.1 , 15.5 ± 0.1 , and $15.6 \pm 0.02^\circ\text{C}$ for tanks in the control, heatwave, hypoxia, and heatwave + hypoxia groups, respectively. From days 2 to 10 of the simulated heatwave (T1 – T5), mean water temperatures for control and hypoxia tanks were $15.4 \pm 0.2^\circ\text{C}$ and $15.6 \pm 0.04^\circ\text{C}$, respectively. In the heatwave group, mean water temperatures were $17.8 \pm 0.1^\circ\text{C}$ on day 2 (T1; 18°C), $19.6 \pm 0.1^\circ\text{C}$ on day 4 (T2; 20°C), $21.9 \pm 0.5^\circ\text{C}$ on day 6 (T3; 22°C), $23.5 \pm 0.2^\circ\text{C}$ on day

8 (T4; 24°C), and $25.6 \pm 0.1^\circ\text{C}$ on day 10 (T5; 26°C). In the heatwave + hypoxia group, mean water temperatures were $17.8 \pm 0.1^\circ\text{C}$ on day 2 (T1; 18°C), $19.7 \pm 0.1^\circ\text{C}$ on day 4 (T2; 20°C), $21.9 \pm 0.5^\circ\text{C}$ on day 6 (T3; 22°C), $23.7 \pm 0.4^\circ\text{C}$ on day 8 (T4; 24°C), and $25.6 \pm 0.1^\circ\text{C}$ on day 10 (T5; 26°C).

Over the 10-d experimental period, mean DO was 7.6 ± 0.4 , 6.6 ± 0.7 , 4.8 ± 1.1 , and 3.9 ± 1.4 mg O₂ L⁻¹ for the control, heatwave, hypoxia, and heatwave + hypoxia treatments, respectively. Over the same period, mean salinity was 29.9 ± 0.2 , 29.9 ± 0.3 , 29.9 ± 0.2 , and 30.0 ± 0.2 ppt and mean pH was 7.8 ± 0.2 , 7.6 ± 0.2 , 7.0 ± 0.3 , and 6.9 ± 0.4 , respectively. Only one mortality was recorded, in the heatwave + hypoxia group on day 10 of the simulated heatwave. No other physical signs of stress (lack of startle response, gaping shell, lack of response to touch) were noted.

3.3.2 Condition index

Mean baseline shell length, wet weight, and condition index (CI) for all sampled individuals was 67.1 ± 4.5 mm, 37.6 ± 7.0 g, and 63.3 ± 10.8 , respectively. On day 8 of the simulated heatwave, mean CI was 53.1 ± 10.6 , 58.7 ± 9.1 , 50.2 ± 7.4 , and 47.8 ± 12.2 for the control (16°C), heatwave (24°C), hypoxia (16°C), and heatwave + hypoxia (24°C) groups, respectively. No significant effect of treatment (one-way ANOVA, $F_{(3,20)} = 1.331$, $p = 0.292$) on CI was observed.

3.3.3 RNA sequencing

Differently expressed genes (DEGs) were seen at all five timepoints during the simulated heatwave for heatwave, hypoxia, and heatwave + hypoxia treatments, where Log₂ fold change

(Log2FC) values were significantly different ($p_{adj} < 0.05$) compared to the control. However, only 22 DEGs were detected in the hypoxia group, none of which were differently expressed at multiple timepoints during the experiment or in the other treatment groups. Therefore, we omitted these samples from the rest of the analysis and focussed exclusively on qPCR verification for the DEGs in the heatwave and heatwave + hypoxia treatments. In both heatwave and heatwave + hypoxia groups, the number of DEGs generally increased at each timepoint as temperature increased with, a dip on day 6 (22°C) (Table 3.2). More DEGs were detected in the heatwave + hypoxia group than the heatwave group at every timepoint during the experiment. On day 10, 45 DEGs were detected in the heatwave group comprising 35 downregulated and 10 upregulated genes (Figure 3.1), while 133 DEGs were observed in the heatwave + hypoxia group comprising 81 downregulated and 52 upregulated genes (Figure 3.2).

A subset of 10 GOIs that were differentially expressed at multiple timepoints during the experiment in both the heatwave and heatwave + hypoxia groups were chosen for further investigation via real time quantitative PCR (qPCR) verification. Those genes were death-associated inhibitor of apoptosis 2 (A2I), high mobility group box 1 (HMGB1), high mobility group protein DSP1 (DSP1), heat shock protein 20 (HSP20), heat shock protein 70 B2 (HSP70), heat shock protein 90 (HSP90), heterogeneous nuclear ribonucleoprotein (HNR), peptidyl-prolyl cis-trans isomerase (PPCTI), stress-induced protein 1 (SIP1), and x-box-binding protein 1 (XBP1) (Table 3.1). RNAseq showed downregulation of DSP1, HMGB1, HNR, and PPCTI during the experiment. In the heatwave only treatment, DSP1 was downregulated on day 6 and 8, HMGB1 was downregulated on day 8 and 10, HNR was downregulated on day 8, and PPCTI was downregulated on day 4, 6, 8 and 10 (Figure 3.3). In the heatwave + hypoxia treatment, DSP1 was downregulated on day 4, 6, 8 and 10, HMGB1 was downregulated on day 4, 8 and 10,

HNR was downregulated on day 10, and PPCTI was downregulated on day 6, 8 and 10. A2I and XBP1 were both upregulated during the experiment based on the RNAseq results. In the heatwave only treatment, A2I was upregulated on day 10 and XBP1 was also upregulated on day 10 (Figure 3.3). In the heatwave + hypoxia treatment, A2I was upregulated on day 10 and XBP1 was upregulated on day 8 and 10 (Figure 3.4). HSP20, HSP70, HSP90 and SIP1 did not show significant changes in expression at any point during the experiment based on the results of RNAseq.

3.3.4 qPCR single-gene responses

Single-gene responses were assessed by ANOVA with the result that five of the 10 GOIs showed relative expression ($2^{\Delta Cq}$) patterns under simulated heatwave and hypoxia conditions that were significantly different from the control. Those genes were A2I, DSP1, HMGB1, HSP90, and PPCTI (Figure 3.5). Three genes—DSP1, HMGB1, and PPCTI—were significantly downregulated in the heatwave and heatwave + hypoxia treatments compared to the control. First, relative expression of DSP1 was significantly affected by treatment (two-way ANOVA, $F_{(2,76)} = 21.854$, $p < 0.001$), timepoint ($F_{(5,76)} = 6.619$, $p < 0.001$), and their interaction ($F_{(8,76)} = 3.302$, $p = 0.008$). Generally, its expression was downregulated in the heatwave and heatwave + hypoxia groups in relation to the control from days 4 to 10, but only significantly so at days 6 and 8 (Figure 3.6). Temperature had a significant effect on the relative expression of DSP1 (LM, $\beta = -0.005$, $SE = 0.001$, $t_{(90)} = -7.22$, $p < 0.001$), explaining approximately 36% of the variance ($R^2 = 0.36$). Second, the relative expression of HMGB1 was significantly affected by treatment (two-way ANOVA, $F_{(2,76)} = 6.012$, $p = 0.004$), timepoint ($F_{(5,76)} = 6.237$, $p = 0.008$), and their interaction ($F_{(8,76)} = 4.940$, $p < 0.001$). Its expression was generally downregulated in relation to

the control from days 6 to 10, but there was only one significant pairwise comparison identified (heatwave + hypoxia vs control on day 8) (Figure 3.7). Temperature also had a significant effect on relative expression of HMGB1 (LM, $\beta = -0.003$, SE = 0.0009, $t_{(90)} = -3.920$, $p < 0.001$), explaining approximately 14% of the variance ($R^2 = 0.14$). Third, the relative expression of PPCTI was also significantly affected by treatment (two-way ANOVA, $F_{(2,76)} = 15.310$, $p < 0.001$), timepoint ($F_{(5,76)} = 3.393$, $p = 0.008$), and their interaction ($F_{(8,76)} = 4.174$, $p < 0.001$). Its expression in the heatwave and heatwave + hypoxia treatments was significantly downregulated in comparison to the control on days 6, 8, and 10 (Figure 3.8). Temperature also had a significant effect on relative expression of PPCTI (LM, $\beta = -0.005$, SE = 0.001, $t_{(90)} = -4.810$, $p < 0.001$), explaining approximately 20% of the variance ($R^2 = 0.20$).

Two genes, A2I and HSP90, were significantly upregulated in the heatwave and heatwave + hypoxia treatments compared to the control. First, relative expression of A2I was significantly affected by treatment (two-way ANOVA, $F_{(2,75)} = 8.885$, $p < 0.001$), and timepoint ($F_{(5,75)} = 2.877$, $p = 0.019$), but not their interaction ($F_{(8,75)} = 1.837$, $p = 0.083$). Its expression was significantly upregulated in the heatwave and heatwave + hypoxia treatment compared to the control (Figure 3.9). In addition, relative expression of A2I was significantly affected by temperature (LM, $\beta = 0.003$, SE = 0.0008, $t_{(89)} = 3.123$, $p = 0.002$), with temperature explaining approximately 9% of the variance ($R^2 = 0.09$). Second, the relative expression of HSP90 was significantly affected by treatment (two-way ANOVA, $F_{(2,76)} = 6.205$, $p = 0.003$), timepoint ($F_{(5,76)} = 3.749$, $p = 0.004$), and their interaction ($F_{(8,76)} = 3.166$, $p = 0.004$). Its expression in the heatwave and heatwave + hypoxia treatments was significantly downregulated in comparison to the control at day 10 (Figure 3.10). The relative expression of HSP90 was significantly affected

by temperature (LM, $\beta = 0.010$, SE = 0.002, $t_{(90)} = 4.435$, $p < 0.001$), with temperature explaining approximately 17% of the variance in HSP90 relative expression ($R^2 = 0.17$).

A third gene, XBP1, was also significantly upregulated. Relative expression of XBP1 was significantly affected by treatment (two-way ANOVA, $F_{(2,76)} = 7.088$, $p = 0.002$), timepoint ($F_{(5,76)} = 2.503$, $p = 0.038$), and not by their interaction ($F_{(8,76)} = 1.829$, $p = 0.084$), but an SNK test failed to reveal any significant differences between the heatwave or heatwave + hypoxia groups and the control for any timepoint during experiment. Furthermore, temperature only explained approximately 4% of the variance ($R^2 = 0.04$) in HSP90 expression (LM, $\beta = 0.001$, SE = 0.0005, $t_{(90)} = 2.197$, $p = 0.031$).

The remaining four genes (HNR, HSP20, HSP70, and SIP1) did not show any significant differences in relative expression compared to the control. Relative expression of HNR was not significantly affected by treatment (two-way ANOVA, $F_{(2,71)} = 0.405$, $p = 0.668$) or by temperature (LM, $\beta = -0.0003$, SE = 0.0003, $t_{(85)} = -0.984$, $p = 0.328$). However, there was a significant effect of timepoint ($F_{(5,71)} = 8.946$, $p < 0.001$) and the interaction of treatment and timepoint ($F_{(8,71)} = 2.730$, $p = 0.011$), but a post-hoc SNK test revealed no significant differences between the heatwave or heatwave + hypoxia groups and the control for any timepoint during experiment. Relative expression of HSP20 was not significantly affected by treatment (two-way ANOVA, $F_{(2,76)} = 2.496$, $p = 0.089$) or the interaction of treatment and timepoint ($F_{(8,76)} = 1.079$, $p = 0.387$). However, timepoint ($F_{(5,76)} = 4.059$, $p = 0.003$) and temperature (LM, $\beta = 0.028$, SE = 0.009, $t_{(90)} = 3.246$, $p = 0.002$) did have a significant effect on relative expression of HSP20 with temperature explaining approximately 9% of the variance ($R^2 = 0.09$). Despite this, a post-hoc SNK test revealed no significant differences between the heatwave or heatwave + hypoxia groups and the control for any timepoint during the experiment (Figure 3.11). Relative

expression of HSP70 was not significantly affected by treatment (two-way ANOVA, $F_{(2,76)} = 0.323, p = 0.725$), timepoint ($F_{(5,76)} = 2.275, p = 0.055$), their interaction ($F_{(8,76)} = 0.787, p = 0.616$), or by temperature (LM, $\beta = 0.001, SE = 0.0005, t_{(90)} = 1.723, p = 0.088$) (Figure 3.12). Finally, relative expression of SIP1 was not significantly affected by treatment (two-way ANOVA, $F_{(2,76)} = 0.773, p = 0.465$), timepoint ($F_{(5,76)} = 1.238, p = 0.300$), their interaction ($F_{(8,76)} = 1.120, p = 0.360$), or by temperature (LM, $\beta = 0.0005, SE = 0.0006, t_{(90)} = 0.813, p = 0.419$).

3.3.5 qPCR multivariate response

A PERMANOVA test (Bray-Curtis dissimilarity, 999 permutations) demonstrated that relative expression of the 10 GOIs in the study was significantly affected by treatment ($F_{(2,79)} = 4.777, R^2 = 0.084, p = 0.003$) and timepoint ($F_{(5,79)} = 5.092, R^2 = 0.223, p = 0.001$). A post-hoc pairwise PERMANOVA test (Bonferroni-corrected) showed that relative expression of the 10 GOIs was significantly different from control on day 8 ($p = 0.005$) for the heatwave group and on day 6 ($p = 0.022$) and day 10 ($p = 0.001$) for the heatwave + hypoxia group. An additional PERMANOVA test (999 permutations) was conducted assessing Bray-Curtis dissimilarity for the relative expression of the five GOIs that showed significant differences in the single-gene response models (A2I, DSP1, HMGB1, HSP90, and PPCTI). The results of that PERMANOVA indicated that relative expression of those five genes was significantly affected by treatment ($F_{(2,79)} = 6.907, R^2 = 0.119, p = 0.001$) and timepoint ($F_{(5,79)} = 3.819, R^2 = 0.165, p = 0.001$). A post-hoc pairwise PERMANOVA test (Bonferroni-corrected) showed that relative expression of those five GOIs was significantly different from control on day 4 ($p = 0.011$), day 8 ($p = 0.001$), and day 10 ($p = 0.001$) for the heatwave group, and on day 6 ($p = 0.003$), day 8 ($p = 0.006$), and day 10 ($p = 0.001$) for the heatwave + hypoxia group.

A SIMPER analysis identified A2I, DSP1, HSP90, and PPCTI as the primary contributors to relative expression differences between treatment groups. In a comparison of the heatwave treatment and the control, differences in DSP1 and PPCTI relative expression accounted for the largest contribution. Lower relative expression of DSP1 and PPCTI in the heatwave treatment explained 6.2% ($p = 0.004$) and 7.2% ($p = 0.001$) of the dissimilarity, respectively. Similarly, in a comparison between the heatwave + hypoxia treatment and the control, lower DSP1 and PPCTI relative expression accounted for 6.4% ($p = 0.001$) and 6.8% ($p = 0.018$), respectively. However, differences in relative expression of HSP90 and A2I were the primary contributors to differences between the heatwave treatment and the heatwave + hypoxia treatment. Higher relative expression of HSP90 in the heatwave + hypoxia treatment accounted for 15.7% ($p = 0.048$) of the dissimilarity and higher A2I relative expression accounted for 6.1% ($p = 0.045$). No other contributions to dissimilarity were statistically significant.

An additional SIMPER analysis comparing treatment groups at each timepoint revealed that those contributions changed over the course of the experiment. Between the heatwave treatment and the control, differences in HMGB1, PPCTI, and DSP1 relative expression contributed most to dissimilarity throughout the experiment. On day 4 of the heatwave, downregulation of HMGB1, PPCTI, and DSP1 accounted for 8.6% ($p = 0.034$), 8.5% ($p = 0.041$), and 8.0% ($p = 0.028$) of the dissimilarity, respectively. Similarly on day 10 of the heatwave, downregulation of HMGB1, PPCTI, and DSP1 accounted for 9.9% ($p = 0.008$), 9.1% ($p = 0.019$), and 8.8% ($p = 0.015$) of the dissimilarity, respectively. No other contributions to dissimilarity between the heatwave treatment and control were statistically significant. In contrast, between the heatwave + hypoxia treatment and the control, differences in HMGB1, PPCTI, and DSP1 contributed most to dissimilarity earlier in the heatwave, but differences in

HSP90 contributed most to dissimilarity at higher temperatures. On day 8 of the experiment, downregulation of HMGB1, PPCTI, and DSP1 accounted for 10.3% ($p = 0.004$), 9.8% ($p = 0.019$), and 9.5% ($p = 0.006$) of the dissimilarity, respectively. However, on day 10 of the experiment, upregulation of HSP90 in the heatwave + hypoxia treatment accounted for 29.2% ($p = 0.001$) of the dissimilarity. No other contributions to dissimilarity between the heatwave + hypoxia treatment and control were statistically significant. Between the heatwave treatment and the heatwave + hypoxia treatment, differences in HMGB1 contributed most to dissimilarity earlier in the heatwave, but differences in HSP90 contributed most to dissimilarity at higher temperatures. On day 8 of the experiment, lower relative expression of HMGB1 in the heatwave + hypoxia treatment accounted for 10.4% ($p = 0.018$) of the dissimilarity. On day 10, however, higher relative expression of HSP90 in the heatwave + hypoxia treatment accounted for 32.3% ($p = 0.002$) of the dissimilarity between groups. No other contributions to dissimilarity between the heatwave and heatwave + hypoxia treatments were statistically significant

A PCA was performed to visualize clustering of relative expression patterns and to identify GOIs that contribute most to those differences between treatments. The first and second principal components (PC1 and PC2) accounted for 60.45% and 24.76% of the total variance, respectively. Cumulative variance explained by the first two components was 85.20%, suggesting that most of the meaningful variability in the data was captured by PC1 and PC2. A PCA score plot revealed partial separation of clustering between the heatwave and heatwave + hypoxia treatments and the control, especially at the lower end of PC1 (Figure 3.13). Relative expression of HSP90 had the highest loading for PC1 (-0.984), suggesting it is a major driver of variation along that axis. Additionally, relative expression of PPCTI (0.744), HMGB1 (0.542), and DSP1 (0.384) contributed strongly to variation along PC2, suggesting that differences in

relative expression of these four genes contributed the most to the variance between treatments (Figure 3.14).

3.4 Discussion

3.4.1 Identification of candidate genes for summer mortality monitoring

Findings of the study suggest that the expression of five candidate genes—death-associated inhibitor of apoptosis 2 (A2I), high mobility group protein DSP1 (DSP1), high mobility group box 1 (HMGB1), heat shock protein 90 (HSP90), and peptidyl-prolyl cis-trans isomerase (PPCTI)—demonstrate potential utility in monitoring heatwave-driven mortality for the Pacific oyster. RNAseq revealed hundreds of DEGs between the heatwave and heatwave + hypoxia treatments and the control, but only a small subset showed consistent expression changes across experimental timepoints and treatments. Given the high polymorphism in the Pacific oyster genome (G. Zhang et al., 2012), this variability is expected and may reinforce the utility of these genes that were consistently differentially expressed. Multivariate analysis demonstrated that the relative expression of the 10 GOIs was significantly different in the heatwave and heatwave + hypoxia treatments compared to the control. However, differences in single-gene relative expression responses were only detected for five of those GOIs—A2I, DSP1, HMGB1, HSP90, and PPCTI. Accordingly, multivariate analysis of only those five GOIs increased the significant difference between heatwave and heatwave + hypoxia treatments compared to the control. In addition, differences in relative expression of PPCTI, DSP1, HMGB1, and HSP90 consistently accounted for the majority of variation between heatwave and heatwave + hypoxia treatments compared to the control. Therefore, it is expected that expression

of PPCTI, DSP1, HMGB1, and HSP90 to be most relevant in terms of monitoring heatwave-driven mortality.

Relative expression differences in those candidate genes were detectable even when whole-organism responses were not. For instance, no significant differences in mean CI was observed between heatwave, hypoxia, heatwave + hypoxia, and control treatments. CI is an established metric for monitoring oyster health (He et al., 2022; Rainier & Mann, 1992) and has been used to assess Pacific oyster health during heatwaves (De Marco et al., 2023). However, CI reductions typically occur during prolonged heatwaves lasting over 30 d (De Marco et al., 2023), and changes in CI have not been reliably demonstrated to correlate with susceptibility to mass mortality (Chávez-Villalba et al., 2007; Mackenzie et al., 2024; Pace et al., 2020). Therefore, the findings align with the existing understanding of CI and summer mortality. Additionally, no clear physical signs of oyster stress were observed in any of the treatments during the experiment. Specifically, shell gaping behavior, an established whole-organism stress metric in bivalves (McMahon, 1988; Oh et al., 2021), was monitored but no notable differences were found during the experiment. Those results further support the concept that genetically based monitoring tools for summer mortality may detect health changes in Pacific oysters that whole-organism metrics, like CI and shell gaping, cannot.

Like other studies (Chaney & Gracey, 2011; De Lorgeril et al., 2011), the present research was not successful at replicating the extent of summer mortality using a laboratory-simulated heatwave. Only a single mortality, in the heatwave + hypoxia treatment on day 10 of the experiment, was recorded. That aligns with the hypothesized role of pathogenic bacteria in summer mortality syndrome (Cowan et al., 2023; Garnier et al., 2007; Go et al., 2017; Wendling & Wegner, 2013) as the only successful laboratory replication of summer mortality to date

involved deliberately selecting oysters with microbiomes consistent with natural mortality events (Green et al., 2019). Seasonal variations in the oyster microbiome were not considered in the present study. Oysters for the experiment were collected in February (winter in the northern hemisphere), so it is unlikely that the bacterial communities in those oysters were representative of those observed during summer mortality events (Conceição et al., 2021; Garnier et al., 2007; Saulnier et al., 2010). Nevertheless, differences in expression of the five candidate genes was detected with simulated heatwave conditions similar to those in the study that successfully triggered mortality (Green et al., 2019). Therefore, differences in gene expression may still be detectable and precede mortality in oysters with bacterial communities that align with seasonal conditions during mortality events. To preserve the seasonal microbiome and validate the potential of those monitoring genes, future laboratory experiments should simulate laboratory heatwaves during summer while collecting oysters prior to a naturally occurring heatwave, as done by Green et al. (2019). Since we were unable to successfully replicate a heatwave-induced mortality event in the present study, the predictive power of those candidate genes remains uncertain.

A potential limitation of the study is the established seasonal variation in gene expression for Pacific oysters that was not considered in this experimental design. Summer mortality is a seasonal phenomenon, and while summer temperatures relevant to mortality were simulated, other aspects of seasonality, which could contribute to mortality, were not accounted for. Seasonal variations in bacterial community have already been noted, but changes to reproductive effort in summer also contribute to mortality and may alter patterns of gene expression (Farcy et al., 2007). Seasonal levels of reproductive effort can be induced with laboratory simulated summer temperatures (Vasquez et al., 2013), so the impact of this discrepancy may be minimal.

However, the expression of stress marker genes such as HSP90 and HSP70 vary seasonally in oysters independent of seasonal changes in temperature (Encomio & Chu, 2005; Farcy et al., 2007). While summer temperatures were simulated in the present study, ultimately relative expression levels of HSP90 and HSP70 for oysters collected in winter are presented. As a result, it is possible that the research has not accurately assessed potential for the GOIs for monitoring summer mortality. The relative expression of stress marker genes during the summer is most relevant for monitoring summer mortality. It is therefore emphasized that future studies should simulate heatwaves with oysters collected in the summer to reduce seasonality-related uncertainty and confirm the effectiveness of the candidate genes in monitoring summer mortality.

3.4.2 Genes involved in stress response

Changes in relative expression for four genes—HSP20, HSP70, HSP90, and SIP1—associated with stress response were assessed in this study, only HSP90 showed significant differences in the heatwave + hypoxia treatment compared to control. Relative expression of HSP90 was significantly higher in the heatwave + hypoxia group than the control on day 10 of the experiment and its expression contributed most to the dissimilarity between the heatwave + hypoxia treatment and the control at higher temperatures. This is consistent with previous research demonstrating reliable upregulation of HSP90 in oysters under acute thermal stress, as well as previous insights that support HSP90 as a molecular biomarker for predicting heatwave-induced mortality in other oyster species (Masanja et al., 2022; Y. Xu, et al., 2022a). However, the majority of those studies detected differences in HSP90 relative expression at seawater temperatures between 32 and 37°C (Farcy et al., 2009; Kim et al., 2017; Lim et al., 2016; Y. Xu et al., 2022a), which is considerably higher than the maximum temperature of 26°C utilized in

the present study. Given that upregulation of HSP90 was observed in the heatwave + hypoxia treatment at relatively low temperatures compared to previous studies, it may be the case that the addition of mild hypoxia exacerbated the expression of this stress response gene. This would be consistent with previous work that has demonstrated that intermittent hypoxia induced by emersion may lower thermal tolerance and amplify stress response in oysters at 30°C, ultimately leading to mortality (Bruhns et al., 2023). However, we provide the first evidence that DO levels of ~4 mg O₂ L⁻¹ may increase stress response at temperatures relevant to summer mortality and thus has the potential to worsen summer mortality.

Furthermore, HSP90 relative expression in the heatwave group was not significantly higher than the control on day 10 or any other timepoint during the experiment. In fact, HSP90 relative expression was significantly lower in the heatwave treatment compared to in the heatwave + hypoxia treatment on day 10 of the experiment, and this difference was a major contributor to dissimilarity between those treatments. Therefore, the lack of artificial aeration in the heatwave + hypoxia group resulted in significantly higher HSP90 relative expression compared to the heatwave treatment with artificial aeration. The study therefore provides some evidence that aeration may reduce thermal stress and thus contribute some resilience to mortality, as suggested by previous studies (H. O. Pörtner et al., 2006). However, HSP90 response to acute thermal stress has the potential to vary seasonally in Pacific oysters (Farcy et al., 2009), therefore, future studies should investigate the effect of artificial aeration on HSP90 relative expression in summer to confirm its potential applicability as a mitigation strategy for Pacific oyster summer mortality.

Despite their established use as stress marker genes in environmental monitoring (Gupta et al., 2010; Hoffmann & Daborn, 2007b; Mukhopadhyay et al., 2003), no significant differences

in relative expression of HSP70 or HSP20 were detected under heatwave or heatwave + hypoxia conditions compared to the control in the present study. In addition, no significant differences in relative expression of SIP1, an orthologue of HSP20 (G. Zhang et al., 2012), were observed. Those results align with the hypothesis that the use of traditional stress biomarkers may not be applicable for monitoring summer mortality, as upregulation of HSP20 and HSP70 usually occurs at temperatures between 32 and 38°C in oysters (Farcy et al., 2009; Lim et al., 2016; Liu et al., 2022; Y. Xu, et al., 2022a; C. Yang et al., 2017; Y. Zhang et al., 2015), well above temperatures that trigger outbreaks of mortality in the field (Garnier et al., 2007; Mackenzie et al., 2024; Whittington et al., 2024) and in appropriate laboratory settings (Green et al., 2019). Therefore, evidence is provided by the current results that novel molecular biomarkers other than HSP20 and HSP70 are needed to effectively monitor and predict Pacific oyster summer mortality. In addition, no significant differences in relative expression of HSP20, HSP70, or SIP1 between heatwave and heatwave + hypoxia treatments were evident, which may suggest that the presence of artificial aeration had little effect on heatwave driven stress response. However, given that HSP90 expression may be a more reliable indicator of heatwave-driven stress in oysters (Masanja et al., 2022; Y. Xu et al., 2022a), and the presence of artificial aeration did result in differences in HSP90 relative expression in the present study, additional research is needed to effectively evaluate the potential for artificial aeration to alleviate thermal stress and confer resilience to summer mortality in Pacific oysters.

3.4.3 Genes involved in regulation of transcription

While upregulation of HSP70 was not induced in this experiment, downregulation of DSP1, a proposed negative regulator of HSP70, was. In the Hong Kong oyster (*Crassostrea*

hongkongensis), a closely related estuarine species (Zhao et al., 2014), DSP1 is a recently discovered negative regulator that suppresses HSP70 transcription through direct binding to its promoter region (Miao et al., 2016). In the present study, relative expression of DSP1 was significantly lower in both the heatwave and heatwave + hypoxia treatments compared to the control. Notably, DSP1 was downregulated on day 6 of the experiment for both treatments, in seawater temperatures that were only slightly elevated (22°C) compared to the control (16°C). Since summer mortality is usually triggered by similar temperatures (Garnier et al., 2007; Green et al., 2019), it is hypothesized that DSP1 expression may be an especially appropriate choice for monitoring summer mortality. Indeed, differences in DSP1 relative expression were consistently one of the primary contributors to dissimilarity between heatwave and heatwave + hypoxia treatments and the control. Since no significant differences in HSP70 relative expression were observed between treatments, it is possible that early detection of DSP1 downregulation before the onset of HSP70 response may provide an early warning signal of stress that can lead to mortality. Previous studies have identified regulators of HSP70 expression as biomarkers for early stress detection in Pacific oyster (Fu et al., 2023; Patterson et al., 2014; Wang et al., 2016) and suggested that regulatory mechanisms may detect vulnerability to mortality where traditional stress biomarkers would not. Therefore, further investigation into the predictive power DSP1 expression for Pacific oyster mortality is warranted.

3.4.4 Genes involved in immune function

Changes in relative expression of three genes associated with immune function—A2I, HMGB1, and PPCTI—were assessed in this study, all of which showed significant differences under heatwave or heatwave + hypoxia conditions compared to the control. Relative expression

of A2I, an inhibitor of apoptosis (IAP) identified by Zhang et al. (2012), was significantly upregulated in heatwave treatment compared to the control on day 8, but not for the heatwave + hypoxia treatment. In addition, A2I relative expression in the heatwave + hypoxia treatment was not significantly different from the control at any timepoint during the experiment. However, A2I relative expression in the heatwave + hypoxia treatment was also not significantly different from the heatwave treatment at any timepoint during the experiment. A2I is involved in innate immunity for oysters, maintaining cell stability in the late stages of infection (Cai et al., 2022; Witkop et al., 2022), and in general, upregulation of IAPs is associated with increased susceptibility to bacterial and viral infection in oysters (Goedken et al., 2005; Segarra et al., 2014; Witkop et al., 2022). Therefore, upregulation of A2I in this study may not only indicate cellular stress, but also increased susceptibility to pathogenic infection. However, given that A2I upregulation was only observed at only one timepoint in the heatwave group and there were no significant differences between the heatwave + hypoxia and control groups at any timepoint, further research is needed to understand the role of IAP expression and apoptosis regulation in Pacific oyster summer mortality.

Significant downregulation of HMGB1 compared to the control was observed on day 8 of the experiment for the heatwave + hypoxia treatment. In *C. gigas*, HMGB1 functions in innate immunity (J. Li et al., 2013; T. Xu et al., 2012) and is significantly upregulated in the presence of pathogenic bacteria such as *Vibrio alginolyticus* and *V. splendidus* (J. Li et al., 2013; Lv et al., 2022). In the absence of bacterial infection, HMGB1 is expressed constitutively in a range of tissues including the gills (J. Li et al., 2013). Therefore, downregulation of HMGB1 in the heatwave + hypoxia treatment may suggest a shift away from innate immune function, leaving oysters susceptible to bacterial infection. That is consistent with previous studies that have

shown negative effects of hypoxia on immune response in oysters (Barnett et al., 2020; David et al., 2005). Interestingly, HMGB1 relative expression in the heatwave treatment was not significantly different from the control at any timepoint during the experiment. Furthermore, HMGB1 relative expression in the heatwave + hypoxia group was significantly lower than the heatwave only treatment on day 8, and this difference was a major contributor to dissimilarity between those treatments. Thus, the results suggest that the addition of hypoxia stress under heatwave conditions may exacerbate negative effects on HMGB1 expression, and therefore innate immunity. This indicates that the presence of artificial aeration may reduce negative impacts of simulated heatwaves on HMGB1 expression, potentially increasing resilience to pathogenic infection.

Finally, significant downregulation of PPCTI compared to the control was observed on days 6 and 8 of the experiment for both heatwave and heatwave + hypoxia treatments. Furthermore, differences in PPCTI relative expression were consistently one of the primary contributors to dissimilarity between heatwave and heatwave + hypoxia treatments and the control. PPCTI describes a domain common to three superfamilies of genes involved in protein folding, usually referred to as PPIases (Takahashi et al., 1989). In molluscs, the most well described PPIases are cyclophilins (CyPs), which likely function in innate immunity, similar to HMGB1. In oysters, CyPs are constitutively expressed in a range of tissues but most highly expressed in the haemocytes (T. Xu et al., 2016), and are also upregulated in response to infection by *V. splendidus* (Huvet et al., 2004) and a pathogenic rickettsia-like organism (T. Xu et al., 2016). Therefore, downregulation of PPCTI in the present study may also indicate a heatwave-driven shift away from innate immunity. That is consistent with previous work that has found that reduced CyP expression is associated with increased susceptibility to summer

mortality following infection by *V. splendidus* (Huvet et al., 2004). Interestingly, no significant differences in PPCTI relative expression between heatwave and heatwave + hypoxia treatments were observed, suggesting no effect of artificial aeration.

While previous studies have challenged the hypothesis that heatwaves impair immune function in oysters and increase susceptibility to summer mortality (Green et al., 2019; Wendling & Wegner, 2013), evidence is provided here that at least three genes—A2I, HMGB1, and PPCTI—involved in immune function show altered relative expression under simulated heatwave and hypoxic conditions. However, relative expression patterns for those three genes were not consistent across treatments. A2I was upregulated only in the heatwave treatment, HMGB1 was downregulated only in the heatwave + hypoxia treatment, and PPCTI was downregulated in both the heatwave and heatwave + hypoxia treatments. Therefore, while the present findings support previous work that demonstrates both heatwaves and hypoxic conditions may impair immune function in the Pacific oyster (Barnett et al., 2020; David et al., 2005; Delaporte et al., 2006; X. Li et al., 2023; Y. Li et al., 2007), limited evidence is provided that artificial aeration would alleviate these negative impacts. However, relative expression of only one of those genes, PPCTI, has been investigated in other studies on summer mortality (Huvet et al., 2004). Expression of A2I and HMGB1 have yet to be explored in the context of heatwave driven summer mortality for Pacific oyster. Thus, further investigation is needed to understand the expression of Pacific oyster immune genes during heatwaves, and the potential for artificial aeration to mitigate negative effects on immunity.

3.4.5 Conclusion

This study examined the effect of simulated heatwave and hypoxic conditions on gene expression in the Pacific oyster to identify candidate monitoring genes and assess the potential for artificial aeration to act as a mitigation strategy for summer mortality. Changes in relative expression of five genes—A2I, DSP1, HMGB1, HSP90, and PPCTI—were assessed and showed altered expression under heatwave and hypoxic conditions, demonstrating potential as monitoring tools for summer mortality. Among traditional stress monitoring genes, HSP90 was upregulated only under a combination of heatwave and hypoxic conditions, indicating potentially exacerbated stress response with limited DO, which was minimized in the presence of artificial aeration. Three immune genes—HMGB1, PPCTI, and A2I—showed altered expression under heatwave and hypoxia conditions, indicating possible impairment of innate immunity in response to elevated temperatures and limited DO, which may contribute to mortality. However, the presence of artificial aeration did not have a clear effect on expression of those immune genes. Taken together, these results indicate that novel molecular biomarkers other than HSP70 and HSP20 are needed to effectively monitor Pacific oyster summer mortality, and artificial aeration may alleviate some thermal stress during heatwaves. However, further investigation is needed to assess aeration as a mitigation strategy for Pacific oyster summer mortality. These findings will inform effective monitoring and mitigation practices to support the adaptation of shellfish aquaculture to the growing impacts of climate change.

3.5 Tables and figures

Table 3.1. Primer sequences used in qPCR verification and associated gene IDs for cDNA sequences used in primer design.

Gene	EnsemblMetazoa gene ID	Forward primer	Reverse primer
Actin	G3054	5' GCCCTGGACTTCGAACAA 3'	5' CGTTGCCAATGGTGATGA 3'
Elongation factor 1- α	G4818	5' GAGCGTGAACGTGGTATCAC 3'	5' ACAGCACAGTCAGCCTGTGA 3'
Heat shock protein 70	G29360	5' TGACCAAGGCAACAGAACCA 3'	5' AATCAGACGGCCGGTATGTG 3'
Heat shock protein 20	G17983	5' CCGAAGGAAGAGGACCAGGAGATG 3'	5' CGAACACCGACAGTCTAACTCTC 3'
Heat shock protein 90	G10994	5' TCACACAGGAGGATATGGC 3'	5' TGAGAAATGCTTCACAGCCAA 3'
High mobility group protein DSP1	G24596	5' CAGCCAAGAAAGCCAAACCTC 3'	5' ACAATGGTGCTTGCCGACT 3'
High mobility group box 1	G31074	5' TCCCACCCAAAACAAGCCA 3'	5' ACTTCCCCTGTTACCCCTC 3'
Peptidyl-prolyl cis-trans isomerase	G21557	5' CCGTTCGATGCTACCCAC 3'	5' ATGAACCAATCCTGGCACACA 3'
Death-associated inhibitor of apoptosis 2	G17932	5' AGGAACGGAAAACAATGACGA 3'	5' ACGTCCTTTGACATCCCCTG 3'
Stress-induced protein 1	G17984	5' AGCCTGACCACATTACCGTC 3'	5' GAACGAGACACCTTGACCCC 3'
Heterogeneous nuclear ribonucleoprotein	G1087	5' CCGGTGACTCCAAAACCATC 3'	5' ACTCACCTGATCGTATCCGT 3'
X-box-binding protein 1	G20574	5' AGTCTGCGGATTTAGCTGGAG 3'	5' GCCAATCACAGAAGCAGCAC 3'

Table 3.2. Numbers of differently expressed genes (DEGs) in each treatment and timepoint with corresponding temperature, including both upregulated and downregulated DEGs.

Timepoint	Temperature (°C)	Treatment	Number of upregulated genes	Number of downregulated genes	Total DEGs
T1	18	Heatwave	2	3	5
T1	18	Heatwave+Hypoxia	4	3	7
T2	20	Heatwave	8	12	20
T2	20	Heatwave+Hypoxia	12	22	34
T3	22	Heatwave	5	7	12
T3	22	Heatwave+Hypoxia	7	8	15
T4	24	Heatwave	10	32	42
T4	24	Heatwave+Hypoxia	27	21	48
T5	26	Heatwave	10	35	45
T5	26	Heatwave+Hypoxia	52	81	133

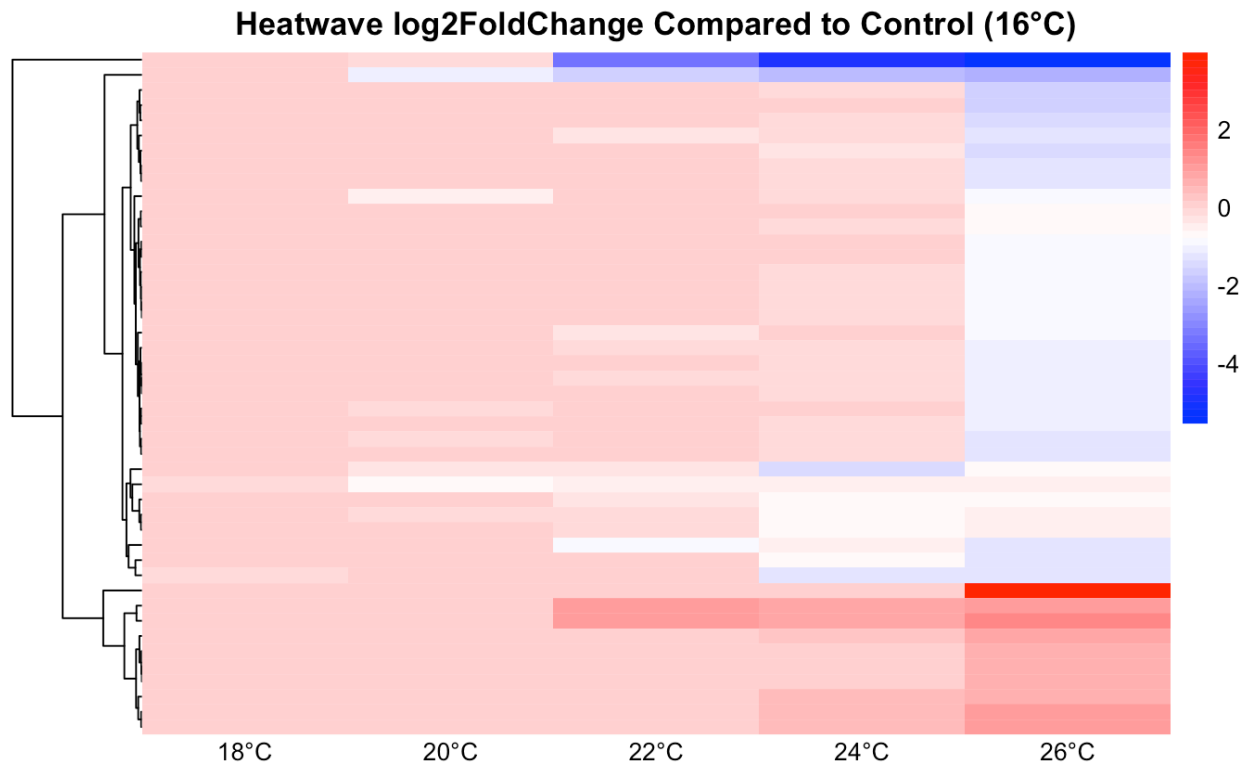


Figure 3.1. Heat map of changes in gene expression (Log₂FC) during the simulated heatwave for the 45 differently expressed genes detected by RNAseq at the height of the heatwave (T5, 26°C) in the heatwave treatment at each timepoint during the experiment. Hierarchical clustering was performed for genes (rows) using Euclidean distance and complete linkage. A colour gradient from blue (low) to red (high) represents Log₂FC values.

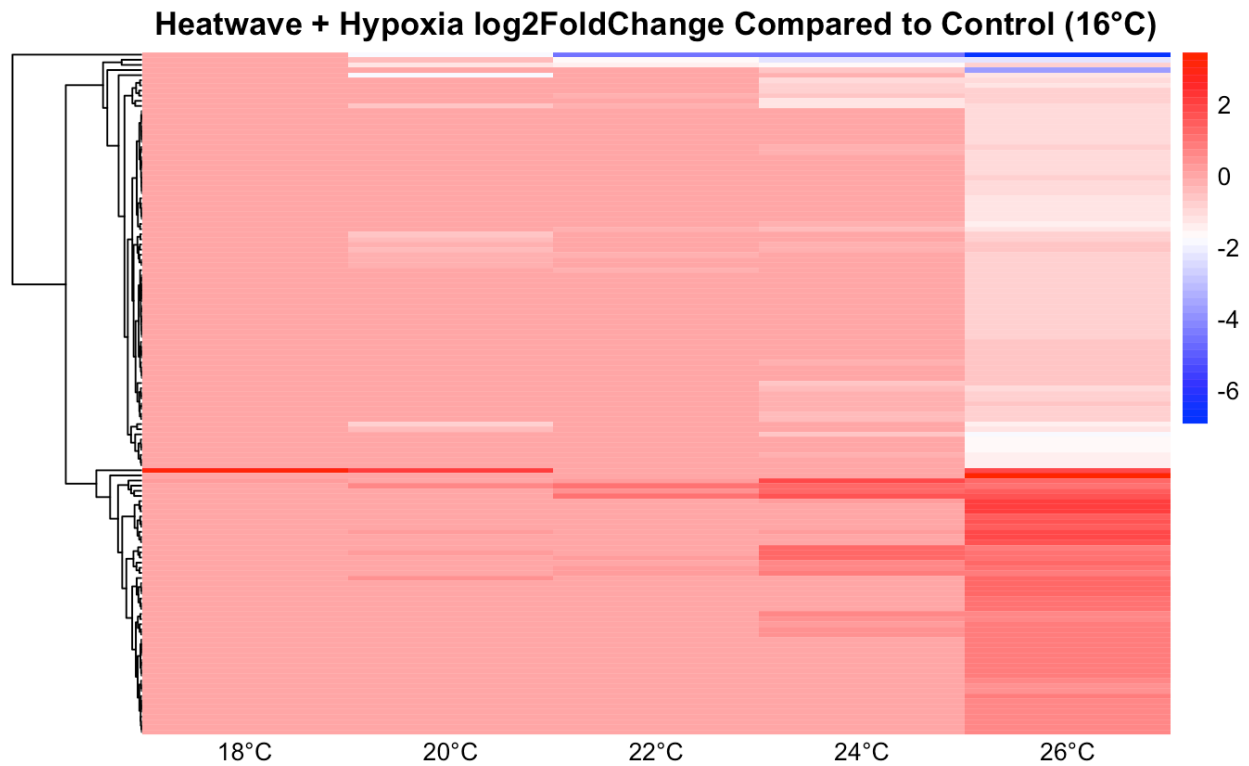


Figure 3.2. Heat map of changes in gene expression (Log₂FC) during the simulated heatwave for the 133 differently expressed genes detected by RNAseq at the height of the heatwave (T5, 26°C) in the heatwave + hypoxia treatment at each timepoint during the experiment. Hierarchical clustering was performed for genes (rows) using Euclidean distance and complete linkage. A colour gradient from blue (low) to red (high) represents Log₂FC values.

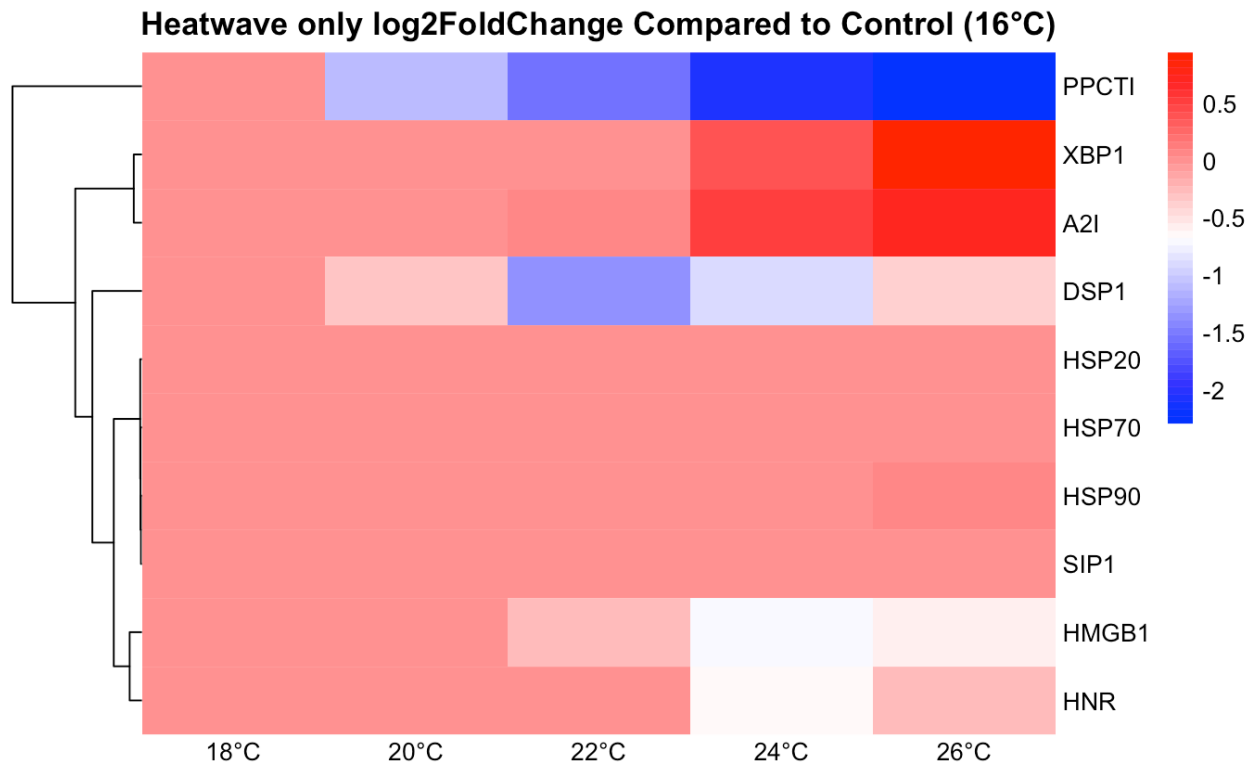


Figure 3.3. Heat map of changes in gene expression (Log2 fold change) detected by RNAseq for the 10 genes of interest— peptidyl-prolyl cis-trans isomerase (PPCTI), x-box-binding protein 1 (XBP1), death-associated inhibitor of apoptosis 2 (A2I), high mobility group protein DSP1 (DSP1), high mobility group box 1 (HMGB1), heat shock protein 20 (HSP20), heat shock protein 70 B2 (HSP70), heat shock protein 90 (HSP90), stress-induced protein 1 (SIP1), and heterogeneous nuclear ribonucleoprotein (HNR)—chosen for qPCR validation across all five timepoints for the heatwave treatment. Hierarchical clustering was performed for genes (rows) using Euclidean distance and complete linkage. A colour gradient from blue (low) to red (high) represents Log2FC values.

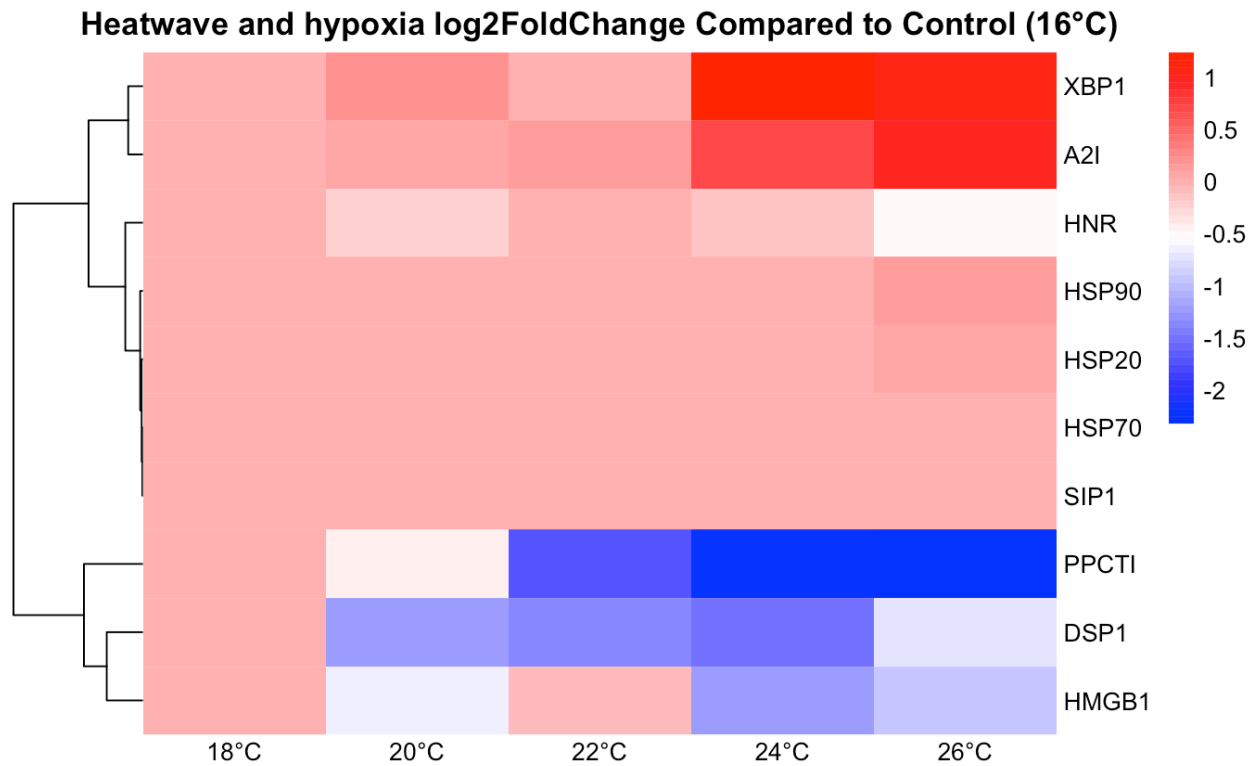


Figure 3.4. Heat map of changes in gene expression (Log2 fold change) detected by RNAseq for the 10 genes of interest— x-box-binding protein 1 (XBP1), death-associated inhibitor of apoptosis 2 (A2I), heterogeneous nuclear ribonucleoprotein (HNR), heat shock protein 90 (HSP90), heat shock protein 20 (HSP20), heat shock protein 70 B2 (HSP70), stress-induced protein 1 (SIP1), peptidyl-prolyl cis-trans isomerase (PPCTI), high mobility group protein DSP1 (DSP1), and high mobility group box 1 (HMGB1)—chosen for qPCR validation across all five timepoints for the heatwave + hypoxia treatment. Hierarchical clustering was performed for genes (rows) using Euclidean distance and complete linkage. A colour gradient from blue (low) to red (high) represents Log2FC values.

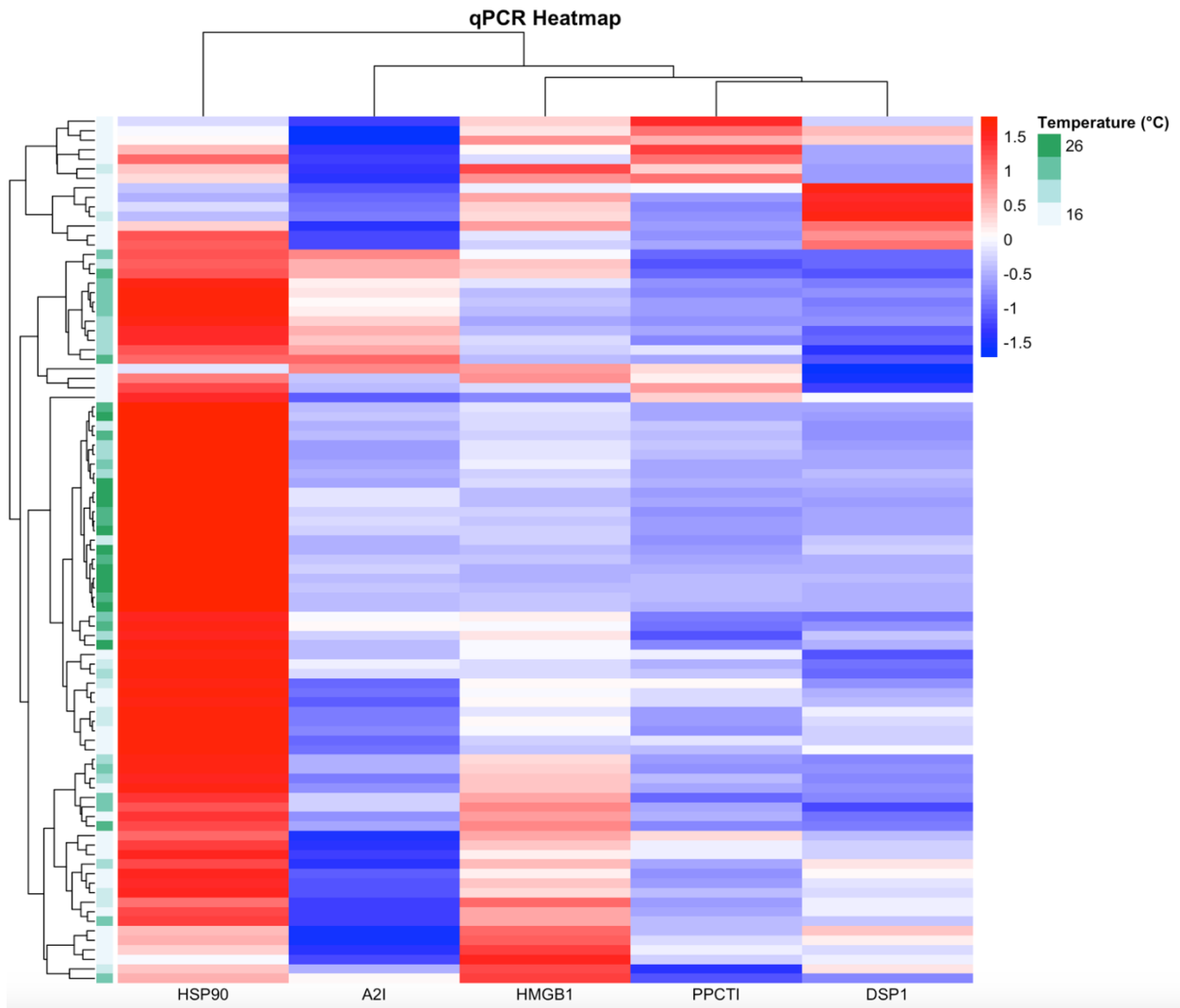


Figure 3.5. Heat map of relative expression ($2\Delta C_q$) for the five genes of interest—heat shock protein 90 (HSP90), death-associated inhibitor of apoptosis 2 (A2I), high mobility group box 1 (HMGB1), peptidyl-prolyl cis-trans isomerase (PPCTI), and high mobility group protein DSP1 (DSP1)—that showed significant ($p < 0.05$) changes under single-gene response assessment. Hierarchical clustering was performed for both genes (columns) and temperatures (rows) using Euclidean distance and complete linkage. A colour gradient from blue (low) to red (high) represents z-transformed relative expression values. Relative expression is similar at higher temperatures, as indicated by clustering of darker green rows.

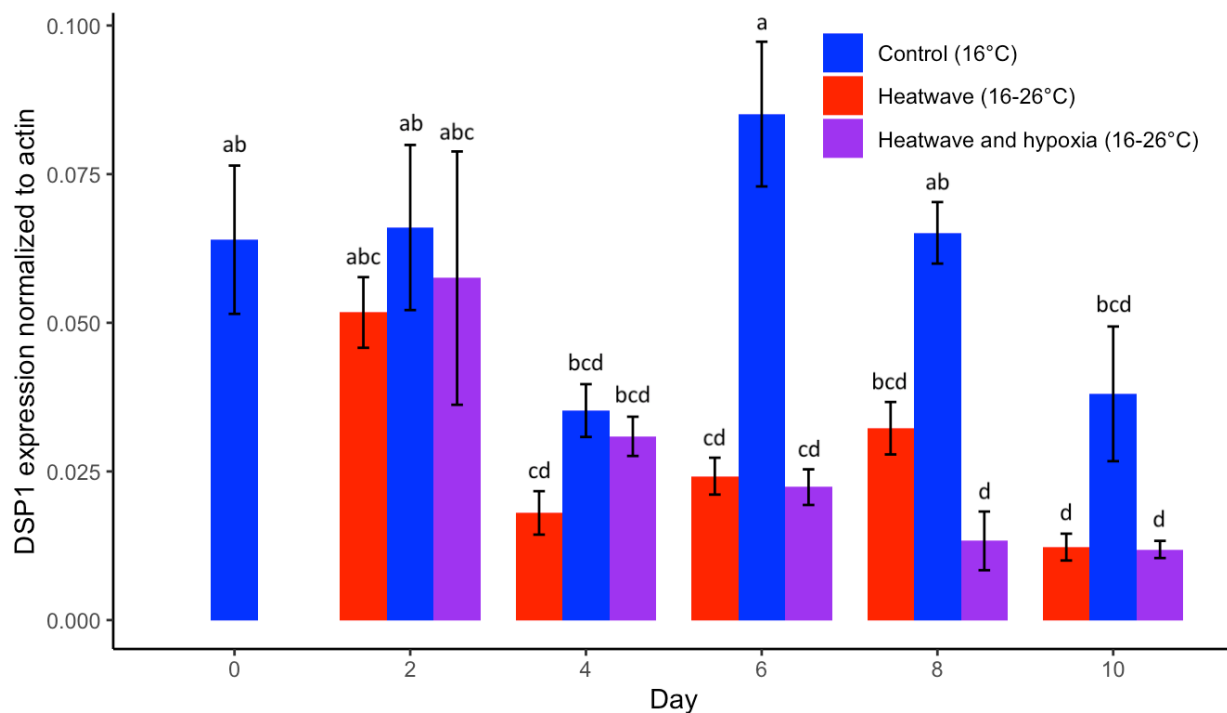


Figure 3.6. Mean relative expression ($2^{\Delta Cq}$) and standard error ($n = 6$) for high mobility group protein DSP1 (DSP1) on day 0 (T0, 16°C), day 2 (T1, 18°C), day 4 (T2, 20°C), day 6 (T3, 22°C), day 8 (T4, 24°C), and day 10 (T5, 26°C) of the simulated heatwave compared to the control (16°C). Relative expression normalized to actin where $\Delta Cq = (Cq_{actin} - Cq_{DSP1})$. Letters show significant ($p < 0.05$) differences identified via post-hoc Student-Newman-Keuls (SNK) test.

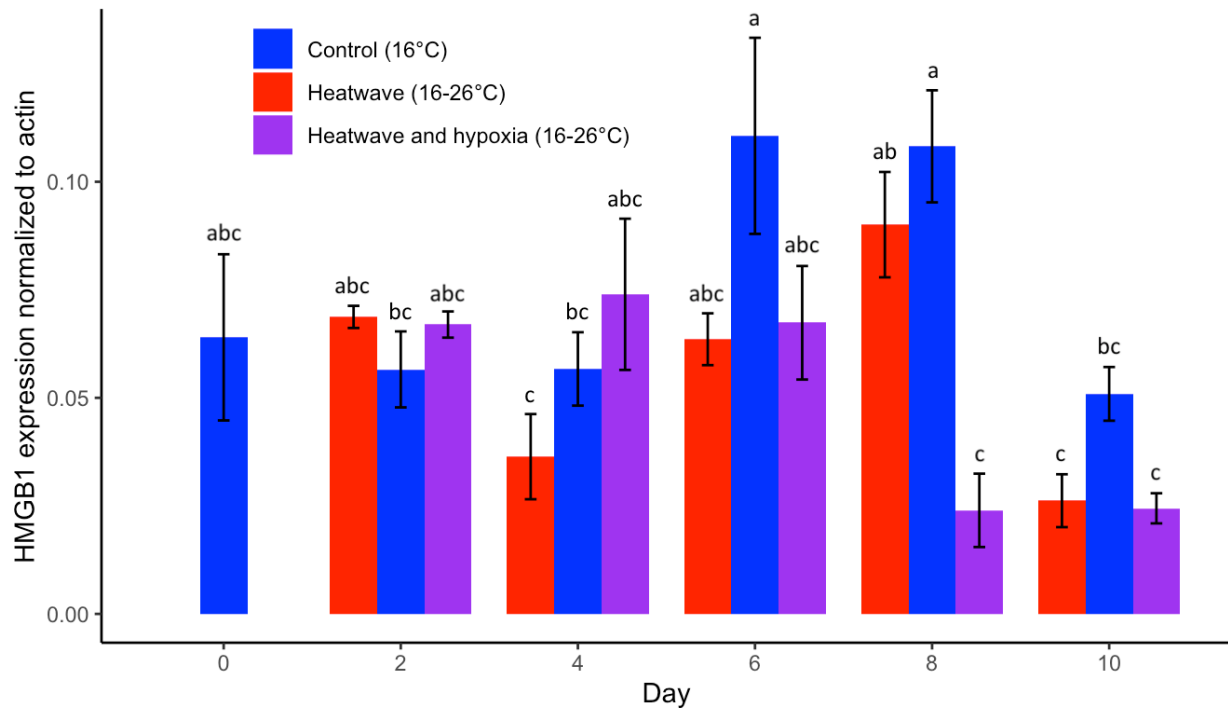


Figure 3.7. Mean relative expression ($2^{\Delta Cq}$) and standard error ($n = 6$) for high mobility group box 1 (HMGB1) on day 0 (T0, 16°C), day 2 (T1, 18°C), day 4 (T2, 20°C), day 6 (T3, 22°C), day 8 (T4, 24°C), and day 10 (T5, 26°C) of the simulated heatwave compared to the control (16°C). Relative expression normalized to actin where $\Delta Cq = (Cq_{actin} - Cq_{HMGB1})$. Letters show significant ($p < 0.05$) differences identified via post-hoc Student-Newman-Keuls (SNK) test.

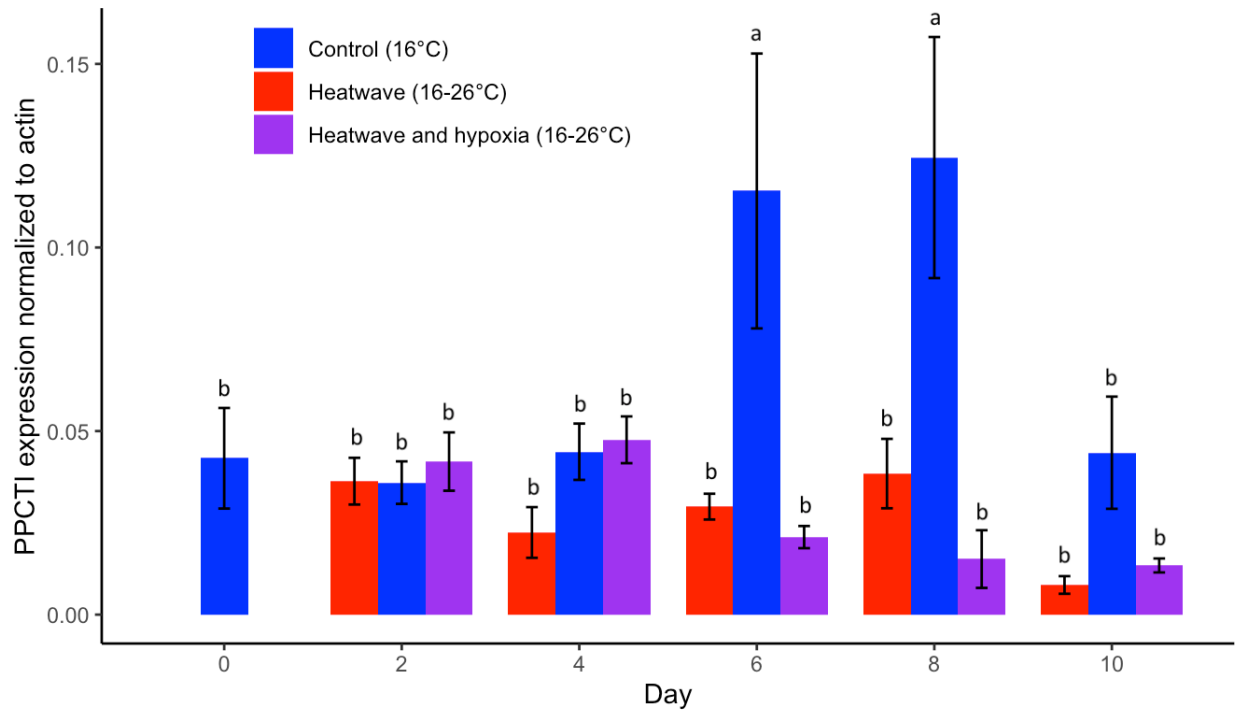


Figure 3.8. Mean relative expression ($2^{\Delta Cq}$) and standard error ($n = 6$) for peptidyl-prolyl cis-trans isomerase (PPCTI) on day 0 (T0, 16°C), day 2 (T1, 18°C), day 4 (T2, 20°C), day 6 (T3, 22°C), day 8 (T4, 24°C), and day 10 (T5, 26°C) of the simulated heatwave compared to the control (16°C). Relative expression normalized to actin where $\Delta Cq = (Cq_{actin} - Cq_{PPCTI})$. Letters show significant ($p < 0.05$) differences identified via post-hoc Student-Newman-Keuls (SNK) test.

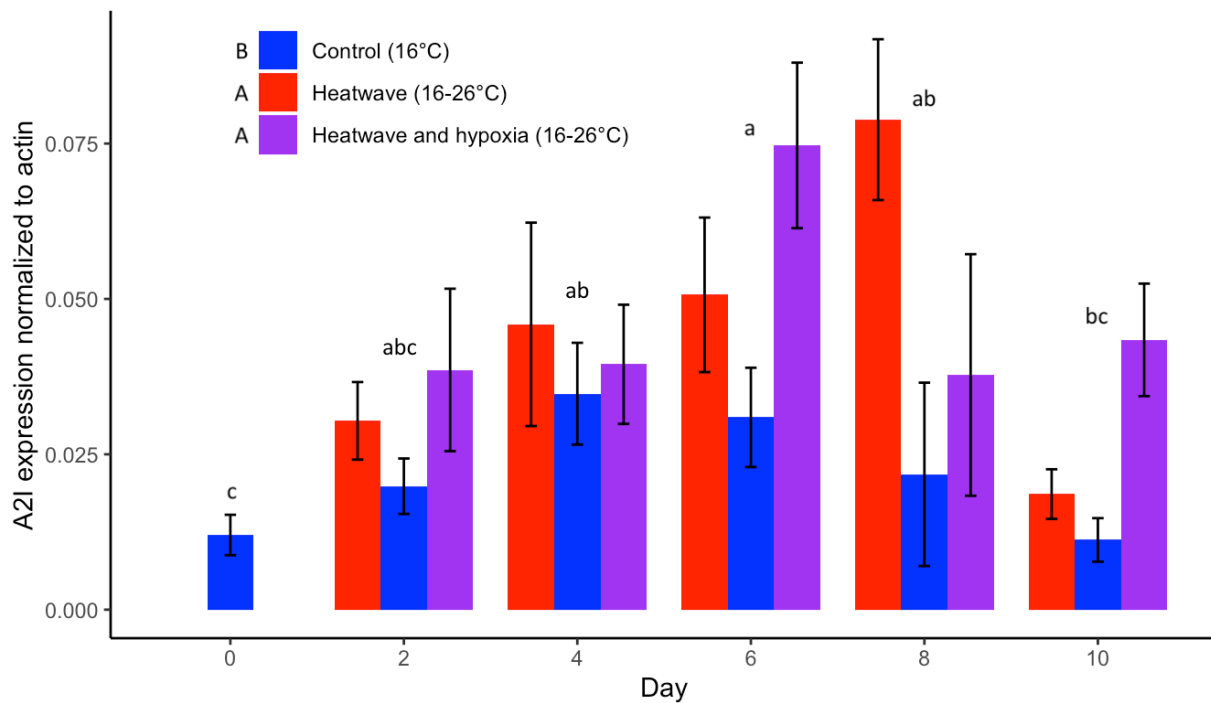


Figure 3.9. Mean relative expression ($2^{\Delta Cq}$) and standard error ($n = 6$) for death-associated inhibitor of apoptosis 2 (A2I) on day 0 (T0, 16°C), day 2 (T1, 18°C), day 4 (T2, 20°C), day 6 (T3, 22°C), day 8 (T4, 24°C), and day 10 (T5, 26°C) of the simulated heatwave compared to the control (16°C). Relative expression normalized to actin where $\Delta Cq = (Cq_{actin} - Cq_{A2I})$. Capital letters in the legend show significant ($p < 0.05$) differences identified for the treatment effect via post-hoc Student-Newman-Keuls (SNK) test, while lower-case letters above the bars show significant ($p < 0.05$) differences between timepoints identified by an additional SNK test.

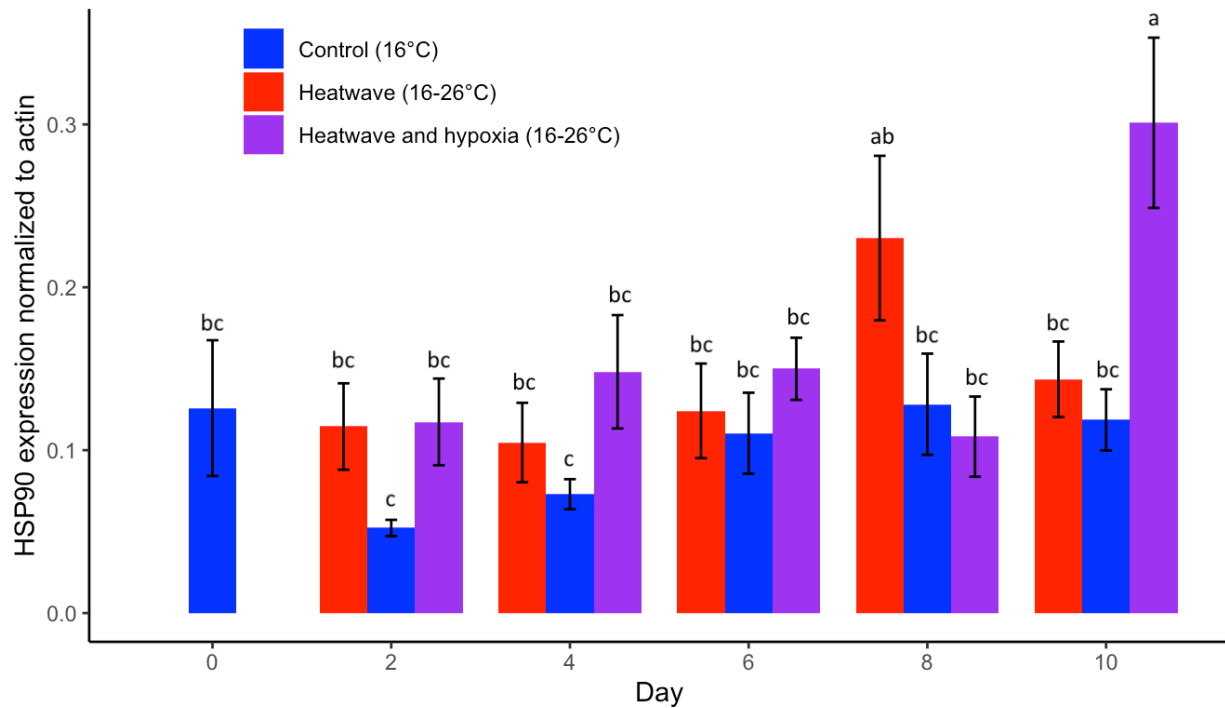


Figure 3.10. Mean relative expression ($2^{\Delta Cq}$) and standard error ($n = 6$) for heat shock protein 90 (HSP90) on day 0 (T0, 16°C), day 2 (T1, 18°C), day 4 (T2, 20°C), day 6 (T3, 22°C), day 8 (T4, 24°C), and day 10 (T5, 26°C) of the simulated heatwave compared to the control (16°C). Relative expression normalized to actin where $\Delta Cq = (Cq_{actin} - Cq_{HSP90})$. Letters show significant ($p < 0.05$) differences identified via post-hoc Student-Newman-Keuls (SNK) test.

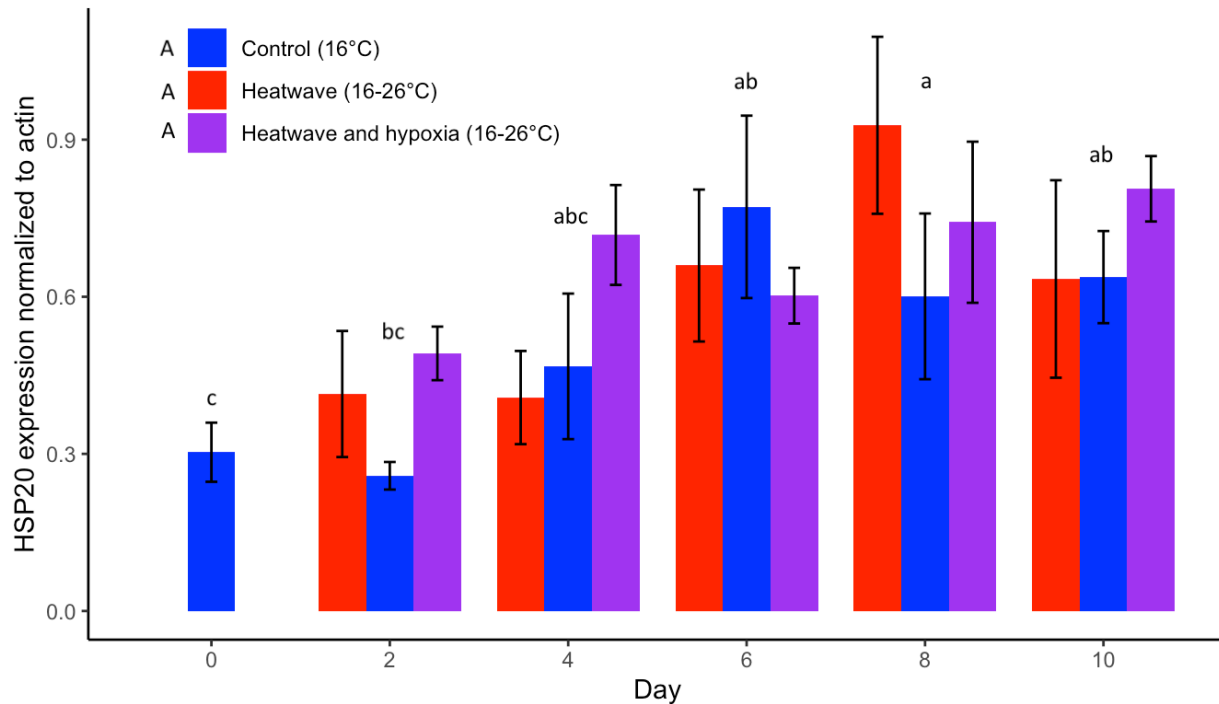


Figure 3.11. Mean relative expression ($2^{\Delta Cq}$) and standard error ($n = 6$) for heat shock protein 20 (HSP20) on day 0 (T0, 16°C), day 2 (T1, 18°C), day 4 (T2, 20°C), day 6 (T3, 22°C), day 8 (T4, 24°C), and day 10 (T5, 26°C) of the simulated heatwave compared to the control (16°C). Relative expression normalized to actin where $\Delta Cq = (Cq_{actin} - Cq_{HSP20})$. Capital letters in the legend show significant ($p < 0.05$) differences identified for the treatment effect via post-hoc Student-Newman-Keuls (SNK) test, while lower-case letters above the bars show significant ($p < 0.05$) differences between timepoints identified by an additional SNK test.

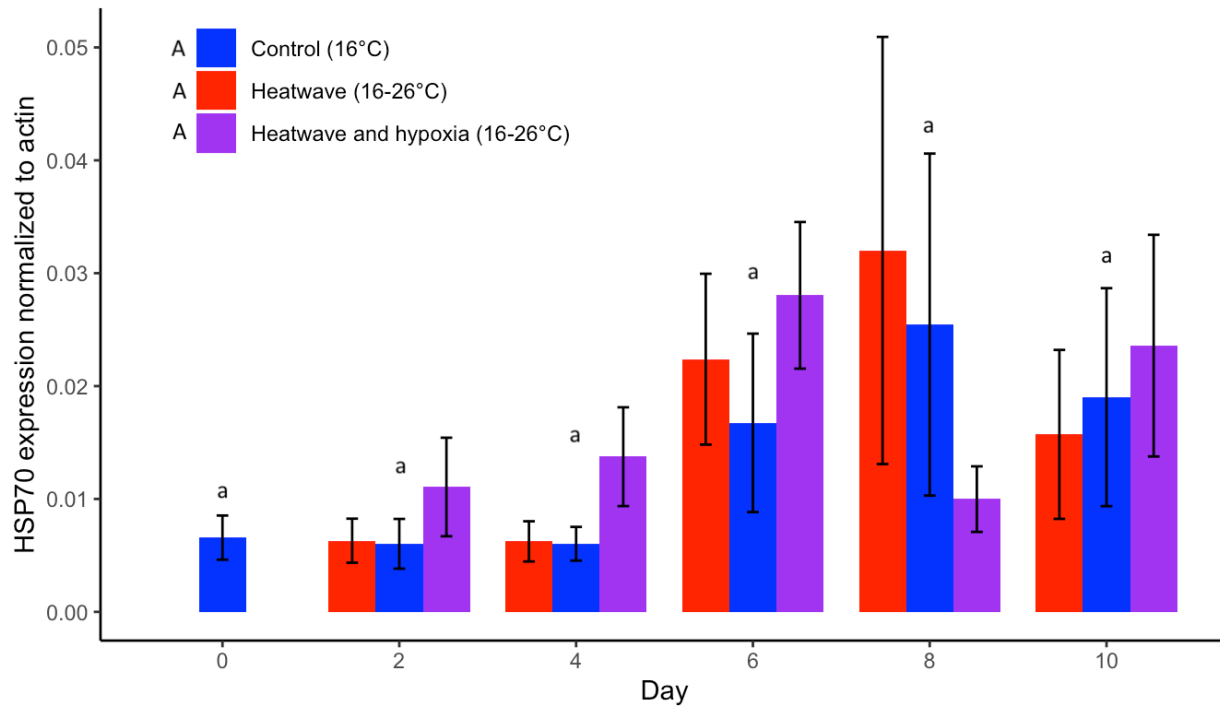


Figure 3.12. Mean relative expression ($2^{\Delta Cq}$) and standard error ($n = 6$) for heat shock protein 70 B2 (HSP70) on day 0 (T0, 16°C), day 2 (T1, 18°C), day 4 (T2, 20°C), day 6 (T3, 22°C), day 8 (T4, 24°C), and day 10 (T5, 26°C) of the simulated heatwave compared to the control (16°C). Relative expression normalized to actin where $\Delta Cq = (Cq_{actin} - Cq_{HSP70})$. Capital letters in the legend show significant ($p < 0.05$) differences identified for the treatment effect via post-hoc Student-Newman-Keuls (SNK) test, while lower-case letters above the bars show significant ($p < 0.05$) differences between timepoints identified by an additional SNK test.

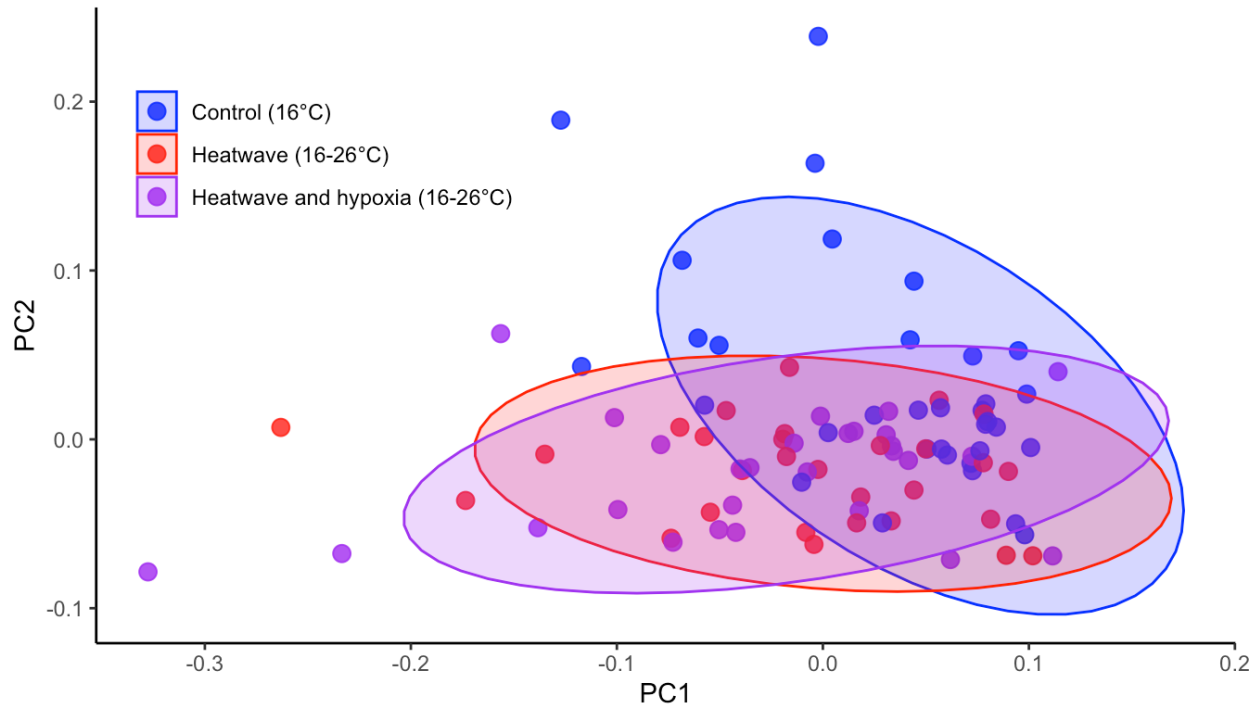


Figure 3.13. Principal Component Analysis (PCA) of relative expression for the five genes of interest—death-associated inhibitor of apoptosis 2 (A2I), high mobility group box 1 (HMGB1), high mobility group protein DSP1 (DSP1), heat shock protein 90 (HSP90), and peptidyl-prolyl cis-trans isomerase (PPCTI)—that showed significant ($p < 0.05$) changes under single-gene response assessment. The first two principal components (PC1 and PC2) are plotted, explaining 43.98% and 39.12% of the total variance, respectively. Samples are colored according to treatment group (control = blue, heatwave = red, heatwave + hypoxia = purple) and ellipses represent 95% confidence intervals for each group. PCA reveals some cluster separation between control and heatwave treatments, especially along PC1.

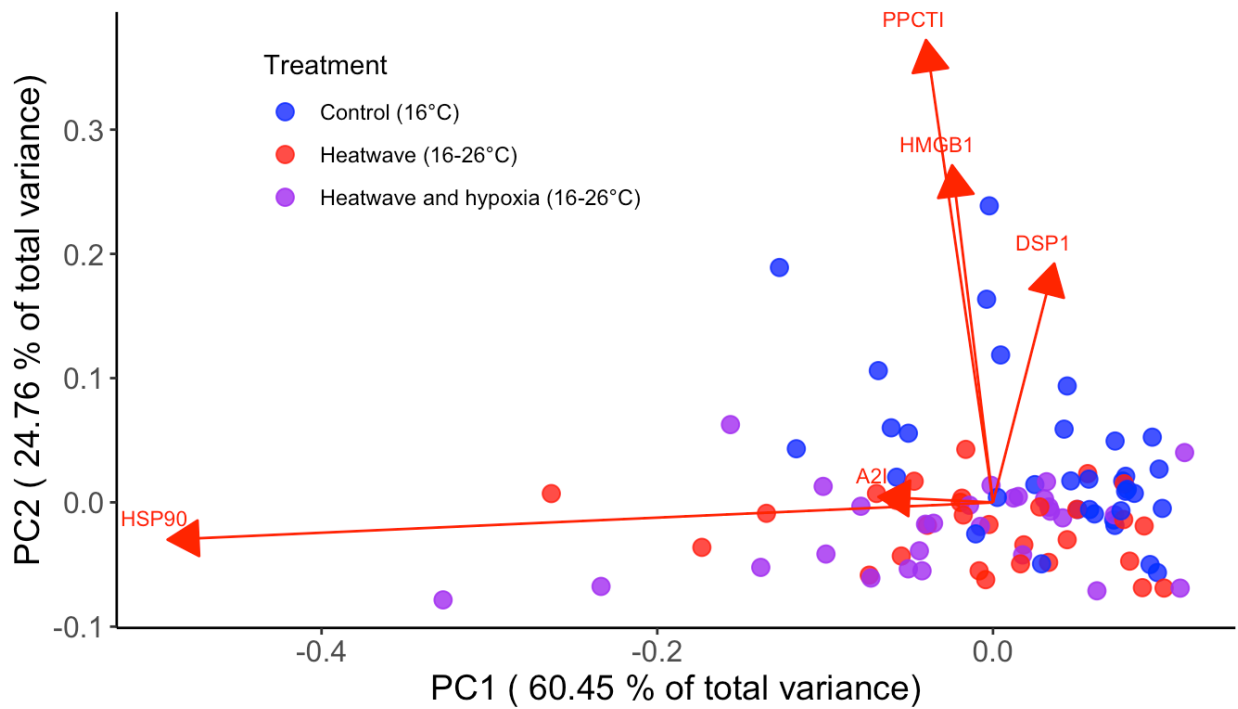


Figure 3.14. Biplot showing the results of Principal Component Analysis (PCA) on relative expression for the five genes of interest—death-associated inhibitor of apoptosis 2 (A2I), high mobility group box 1 (HMGB1), high mobility group protein DSP1 (DSP1), heat shock protein 90 (HSP90), and peptidyl-prolyl cis-trans isomerase (PPCTI)—that showed significant ($p < 0.05$) changes under single-gene response assessment. Samples are colored according to treatment group (control = blue, heatwave = red, heatwave + hypoxia = purple) and arrows represent the loadings of individual genes, with longer arrows indicating stronger contributions to the corresponding principal components. HSP90 is strongly associated with PC1, while PPCTI, HMGB1, and DSP1 are associated with PC2.

Chapter 4. Conclusion and perspectives

4.1 Candidate genes for summer mortality monitoring

A primary objective of this thesis was to identify candidate genes that show altered expression under conditions that may lead to mortality and to contribute to the development of genetically-based monitoring tools. In both experiments, five candidate genes—A2I, DSP1, HMGB1, HSP90, and PPCTI—were consistently differentially expressed under simulated heatwave conditions. Notably, changes in relative expression of those five candidate genes were detectable, even when changes in whole-organism and behavioural health metrics were not. Shell gaping and CI were assessed in both experiments, and no significant changes were observed between heatwave treatments compared to the controls. Therefore, this thesis provides additional evidence that genetically-based monitoring tools for summer mortality can detect changes in organism health that traditional whole-organism metrics cannot. In addition, the present work provides reproducible evidence that expression of those five candidate genes is altered under simulated temperature conditions similar to those that lead to mortality in the field. Thus, further investigation into the expression patterns and molecular products associated with those genes is recommended to develop reliable monitoring tools for oyster summer mortality.

Changes in relative expression of four genes related specifically to stress response in both experiments were assessed, only HSP90 showing significant differences under simulated heatwave conditions. Traditional stress marker genes like HSP70 and HSP20 were hypothesized to be potentially inappropriate for monitoring summer mortality given that their upregulation usually occurs between 32 and 38°C in Pacific oysters (Farcy et al., 2009; Lim et al., 2016; Liu et al., 2022; Y. Xu et al., 2022a; C. Yang et al., 2017; Y. Zhang et al., 2015) while summer

mortality can be triggered by water temperatures as low as $>20^{\circ}\text{C}$ (Garnier et al., 2007; Green et al., 2019; Whittington et al., 2024). The findings of the present work are consistent with that hypothesis, as no significant differences in HSP70/HSP20 relative expression were observed for simulated heatwave and hypoxia conditions in either experiment (Chapter 2 or 3). Therefore, reproducible evidence is provided that novel genetic biomarkers, beyond those already used in environmental monitoring, are needed to effectively predict the onset of summer mortality. However, HSP90 is also an established stress marker gene (Richter & Buchner, 2001), and significant differences in its relative expression were detected in both experiments. That is consistent with previous work that has supported HSP90 as a monitoring tool for heatwave-driven stress in other oyster species (Masanja et al., 2022), though it is unclear why HSP90 might be upregulated while HSP70/HSP20 are not, given that they are closely related molecular chaperones. HSP90 is involved in protein stabilization while HSP70 acts to refold denatured proteins (Richter & Buchner, 2001), so it may be that relatively mild temperature increases induce protein instability but not denaturation, resulting in exclusively HSP90 upregulation. Regardless, this thesis provides evidence that HSP90 may act as a reliable stress marker for predicting onset of summer mortality, and further investigation into its expression pattern during heatwaves is recommended.

While only one stress marker gene, HSP90, showed significant changes in relative expression for both experiments, genes associated with regulation of transcription and immune function were consistently differentially expressed in both experiments. DSP1 is a recently discovered negative regulator of HSP70 expression in *C. hongkongensis* (Miao et al., 2016), an estuarine species closely related to *C. gigas* (Zhao et al., 2014). Significant downregulation of DSP1 was observed in both experiments (Chapter 2 and 3), indicating a shift away from heat

shock suppression during the simulated heatwaves. Thus, the results of the present work provide the first indirect evidence of this regulatory mechanism in the Pacific oyster, and indicate that genes involved in HSP70 regulation may provide an early warning of heatwave-driven stress where measurement of direct HSP70 expression cannot. In addition, three genes involved in innate immune function—A2I, HMGB1, and PPCTI—showed significant changes in relative expression in both experiments (Chapter 2 and 3). Therefore, the results of the present work indicate that while traditional stress marker genes demonstrate limited utility in early prediction of summer mortality, the expression of certain regulatory and immune genes represents a promising avenue for the development of monitoring tools for heatwave-driven mortality in the Pacific oyster. Thus, future research should prioritise further investigation into the expression of immune genes during heatwaves and the characterization of regulatory pathways for stress marker genes.

4.2 Simulated heatwaves impact immune function

This thesis sought to investigate the impacts of heatwaves and hypoxia on Pacific oysters to speculate on their roles in driving summer mortality and provides evidence that those acute stressors may negatively impact immune function increasing susceptibility to mortality. Previous evidence challenged the hypothesis that marine heatwaves may impair immune function in the Pacific oyster increasing susceptibility to pathogenic infection (Green et al., 2019; Wendling & Wegner, 2013), as heat stressed oysters can still successfully activate immune response during laboratory-simulated and naturally occurring heatwaves (Green et al., 2019; Siboni et al., 2024). However, more recent evidence has demonstrated that heatwaves do indeed drive reductions in innate immunity in the early stages of infection, while immune genes become upregulated in the

late stages of infection prior to mortality (X. Li et al., 2023). The results of this thesis are consistent with that previous work, as consistent downregulation of HMGB1 and PPCTI, as well as upregulation of A2I, were observed in both experiments (Chapter 2 and 3). HMGB1 and PPCTI are both involved in innate immunity (J. Li et al., 2013; T. Xu et al., 2012; T. Xu et al., 2016) and their downregulation is associated with susceptibility to pathogenic infection (Huvet et al., 2004; J. Li et al., 2013; Lv et al., 2022). Similarly, A2I is an inhibitor of apoptosis whose upregulation may indicate a shift away from innate immunity towards cell stability (Cai et al., 2022; Witkop et al., 2022). Thus, this thesis provides evidence that simulated heatwaves drive reductions in innate immunity that may increase susceptibility to infection with pathogenic bacteria and trigger eventual mortality. However, I only assessed changes in relative expression specific to gill tissue in the present thesis. Expression in the hemocytes may be more appropriate for evaluating immune response during heatwaves, as Pacific oysters modulate gene expression differently across tissues during immune challenge (Schmitt et al., 2012) and the hemocytes are the primary immune cells in oysters. It is therefore recommended that future studies assess the tissue-specific expression of these immune genes during heatwaves.

The present thesis also provides evidence that oxygen limitation may exacerbate the negative impacts of heatwaves on immune function. In Chapter 3, a combination of heatwave and hypoxia stress resulted in significantly lower HMGB1 expression compared to a heatwave alone. Previous work has shown that DO limitation may impair immune function in oysters independent of heatwaves (Barnett et al., 2020; David et al., 2005), and research on other species has demonstrated that coinciding heatwave and hypoxia stress may exacerbate negative impacts (Del Rio et al., 2019; Earhart et al., 2022; Frakes et al., 2021; Krishna et al., 2025; Roman et al., 2019). Observed expression of HMGB1 in Chapter 3 is consistent with that previous work,

suggesting that hypoxia may exacerbate negative impacts of heatwaves on immune function and potentially increase the likelihood of summer mortality outbreaks. However, the addition of hypoxia had no significant effect on the relative expression of the other two immune genes—A2I and PPCTI—during the simulated heatwave. Given that all three of those immune genes were identified as appropriate candidates for summer mortality monitoring in Chapter 1, it is recommended that their expression in response to heatwaves and hypoxia be investigated further to better understand the role of oxygen limitation on heatwave-driven mortality of the Pacific oyster.

4.3 Artificial aeration may mitigate stress response during heatwaves

Given previous work that has identified artificial aeration as a method for increasing thermal tolerance limits in bivalves (H. O. Pörtner et al., 2006; Srisunont et al., 2022), one primary objective of this thesis was to assess the potential for artificial aeration to act as a mitigation strategy for Pacific oyster summer mortality. To this end, the experiment in Chapter 3 utilized the presence or absence of artificial aeration to simulate different oxic levels, and those results indicated that the presence of artificial aeration may alleviate thermal stress during heatwaves. Specifically, the relative expression of HSP90 was significantly higher in the heatwave treatment without artificial aeration than in the heatwave treatment with it. HSP90 is an established biomarker for heatwave-driven stress in other oyster species (Masanja et al., 2022) and was identified as an appropriate candidate gene for summer mortality monitoring in Chapter 1 of the present thesis. Given that HSP90 was the only stress marker gene reliably upregulated in both experiments, differences in its relative expression likely indicate meaningful differences in thermal stress during heatwaves. Therefore, the results of this thesis suggest that artificial

aeration may mitigate thermal stress during heatwaves, potentially conferring some resilience to summer mortality.

This thesis also provides evidence that artificial aeration may alleviate some negative impacts of heatwaves on immune function. Specifically, HMGB1 relative expression was significantly lower in the heatwave treatment without artificial aeration than in the heatwave treatment with it. Given the established role of HMGB1 in innate immunity for Pacific oysters (J. Li et al., 2013; Lv et al., 2022), those results suggest that DO limitation may exacerbate negative effects on immune function during heatwaves, and that artificial aeration could mitigate some of those negative impacts, potentially increasing resilience to mortality. That would be consistent with previous research demonstrating negative impacts of DO limitation on immune function in oysters (Barnett et al., 2020; David et al., 2005). However, no significant differences in relative expression of the other two immune genes—A2I and PPCTI—were detected between heatwave treatments with and without artificial aeration. All three of those immune genes were identified as appropriate candidates for summer mortality monitoring in Chapter 1. If artificial aeration strongly alleviated negative impacts to immune function during heatwaves, it is likely that multiple immune genes would show differences in expression. Since differences in the expression of only one of those immune genes was detected, the findings of this thesis suggest that artificial aeration likely has a neutral to slightly positive effect on immune function during heatwaves. However, as previously stated, only expression of PPCTI has been explored in other studies on summer mortality (Huvet et al., 2004). Therefore, further research is recommended into expression of these immune genes during heatwaves to further assess the potential for artificial aeration, at various levels, to mitigate negative impacts.

4.4 Conclusion

This thesis examined the effects of simulated heatwave and hypoxic conditions on gene expression in the Pacific oyster to identify candidate monitoring genes and assess the potential for artificial aeration to act as a mitigation strategy for summer mortality. Changes in relative expression of five genes—A2I, DSP1, HMGB1, HSP90, and PPCTI—demonstrated altered expression under heatwave and hypoxic conditions across two independent laboratory experiments (Chapter 2 and 3), providing reproducible evidence for their utility as monitoring tools for summer mortality. In Chapter 3, HSP90 was highly upregulated under a combination of heatwave and hypoxic conditions, indicating potentially exacerbated stress response with lowered DO, which was minimized in the presence of artificial aeration. This thesis also provides the first indirect evidence of HSP70 negative regulation by DSP1 in the Pacific oyster. Three immune genes—HMGB1, PPCTI, and A2I—showed consistently altered expression under heatwave and hypoxia conditions, indicating possible impairment of innate immunity in response to elevated temperatures and lowered DO, which may contribute to mortality. The presence of artificial aeration did alleviate some negative effects on HMGB1 expression, but did not have a clear effect on expression of other immune genes. Taken together, the results of this thesis suggest that novel molecular biomarkers other than HSP70 and HSP20 are needed to effectively predict Pacific oyster summer mortality and that immune and regulatory genes represent a promising alternative to traditional stress marker genes. In addition, artificial aeration likely alleviates some thermal stress during heatwaves and may have a neutral to positive effect on immune function (Figure 4.1). However, further investigation is needed to assess aeration as a mitigation strategy for Pacific oyster summer mortality, and to understand the role of oxygen limitation in driving that mortality. The present findings will inform effective monitoring and

mitigation practices to support the adaptation of shellfish aquaculture to the growing impacts of climate change.

4.5 Tables and figures

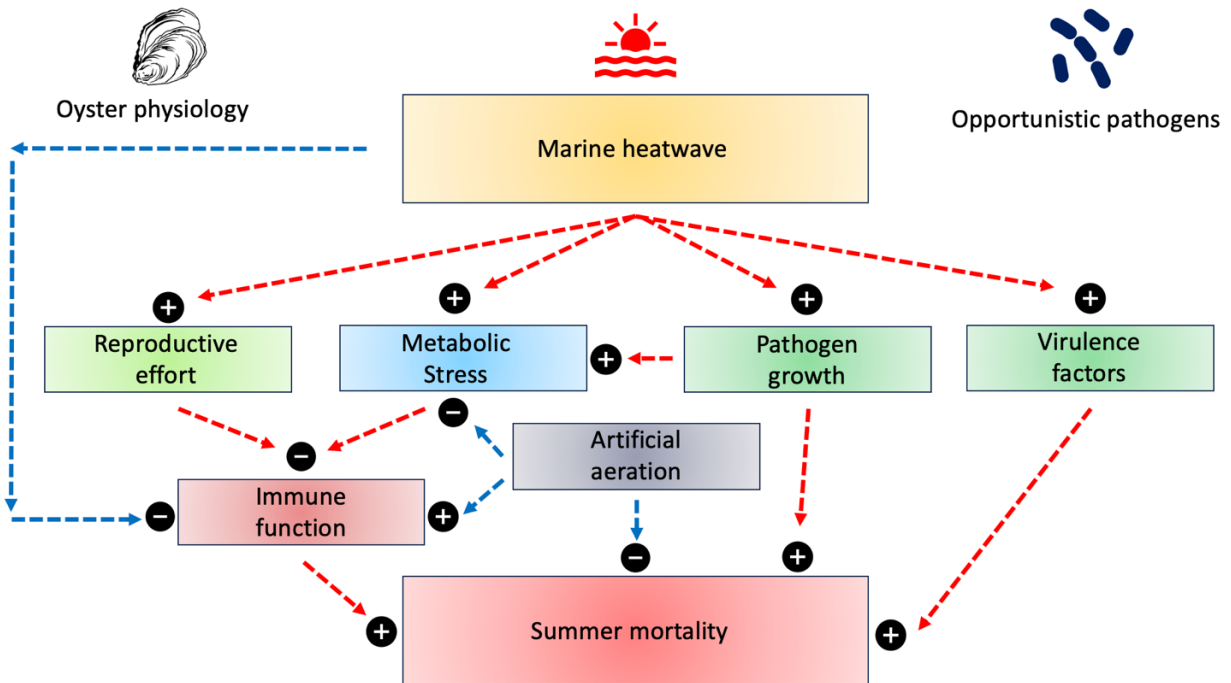


Figure 4.1. Hypothesized mechanisms by which marine heatwaves affect oyster physiology and pathogenic bacteria, contributing to Pacific oyster summer mortality, along with the proposed mitigating effects of artificial aeration. Arrows represent interactions between factors: red arrows indicate relationships established in previous studies, while blue arrows indicate potential interactions suggested by findings from this thesis. Increases and decreases in individual factors are indicated by (+) and (-), respectively.

References

- Anders, S., Pyl, P. T., & Huber, W. (2015). HTSeq—A Python framework to work with high-throughput sequencing data. *Bioinformatics*, *31*(2), 166–169.
<https://doi.org/10.1093/bioinformatics/btu638>
- Anthony, K. R. N., Kline, D. I., Diaz-Pulido, G., Dove, S., & Hoegh-Guldberg, O. (2008). Ocean acidification causes bleaching and productivity loss in coral reef builders. *Proceedings of the National Academy of Sciences*, *105*(45), 17442–17446.
<https://doi.org/10.1073/pnas.0804478105>
- Arrhenius, S. (1897). On the Influence of Carbonic Acid in the Air upon the Temperature of the Earth. *Publications of the Astronomical Society of the Pacific*, *9*, 14.
<https://doi.org/10.1086/121158>
- Bahrndorff, S., Mariën, J., Loeschke, V., & Ellers, J. (2009). Dynamics of heat-induced thermal stress resistance and hsp70 expression in the springtail, *Orchesella cincta*. *Functional Ecology*, *23*(2), 233–239. <https://doi.org/10.1111/j.1365-2435.2009.01541.x>
- Baker, A. C., Glynn, P. W., & Riegl, B. (2008). Climate change and coral reef bleaching: An ecological assessment of long-term impacts, recovery trends and future outlook. *Estuarine, Coastal and Shelf Science*, *80*(4), 435–471.
<https://doi.org/10.1016/j.ecss.2008.09.003>
- Bakun, A., Black, B. A., Bograd, S. J., García-Reyes, M., Miller, A. J., Rykaczewski, R. R., & Sydeman, W. J. (2015). Anticipated Effects of Climate Change on Coastal Upwelling Ecosystems. *Current Climate Change Reports*, *1*(2), 85–93.
<https://doi.org/10.1007/s40641-015-0008-4>

- Barbeaux, S. J., Holsman, K., & Zador, S. (2020). Marine Heatwave Stress Test of Ecosystem-Based Fisheries Management in the Gulf of Alaska Pacific Cod Fishery. *Frontiers in Marine Science*, 7, 703. <https://doi.org/10.3389/fmars.2020.00703>
- Barber, G. N. (2001). Host defense, viruses and apoptosis. *Cell Death & Differentiation*, 8(2), 113–126. <https://doi.org/10.1038/sj.cdd.4400823>
- Barnett, A. F., Gledhill, J. H., Griffith, R. J., Slattery, M., Gochfeld, D. J., & Willett, K. L. (2020). Combined and independent effects of hypoxia and tributyltin on mRNA expression and physiology of the Eastern oyster (*Crassostrea virginica*). *Scientific Reports*, 10(1), 10605. <https://doi.org/10.1038/s41598-020-67650-x>
- Bastaki, N. K., Albarjas, T. A., Almoosa, F. A., & Al-Adsani, A. M. (2023). Chronic heat stress induces the expression of HSP genes in the retina of chickens (*Gallus gallus*). *Frontiers in Genetics*, 14, 1085590. <https://doi.org/10.3389/fgene.2023.1085590>
- Berillis, P., Mente, E., Nikouli, E., Makridis, P., Grundvig, H., Bergheim, A., & Gausen, M. (2016). Improving aeration for efficient oxygenation in sea bass sea cages. Blood, brain and gill histology. *Open Life Sciences*, 11(1), 270–279. <https://doi.org/10.1515/biol-2016-0028>
- Beveridge, M. C. M., Thilsted, S. H., Phillips, M. J., Metian, M., Troell, M., & Hall, S. J. (2013). Meeting the food and nutrition needs of the poor: The role of fish and the opportunities and challenges emerging from the rise of aquaculture. *Journal of Fish Biology* 83(4), 1067–1084. <https://doi.org/10.1111/jfb.12187>
- Bolger, A. M., Lohse, M., & Usadel, B. (2014). Trimmomatic: A flexible trimmer for Illumina sequence data. *Bioinformatics*, 30(15), 2114–2120. <https://doi.org/10.1093/bioinformatics/btu170>

- Bougrier, S., Geairon, P., Deslous-Paoli, J. M., Bacher, C., & Jonquière, G. (1995). Allometric relationships and effects of temperature on clearance and oxygen consumption rates of *Crassostrea gigas* (Thunberg). *Aquaculture*, *134*(1–2), 143–154.
[https://doi.org/10.1016/0044-8486\(95\)00036-2](https://doi.org/10.1016/0044-8486(95)00036-2)
- Bourgey, M., Dali, R., Eveleigh, R., Chen, K. C., Letourneau, L., Fillon, J., Michaud, M., Caron, M., Sandoval, J., Lefebvre, F., Leveque, G., Mercier, E., Bujold, D., Marquis, P., Van, P. T., Anderson De Lima Morais, D., Tremblay, J., Shao, X., Henrion, E., & Bourque, G. (2019). GenPipes: An open-source framework for distributed and scalable genomic analyses. *GigaScience*, *8*(6), giz037. <https://doi.org/10.1093/gigascience/giz037>
- Boyd, C. E., McNevin, A. A., & Davis, R. P. (2022). The contribution of fisheries and aquaculture to the global protein supply. *Food Security*, *14*(3), 805–827.
<https://doi.org/10.1007/s12571-021-01246-9>
- Brandt, S., Wassmann, P., & Piepenburg, D. (2023). Revisiting the footprints of climate change in Arctic marine food webs: An assessment of knowledge gained since 2010. *Frontiers in Marine Science*, *10*, 1096222. <https://doi.org/10.3389/fmars.2023.1096222>
- Breitburg, D., Levin, L. A., Oschlies, A., Grégoire, M., Chavez, F. P., Conley, D. J., Garçon, V., Gilbert, D., Gutiérrez, D., Isensee, K., Jacinto, G. S., Limburg, K. E., Montes, I., Naqvi, S. W. A., Pitcher, G. C., Rabalais, N. N., Roman, M. R., Rose, K. A., Seibel, B. A., & Zhang, J. (2018). Declining oxygen in the global ocean and coastal waters. *Science*, *359*(6371), eaam7240. <https://doi.org/10.1126/science.aam7240>
- Bruhns, T., Timm, S., Feußner, N., Engelhaupt, S., Labrenz, M., Wegner, M., & Sokolova, I. M. (2023). Combined effects of temperature and emersion-immersion cycles on metabolism

- and bioenergetics of the Pacific oyster *Crassostrea (Magallana) gigas*. *Marine Environmental Research*, 192, 106231. <https://doi.org/10.1016/j.marenvres.2023.106231>
- Burke, M., Grant, J., Filgueira, R., & Swanson, A. (2022). Oxygenation effects on temperature and dissolved oxygen at a commercial Atlantic salmon farm. *Aquacultural Engineering*, 99, 102287. <https://doi.org/10.1016/j.aquaeng.2022.102287>
- Cai, X., Chen, H., Qian, M., Wu, Y., Yang, Q., Fang, J., & Wu, X. (2022). A novel inhibitor of apoptosis protein (IAPs) from *Crassostrea gigas* is involved in anti-apoptosis and innate defense role under *Vibrio alginolyticus* stimulation. *Aquaculture Reports*, 27, 101379. <https://doi.org/10.1016/j.aqrep.2022.101379>
- Calvin, K., Dasgupta, D., Krinner, G., Mukherji, A., Thorne, P. W., Trisos, C., Romero, J., Aldunce, P., Barrett, K., Blanco, G., Cheung, W. W. L., Connors, S., Denton, F., Diongue-Niang, A., Dodman, D., Garschagen, M., Geden, O., Hayward, B., Jones, C., & Péan, C. (2023). *IPCC, 2023: Climate Change 2023: Synthesis Report. Contribution of Working Groups I, II and III to the Sixth Assessment Report of the Intergovernmental Panel on Climate Change [Core Writing Team, H. Lee and J. Romero (eds.)]. IPCC, Geneva, Switzerland*. (First). Intergovernmental Panel on Climate Change (IPCC). <https://doi.org/10.59327/IPCC/AR6-9789291691647>
- Caputi, N., Kangas, M., Chandrapavan, A., Hart, A., Feng, M., Marin, M., & Lestang, S. D. (2019). Factors Affecting the Recovery of Invertebrate Stocks From the 2011 Western Australian Extreme Marine Heatwave. *Frontiers in Marine Science*, 6, 484. <https://doi.org/10.3389/fmars.2019.00484>

- Carrier-Belleau, C., Drolet, D., McKindsey, C. W., & Archambault, P. (2021). Environmental stressors, complex interactions and marine benthic communities' responses. *Scientific Reports*, *11*(1), 4194. <https://doi.org/10.1038/s41598-021-83533-1>
- Chaney, M. L., & Gracey, A. Y. (2011). Mass mortality in Pacific oysters is associated with a specific gene expression signature. *Molecular Ecology*, *20*(14), 2942–2954. <https://doi.org/10.1111/j.1365-294X.2011.05152.x>
- Chávez-Villalba, J., Villelas-Ávila, R., & Cáceres-Martínez, C. (2007). Reproduction, condition and mortality of the Pacific oyster *Crassostrea gigas* (Thunberg) in Sonora, México: Reproduction, condition, and mortality of *C. gigas*. *Aquaculture Research*, *38*(3), 268–278. <https://doi.org/10.1111/j.1365-2109.2007.01662.x>
- Chen, L., Mu, C., Zhao, J., & Wang, C. (2011). Molecular cloning and characterization of two isoforms of cyclophilin A gene from *Venerupis philippinarum*. *Fish & Shellfish Immunology*, *31*(6), 1218–1223. <https://doi.org/10.1016/j.fsi.2011.07.001>
- Chung-Do, J. J., Hwang, P. W., Ho-Lastimosa, I., Rogerson, I., Ho, K., DeMello, K., Kauahikaua, D., & Ahn, H. J. (2024). MALAMA: Cultivating Food Sovereignty through Backyard Aquaponics with Native Hawaiian Families. *Genealogy*, *8*(3), 101. <https://doi.org/10.3390/genealogy8030101>
- Clarke, A., Murphy, E. J., Meredith, M. P., King, J. C., Peck, L. S., Barnes, D. K. A., & Smith, R. C. (2007). Climate change and the marine ecosystem of the western Antarctic Peninsula. *Philosophical Transactions of the Royal Society B: Biological Sciences*, *362*(1477), 149–166. <https://doi.org/10.1098/rstb.2006.1958>

- Coen, L., Brumbaugh, R., Bushek, D., Grizzle, R., Luckenbach, M., Posey, M., Powers, S., & Tolley, S. (2007). Ecosystem services related to oyster restoration. *Marine Ecology Progress Series*, 341, 303–307. <https://doi.org/10.3354/meps341303>
- Coffin, M. R. S., Clements, J. C., Comeau, L. A., Guyondet, T., Maillet, M., Steeves, L., Winterburn, K., Babarro, J. M. F., Mallet, M. A., Haché, R., Poirier, L. A., Deb, S., & Filgueira, R. (2021). The killer within: Endogenous bacteria accelerate oyster mortality during sustained anoxia. *Limnology and Oceanography*, 66(7), 2885–2900. <https://doi.org/10.1002/lno.11798>
- Conceição, M. V. R., Costa, S. S., Schaan, A. P., Ribeiro-dos-Santos, Â. K. C., Silva, A., Das Graças, D. A., Schneider, M. P. C., & Baraúna, R. A. (2021). Amazonia Seasons Have an Influence in the Composition of Bacterial Gut Microbiota of Mangrove Oysters (*Crassostrea gasar*). *Frontiers in Genetics*, 11, 602608. <https://doi.org/10.3389/fgene.2020.602608>
- Connolly, T. P., Hickey, B. M., Geier, S. L., & Cochlan, W. P. (2010). Processes influencing seasonal hypoxia in the northern California Current System. *Journal of Geophysical Research: Oceans*, 115(C3), 2009JC005283. <https://doi.org/10.1029/2009JC005283>
- Cowan, M. W., Pearce, C. M., Finston, T., Meyer, G. R., Marshall, R., Evans, W., Sutherland, T. F., & De La Bastide, P. Y. (2023). Role of the *Vibrio* community, reproductive effort, and environmental parameters in intertidal Pacific oyster summer mortality in British Columbia, Canada. *Aquaculture*, 565, 739094. <https://doi.org/10.1016/j.aquaculture.2022.739094>
- Cowan, M. W., Pearce, C. M., Green, T. J., Finston, T., Meyer, G. R., McAmmond, B., Van Hamme, J. D., Bottos, E. M., Marshall, R., Evans, W., Sutherland, T. F., & De La Bastide,

- P. Y. (2024). Abundance of *Vibrio aestuarianus*, water temperature, and stocking density are associated with summer mortality of Pacific oysters in suspended culture. *Aquaculture International*, 32(4), 5045–5066. <https://doi.org/10.1007/s10499-024-01415-5>
- Cuff, S., & Ruby, J. (1996). Evasion of apoptosis by DNA viruses. *Immunology & Cell Biology*, 74(6), 527–537. <https://doi.org/10.1038/icb.1996.86>
- Cunning, R., & Baker, A. C. (2013). Excess algal symbionts increase the susceptibility of reef corals to bleaching. *Nature Climate Change*, 3(3), 259–262. <https://doi.org/10.1038/nclimate1711>
- Curnock, M. I., Marshall, N. A., Thiault, L., Heron, S. F., Hoey, J., Williams, G., Taylor, B., Pert, P. L., & Goldberg, J. (2019). Shifts in tourists' sentiments and climate risk perceptions following mass coral bleaching of the Great Barrier Reef. *Nature Climate Change*, 9(7), 535–541. <https://doi.org/10.1038/s41558-019-0504-y>
- David, E., Tanguy, A., Pichavant, K., & Moraga, D. (2005). Response of the Pacific oyster *Crassostrea gigas* to hypoxia exposure under experimental conditions. *The FEBS Journal*, 272(21), 5635–5652. <https://doi.org/10.1111/j.1742-4658.2005.04960.x>
- De La Maza, L., & Fariás, L. (2023). The intensification of coastal hypoxia off central Chile: Long term and high frequency variability. *Frontiers in Earth Science*, 10, 929271. <https://doi.org/10.3389/feart.2022.929271>
- De Lorgeril, J., Zenagui, R., Rosa, R. D., Piquemal, D., & Bachère, E. (2011). Whole Transcriptome Profiling of Successful Immune Response to *Vibrio* Infections in the Oyster *Crassostrea gigas* by Digital Gene Expression Analysis. *PLoS ONE*, 6(8), e23142. <https://doi.org/10.1371/journal.pone.0023142>

- De Marco, A., Baldassarro, V. A., Calzà, L., Giardino, L., Dondi, F., Ferrari, M. G., Bignami, G., Parma, L., & Bonaldo, A. (2023). Prolonged heat waves reduce the condition index and alter the molecular parameters in the pacific oyster *Crassostrea gigas*. *Fish & Shellfish Immunology*, *133*, 108518. <https://doi.org/10.1016/j.fsi.2023.108518>
- Deb, J. C., & Bailey, S. A. (2023). Arctic marine ecosystems face increasing climate stress. *Environmental Reviews*, *31*(3), 403–451. <https://doi.org/10.1139/er-2022-0101>
- Dégremont, L., Bédier, E., & Boudry, P. (2010). Summer mortality of hatchery-produced Pacific oyster spat (*Crassostrea gigas*). II. Response to selection for survival and its influence on growth and yield. *Aquaculture*, *299*(1–4), 21–29. <https://doi.org/10.1016/j.aquaculture.2009.11.017>
- Del Rio, A. M., Davis, B. E., Fangue, N. A., & Todgham, A. E. (2019). Combined effects of warming and hypoxia on early life stage Chinook salmon physiology and development. *Conservation Physiology*, *7*(1). <https://doi.org/10.1093/conphys/coy078>
- Delaporte, M., Soudant, P., Lambert, C., Moal, J., Pouvreau, S., & Samain, J.-F. (2006). Impact of food availability on energy storage and defense related hemocyte parameters of the Pacific oyster *Crassostrea gigas* during an experimental reproductive cycle. *Aquaculture*, *254*(1–4), 571–582. <https://doi.org/10.1016/j.aquaculture.2005.10.006>
- Department of Fisheries and Oceans Canada. (2023). *Aquaculture production quantities and value*. <https://www.dfo-mpo.gc.ca/stats/aqua/aqua23-eng.html>
- Diaz, R. J. (2001). Overview of Hypoxia around the World. *Journal of Environmental Quality*, *30*(2), 275–281. <https://doi.org/10.2134/jeq2001.302275x>
- Dimitriadis, V. K., Gougoula, C., Anestis, A., Pörtner, H. O., & Michaelidis, B. (2012). Monitoring the biochemical and cellular responses of marine bivalves during thermal

- stress by using biomarkers. *Marine Environmental Research*, 73, 70–77.
<https://doi.org/10.1016/j.marenvres.2011.11.004>
- Dobin, A., Davis, C. A., Schlesinger, F., Drenkow, J., Zaleski, C., Jha, S., Batut, P., Chaisson, M., & Gingeras, T. R. (2013). STAR: Ultrafast universal RNA-seq aligner. *Bioinformatics*, 29(1), 15–21. <https://doi.org/10.1093/bioinformatics/bts635>
- Dondero, F., Dagnino, A., Jonsson, H., Capri, F., Gastaldi, L., & Viarengo, A. (2006). Assessing the occurrence of a stress syndrome in mussels (*Mytilus edulis*) using a combined biomarker/gene expression approach. *Aquatic Toxicology*, 78, S13–S24.
<https://doi.org/10.1016/j.aquatox.2006.02.025>
- Doney, S. C., Fabry, V. J., Feely, R. A., & Kleypas, J. A. (2009). Ocean Acidification: The Other CO₂ Problem. *Annual Review of Marine Science*, 1(1), 169–192.
<https://doi.org/10.1146/annurev.marine.010908.163834>
- Doney, S. C., Ruckelshaus, M., Emmett Duffy, J., Barry, J. P., Chan, F., English, C. A., Galindo, H. M., Grebmeier, J. M., Hollowed, A. B., Knowlton, N., Polovina, J., Rabalais, N. N., Sydeman, W. J., & Talley, L. D. (2012). Climate Change Impacts on Marine Ecosystems. *Annual Review of Marine Science*, 4(1), 11–37. <https://doi.org/10.1146/annurev-marine-041911-111611>
- Doshi, A., Pascoe, S., Thébaud, O., Thomas, C. R., Setiasih, N., Hong, J. T. C., True, J., Schuttenberg, H. Z., & Heron, S. F. (2012). *Loss of economic value from coral bleaching in S.E. Asia*.
- Doyle, S. M., Self, M. J., Hayes, J., Shamberger, K. E. F., Correa, A. M. S., Davies, S. W., Santiago-Vázquez, L. Z., & Sylvan, J. B. (2022). Microbial Community Dynamics

- Provide Evidence for Hypoxia during a Coral Reef Mortality Event. *Applied and Environmental Microbiology*, 88(9), e00347-22. <https://doi.org/10.1128/aem.00347-22>
- Earhart, M. L., Blanchard, T. S., Harman, A. A., & Schulte, P. M. (2022). Hypoxia and High Temperature as Interacting Stressors: Will Plasticity Promote Resilience of Fishes in a Changing World? *The Biological Bulletin*, 243(2), 149–170.
<https://doi.org/10.1086/722115>
- EFSA Panel on Animal Health and Welfare (AHAW). (2015). Oyster mortality. *EFSA Journal*, 13(6). <https://doi.org/10.2903/j.efsa.2015.4122>
- Encomio, V., & Chu, F. (2005). Seasonal Variation Of Heat Shock Protein 70 In Eastern Oysters (*Crassostrea Virginica*) Infected With Perkinsus Marinus (Dermo). *Journal of Shellfish Research*, 24(1), 167–175.
- Engelhard, G. H., Righton, D. A., & Pinnegar, J. K. (2014). Climate change and fishing: A century of shifting distribution in North Sea cod. *Global Change Biology*, 20(8), 2473–2483. <https://doi.org/10.1111/gcb.12513>
- Evans, T. G., & Hofmann, G. E. (2012). Defining the limits of physiological plasticity: How gene expression can assess and predict the consequences of ocean change. *Philosophical Transactions of the Royal Society B: Biological Sciences*, 367(1596), 1733–1745.
<https://doi.org/10.1098/rstb.2012.0019>
- Farcy, E., Voiseux, C., Lebel, J.-M., & Fievet, B. (2007). Seasonal changes in mRNA encoding for cell stress markers in the oyster *Crassostrea gigas* exposed to radioactive discharges in their natural environment. *Science of The Total Environment*, 374(2–3), 328–341.
<https://doi.org/10.1016/j.scitotenv.2006.11.014>

- Farcy, E., Voiseux, C., Lebel, J.-M., & Fiévet, B. (2009). Transcriptional expression levels of cell stress marker genes in the Pacific oyster *Crassostrea gigas* exposed to acute thermal stress. *Cell Stress and Chaperones*, *14*(4), 371–380. <https://doi.org/10.1007/s12192-008-0091-8>
- Fisher, R., O’Leary, R. A., Low-Choy, S., Mengersen, K., Knowlton, N., Brainard, R. E., & Caley, M. J. (2015). Species Richness on Coral Reefs and the Pursuit of Convergent Global Estimates. *Current Biology*, *25*(4), 500–505. <https://doi.org/10.1016/j.cub.2014.12.022>
- Frakes, J. I., Birrell, J. H., Shah, A. A., & Woods, H. A. (2021). Flow increases tolerance of heat and hypoxia of an aquatic insect. *Biology Letters*, *17*(5), rsbl.2021.0004, 20210004. <https://doi.org/10.1098/rsbl.2021.0004>
- Fu, H., Li, Y., Tian, J., Yang, B., Li, Y., Li, Q., & Liu, S. (2023). Contribution of HIF-1 α to Heat Shock Response by Transcriptional Regulation of HSF1/HSP70 Signaling Pathway in Pacific Oyster, *Crassostrea gigas*. *Marine Biotechnology*, *25*(5), 691–700. <https://doi.org/10.1007/s10126-023-10231-6>
- Gagnaire, B., Frouin, H., Moreau, K., Thomas-Guyon, H., & Renault, T. (2006). Effects of temperature and salinity on haemocyte activities of the Pacific oyster, *Crassostrea gigas* (Thunberg). *Fish & Shellfish Immunology*, *20*(4), 536–547. <https://doi.org/10.1016/j.fsi.2005.07.003>
- Galappaththi, E. K., Ford, J. D., Bennett, E. M., & Berkes, F. (2021). Adapting to climate change in small-scale fisheries: Insights from indigenous communities in the global north and south. *Environmental Science & Policy*, *116*, 160–170. <https://doi.org/10.1016/j.envsci.2020.11.009>

- Gammelsrød, T., Bartholomae, C. H., Boyer, D. C., Filipe, V. L. L., & O'Toole, M. J. (1998). Intrusion of warm surface water along the Angolan-Namibian coast in February–March 1995: The 1995 Benguela *Nino*. *South African Journal of Marine Science*, *19*(1), 41–56. <https://doi.org/10.2989/025776198784126719>
- García Molinos, J., Hunt, H. L., Green, M. E., Champion, C., Hartog, J. R., & Pecl, G. T. (2022). Climate, currents and species traits contribute to early stages of marine species redistribution. *Communications Biology*, *5*(1), 1329. <https://doi.org/10.1038/s42003-022-04273-0>
- Garlock, T. M., Asche, F., Anderson, J. L., Eggert, H., Anderson, T. M., Che, B., Chávez, C. A., Chu, J., Chukwuone, N., Dey, M. M., Fitzsimmons, K., Flores, J., Guillen, J., Kumar, G., Liu, L., Llorente, I., Nguyen, L., Nielsen, R., Pincinato, R. B. M., & Tveteras, R. (2024). Environmental, economic, and social sustainability in aquaculture: The aquaculture performance indicators. *Nature Communications*, *15*(1), 5274. <https://doi.org/10.1038/s41467-024-49556-8>
- Garner, J. B., Chamberlain, A. J., Vander Jagt, C., Nguyen, T. T. T., Mason, B. A., Marett, L. C., Leury, B. J., Wales, W. J., & Hayes, B. J. (2020). Gene expression of the heat stress response in bovine peripheral white blood cells and milk somatic cells in vivo. *Scientific Reports*, *10*(1), 19181. <https://doi.org/10.1038/s41598-020-75438-2>
- Garnier, M., Labreuche, Y., Garcia, C., Robert, M., & Nicolas, J.-L. (2007). Evidence for the Involvement of Pathogenic Bacteria in Summer Mortalities of the Pacific Oyster *Crassostrea gigas*. *Microbial Ecology*, *53*(2), 187–196. <https://doi.org/10.1007/s00248-006-9061-9>

- Garrabou, J., Gómez-Gras, D., Ledoux, J.-B., Linares, C., Bensoussan, N., López-Sendino, P., Bazairi, H., Espinosa, F., Ramdani, M., Grimes, S., Benabdi, M., Souissi, J. B., Soufi, E., Khamassi, F., Ghanem, R., Ocaña, O., Ramos-Esplà, A., Izquierdo, A., Anton, I., & Harmelin, J. G. (2019). Collaborative Database to Track Mass Mortality Events in the Mediterranean Sea. *Frontiers in Marine Science*, 6, 707.
<https://doi.org/10.3389/fmars.2019.00707>
- Gentemann, C. L., Fewings, M. R., & García-Reyes, M. (2017). Satellite sea surface temperatures along the West Coast of the United States during the 2014–2016 northeast Pacific marine heat wave. *Geophysical Research Letters*, 44(1), 312–319.
<https://doi.org/10.1002/2016GL071039>
- Go, J., Deutscher, A., Spiers, Z., Dahle, K., Kirkland, P., & Jenkins, C. (2017). Mass mortalities of unknown aetiology in Pacific oysters *Crassostrea gigas* in Port Stephens, New South Wales, Australia. *Diseases of Aquatic Organisms*, 125(3), 227–242.
<https://doi.org/10.3354/dao03146>
- Goedken, M., Morsey, B., Sunila, I., & De Guise, S. (2005). Immunomodulation of *Crassostrea gigas* and *Crassostrea virginica* cellular defense mechanisms by *Perkinsus marinus*. *Journal of Shellfish Research*, 24(2), 487–496. [https://doi.org/10.2983/0730-8000\(2005\)24\[487:IOCGAC\]2.0.CO;2](https://doi.org/10.2983/0730-8000(2005)24[487:IOCGAC]2.0.CO;2)
- Golden, C. D., Koehn, J. Z., Shepon, A., Passarelli, S., Free, C. M., Viana, D. F., Matthey, H., Eurich, J. G., Gephart, J. A., Fluet-Chouinard, E., Nyboer, E. A., Lynch, A. J., Kjellevold, M., Bromage, S., Charlebois, P., Barange, M., Vannuccini, S., Cao, L., Kleisner, K. M., & Thilsted, S. H. (2021). Aquatic foods to nourish nations. *Nature*, 598(7880), 315–320.
<https://doi.org/10.1038/s41586-021-03917-1>

- Green, T. J., & Montagnani, C. (2013). Poly I:C induces a protective antiviral immune response in the Pacific oyster (*Crassostrea gigas*) against subsequent challenge with Ostreid herpesvirus (OsHV-1 μ var). *Fish & Shellfish Immunology*, 35(2), 382–388.
<https://doi.org/10.1016/j.fsi.2013.04.051>
- Green, T. J., Siboni, N., King, W. L., Labbate, M., Seymour, J. R., & Raftos, D. (2019). Simulated Marine Heat Wave Alters Abundance and Structure of *Vibrio* Populations Associated with the Pacific Oyster Resulting in a Mass Mortality Event. *Microbial Ecology*, 77(3), 736–747. <https://doi.org/10.1007/s00248-018-1242-9>
- Gupta, S. C., Sharma, A., Mishra, M., Mishra, R. K., & Chowdhuri, D. K. (2010). Heat shock proteins in toxicology: How close and how far? *Life Sciences*, 86(11–12), 377–384.
<https://doi.org/10.1016/j.lfs.2009.12.015>
- Hamdoun, A. M., Cheney, D. P., & Cherr, G. N. (2003). Phenotypic Plasticity of HSP70 and HSP70 Gene Expression in the Pacific Oyster (*Crassostrea gigas*): Implications for Thermal Limits and Induction of Thermal Tolerance. *The Biological Bulletin*, 205(2), 160–169. <https://doi.org/10.2307/1543236>
- Hamilton, M., Robinson, J. P. W., Benkwitt, C. E., Wilson, S. K., MacNeil, M. A., Ebrahim, A., & Graham, N. A. J. (2022). Climate impacts alter fisheries productivity and turnover on coral reefs. *Coral Reefs*, 41(4), 921–935. <https://doi.org/10.1007/s00338-022-02265-4>
- Harada, E., & Goto, S. G. (2017). Upregulation of heat-shock proteins in larvae, but not adults, of the flesh fly during hot summer days. *Cell Stress and Chaperones*, 22(6), 823–831.
<https://doi.org/10.1007/s12192-017-0812-y>
- He, X., Wu, F., Wang, L., Li, L., & Zhang, G. (2022). Integrated application of transcriptomics and metabolomics provides insights into condition index difference mechanisms in the

- Pacific oyster (*Crassostrea gigas*). *Genomics*, 114(4), 110413.
<https://doi.org/10.1016/j.ygeno.2022.110413>
- Heo, J.-M., Kim, S.-S., Kim, D.-Y., Lee, S. W., Lee, J. S., Kang, M. H., & Kim, S. E. (2023). Impact of exposure temperature rise on mass mortality of tidal flat pacific oysters. *Frontiers in Marine Science*, 10, 1275521. <https://doi.org/10.3389/fmars.2023.1275521>
- Hilborn, R., Amoroso, R. O., Anderson, C. M., Baum, J. K., Branch, T. A., Costello, C., De Moor, C. L., Faraj, A., Hively, D., Jensen, O. P., Kurota, H., Little, L. R., Mace, P., McClanahan, T., Melnychuk, M. C., Minto, C., Osio, G. C., Parma, A. M., Pons, M., & Ye, Y. (2020). Effective fisheries management instrumental in improving fish stock status. *Proceedings of the National Academy of Sciences*, 117(4), 2218–2224.
<https://doi.org/10.1073/pnas.1909726116>
- Hobday, A. J., Alexander, L. V., Perkins, S. E., Smale, D. A., Straub, S. C., Oliver, E. C. J., Benthuisen, J. A., Burrows, M. T., Donat, M. G., Feng, M., Holbrook, N. J., Moore, P. J., Scannell, H. A., Sen Gupta, A., & Wernberg, T. (2016). A hierarchical approach to defining marine heatwaves. *Progress in Oceanography*, 141, 227–238.
<https://doi.org/10.1016/j.pocean.2015.12.014>
- Hoegh-Guldberg, O., Poloczanska, E. S., Skirving, W., & Dove, S. (2017). Coral Reef Ecosystems under Climate Change and Ocean Acidification. *Frontiers in Marine Science*, 4, 158. <https://doi.org/10.3389/fmars.2017.00158>
- Hoffmann, A. A., & Daborn, P. J. (2007a). Towards genetic markers in animal populations as biomonitors for human-induced environmental change. *Ecology Letters*, 10(1), 63–76.
<https://doi.org/10.1111/j.1461-0248.2006.00985.x>

- Hoffmann, A. A., & Daborn, P. J. (2007b). Towards genetic markers in animal populations as biomonitors for human-induced environmental change. *Ecology Letters*, *10*(1), 63–76. <https://doi.org/10.1111/j.1461-0248.2006.00985.x>
- Huang, L., Smith, M. D., & Craig, J. K. (2010). Quantifying the Economic Effects of Hypoxia on a Fishery for Brown Shrimp *Farfantepenaeus aztecus*. *Marine and Coastal Fisheries*, *2*(1), 232–248. <https://doi.org/10.1577/C09-048.1>
- Huvet, A., Herpin, A., Dégremont, L., Labreuche, Y., Samain, J.-F., & Cunningham, C. (2004). The identification of genes from the oyster *Crassostrea gigas* that are differentially expressed in progeny exhibiting opposed susceptibility to summer mortality. *Gene*, *343*(1), 211–220. <https://doi.org/10.1016/j.gene.2004.09.008>
- Ingels, J., Vanreusel, A., Brandt, A., Catarino, A. I., David, B., De Ridder, C., Dubois, P., Gooday, A. J., Martin, P., Pasotti, F., & Robert, H. (2012). Possible effects of global environmental changes on Antarctic benthos: A synthesis across five major taxa. *Ecology and Evolution*, *2*(2), 453–485. <https://doi.org/10.1002/ece3.96>
- Intergovernmental Panel On Climate Change (Ipcc). (2022). *The Ocean and Cryosphere in a Changing Climate: Special Report of the Intergovernmental Panel on Climate Change* (1st ed.). Cambridge University Press. <https://doi.org/10.1017/9781009157964>
- Intergovernmental Panel On Climate Change (Ipcc). (2023). *Climate Change 2021 – The Physical Science Basis: Working Group I Contribution to the Sixth Assessment Report of the Intergovernmental Panel on Climate Change* (1st ed.). Cambridge University Press. <https://doi.org/10.1017/9781009157896>

- James, N. C., & Whitfield, A. K. (2023). The role of macroalgae as nursery areas for fish species within coastal seascapes. *Cambridge Prisms: Coastal Futures, 1*, e3.
<https://doi.org/10.1017/cft.2022.3>
- Jeyachandran, S., Chellapandian, H., Park, K., & Kwak, I.-S. (2023). A Review on the Involvement of Heat Shock Proteins (Extrinsic Chaperones) in Response to Stress Conditions in Aquatic Organisms. *Antioxidants, 12*(7), 1444.
<https://doi.org/10.3390/antiox12071444>
- Johnson, M. D., Scott, J. J., Leray, M., Lucey, N., Bravo, L. M. R., Wied, W. L., & Altieri, A. H. (2021). Rapid ecosystem-scale consequences of acute deoxygenation on a Caribbean coral reef. *Nature Communications, 12*(1), 4522. <https://doi.org/10.1038/s41467-021-24777-3>
- Jones, T., Parrish, J. K., Peterson, W. T., Bjorkstedt, E. P., Bond, N. A., Ballance, L. T., Bowes, V., Hipfner, J. M., Burgess, H. K., Dolliver, J. E., Lindquist, K., Lindsey, J., Nevins, H. M., Robertson, R. R., Roletto, J., Wilson, L., Joyce, T., & Harvey, J. (2018). Massive Mortality of a Planktivorous Seabird in Response to a Marine Heatwave. *Geophysical Research Letters, 45*(7), 3193–3202. <https://doi.org/10.1002/2017GL076164>
- Joyce, A. L., & Satterfield, T. A. (2010). Shellfish aquaculture and First Nations' sovereignty: The quest for sustainable development in contested sea space. *Natural Resources Forum, 34*(2), 106–123. <https://doi.org/10.1111/j.1477-8947.2010.01297.x>
- Kajtar, J. B., Holbrook, N. J., Lyth, A., Hobday, A. J., Mundy, C. N., & Ugalde, S. C. (2024). A stakeholder-guided marine heatwave hazard index for fisheries and aquaculture. *Climatic Change, 177*(2), 26. <https://doi.org/10.1007/s10584-024-03684-8>

- Kawabe, S., & Yokoyama, Y. (2012). Role of Hypoxia-Inducible Factor α in Response to Hypoxia and Heat Shock in the Pacific Oyster *Crassostrea gigas*. *Marine Biotechnology*, *14*(1), 106–119. <https://doi.org/10.1007/s10126-011-9394-3>
- Kawai, Y., Oka, E., Sato, K., Hosoda, S., & Kido, S. (2025). Marine heatwave in the Oyashio region in 2022/23 and its impact on subsurface dissolved oxygen. *Journal of Oceanography*, *81*(1), 23–39. <https://doi.org/10.1007/s10872-024-00731-x>
- Kikstra, J. S., Nicholls, Z. R. J., Smith, C. J., Lewis, J., Lamboll, R. D., Byers, E., Sandstad, M., Meinshausen, M., Gidden, M. J., Rogelj, J., Kriegler, E., Peters, G. P., Fuglestedt, J. S., Skeie, R. B., Samset, B. H., Wienpahl, L., Van Vuuren, D. P., Van Der Wijst, K.-I., Al Khourdajie, A., & Riahi, K. (2022). The IPCC Sixth Assessment Report WGIII climate assessment of mitigation pathways: From emissions to global temperatures. *Geoscientific Model Development*, *15*(24), 9075–9109. <https://doi.org/10.5194/gmd-15-9075-2022>
- Kim, B.-M., Kim, K., Choi, I.-Y., & Rhee, J.-S. (2017). Transcriptome response of the Pacific oyster, *Crassostrea gigas* susceptible to thermal stress: A comparison with the response of tolerant oyster. *Molecular & Cellular Toxicology*, *13*(1), 105–113. <https://doi.org/10.1007/s13273-017-0011-z>
- Kimes, N. E., Grim, C. J., Johnson, W. R., Hasan, N. A., Tall, B. D., Kothary, M. H., Kiss, H., Munk, A. C., Tapia, R., Green, L., Detter, C., Bruce, D. C., Brettin, T. S., Colwell, R. R., & Morris, P. J. (2012). Temperature regulation of virulence factors in the pathogen *Vibrio coralliilyticus*. *The ISME Journal*, *6*(4), 835–846. <https://doi.org/10.1038/ismej.2011.154>
- King, W. L., Jenkins, C., Go, J., Siboni, N., Seymour, J. R., & Labbate, M. (2019). Characterisation of the Pacific Oyster Microbiome During a Summer Mortality Event. *Microbial Ecology*, *77*(2), 502–512. <https://doi.org/10.1007/s00248-018-1226-9>

- Krishna, S., Lemmen, C., Örey, S., Rehren, J., Pane, J. D., Mathis, M., Püts, M., Hokamp, S., Pradhan, H. K., Hasenbein, M., Scheffran, J., & Wirtz, K. W. (2025). Interactive effects of multiple stressors in coastal ecosystems. *Frontiers in Marine Science*, *11*, 1481734. <https://doi.org/10.3389/fmars.2024.1481734>
- La, V. T., & Cooke, S. J. (2011). Advancing the Science and Practice of Fish Kill Investigations. *Reviews in Fisheries Science*, *19*(1), 21–33. <https://doi.org/10.1080/10641262.2010.531793>
- Lam, V. W. Y., Cheung, W. W. L., Reygondeau, G., & Sumaila, U. R. (2016). Projected change in global fisheries revenues under climate change. *Scientific Reports*, *6*(1), 32607. <https://doi.org/10.1038/srep32607>
- Lan, J., Liu, P., Hu, X., & Zhu, S. (2024). Harmful Algal Blooms in Eutrophic Marine Environments: Causes, Monitoring, and Treatment. *Water*, *16*(17), 2525. <https://doi.org/10.3390/w16172525>
- Le, C.-Y., Feng, J.-C., Sun, L., Yuan, W., Wu, G., Zhang, S., & Yang, Z. (2023). Co-benefits of carbon sink and low carbon food supply via shellfish and algae farming in China from 2003 to 2020. *Journal of Cleaner Production*, *414*, 137436. <https://doi.org/10.1016/j.jclepro.2023.137436>
- Le Moullac, G., Quéau, I., Le Souchu, P., Pouvreau, S., Moal, J., René Le Coz, J., & François Samain, J. (2007). Metabolic adjustments in the oyster *Crassostrea gigas* according to oxygen level and temperature. *Marine Biology Research*, *3*(5), 357–366. <https://doi.org/10.1080/17451000701635128>

- Lebel, L., Lebel, P., & Lebel, B. (2016). Impacts, Perceptions and Management of Climate-Related Risks to Cage Aquaculture in the Reservoirs of Northern Thailand. *Environmental Management*, 58(6), 931–945. <https://doi.org/10.1007/s00267-016-0764-5>
- Lee, S., Jo, Q., Han, J., Park, Y., & Park, T. (2017). Pelagic oxycline and damage potential of hypoxia to the Pacific oyster *Crassostrea gigas* suspended in longline aquaculture systems. *Aquaculture Environment Interactions*, 9, 461–468. <https://doi.org/10.3354/aei00245>
- Lefcheck, J. S., Hughes, B. B., Johnson, A. J., Pfirmann, B. W., Rasher, D. B., Smyth, A. R., Williams, B. L., Beck, M. W., & Orth, R. J. (2019). Are coastal habitats important nurseries? A meta-analysis. *Conservation Letters*, 12(4), e12645. <https://doi.org/10.1111/conl.12645>
- Lemasson, A. J., Fletcher, S., Hall-Spencer, J. M., & Knights, A. M. (2017). Linking the biological impacts of ocean acidification on oysters to changes in ecosystem services: A review. *Journal of Experimental Marine Biology and Ecology*, 492, 49–62. <https://doi.org/10.1016/j.jembe.2017.01.019>
- Levin, L. A., Ekau, W., Gooday, A. J., Jorissen, F., Middelburg, J. J., Naqvi, S. W. A., Neira, C., Rabalais, N. N., & Zhang, J. (2009). *Effects of natural and human-induced hypoxia on coastal benthos*.
- Li, C., Huang, J., Liu, X., Ding, L., He, Y., & Xie, Y. (2024). The ocean losing its breath under the heatwaves. *Nature Communications*, 15(1), 6840. <https://doi.org/10.1038/s41467-024-51323-8>
- Li, J., Kokkola, R., Tabibzadeh, S., Yang, R., Ochani, M., Qiang, X., Harris, H. E., Czura, C. J., Wang, H., Ulloa, L., Wang, H., Warren, H. S., Moldawer, L. L., Fink, M. P., Andersson,

- U., Tracey, K. J., & Yang, H. (2003). Structural Basis for the Proinflammatory Cytokine Activity of High Mobility Group Box 1. *Molecular Medicine*, 9(1–2), 37–45.
<https://doi.org/10.1007/BF03402105>
- Li, J., Zhang, Y., Xiang, Z., Xiao, S., Yu, F., & Yu, Z. (2013). High mobility group box 1 can enhance NF- κ B activation and act as a pro-inflammatory molecule in the Pacific oyster, *Crassostrea gigas*. *Fish & Shellfish Immunology*, 35(1), 63–70.
<https://doi.org/10.1016/j.fsi.2013.04.001>
- Li, W., Li, X., Song, C., & Gao, G. (2024). Carbon removal, sequestration and release by mariculture in an important aquaculture area, China. *Science of The Total Environment*, 927, 172272. <https://doi.org/10.1016/j.scitotenv.2024.172272>
- Li, X., Shi, C., Yang, B., Li, Q., & Liu, S. (2023). High temperature aggravates mortalities of the Pacific oyster (*Crassostrea gigas*) infected with *Vibrio*: A perspective from homeostasis of digestive microbiota and immune response. *Aquaculture*, 568, 739309.
<https://doi.org/10.1016/j.aquaculture.2023.739309>
- Li, Y., Qin, J. G., Abbott, C. A., Li, X., & Benkendorff, K. (2007). Synergistic impacts of heat shock and spawning on the physiology and immune health of *Crassostrea gigas*: An explanation for summer mortality in Pacific oysters. *American Journal of Physiology-Regulatory, Integrative and Comparative Physiology*, 293(6), R2353–R2362.
<https://doi.org/10.1152/ajpregu.00463.2007>
- Li, Y., Qin, J. G., Li, X., & Benkendorff, K. (2009). Spawning-dependent stress responses in pacific oysters *Crassostrea gigas*: A simulated bacterial challenge in oysters. *Aquaculture*, 293(3–4), 164–171. <https://doi.org/10.1016/j.aquaculture.2009.04.044>

- Lim, H.-J., Kim, B.-M., Hwang, I. J., Lee, J.-S., Choi, I.-Y., Kim, Y.-J., & Rhee, J.-S. (2016). Thermal stress induces a distinct transcriptome profile in the Pacific oyster *Crassostrea gigas*. *Comparative Biochemistry and Physiology Part D: Genomics and Proteomics*, *19*, 62–70. <https://doi.org/10.1016/j.cbd.2016.06.006>
- Liu, Y., Bao, Z., Lin, Z., & Xue, Q. (2022). Transcriptomic identification of key genes in Pacific oysters *Crassostrea gigas* responding to major abiotic and biotic stressors. *Fish & Shellfish Immunology*, *131*, 1027–1039. <https://doi.org/10.1016/j.fsi.2022.11.009>
- Love, M. I., Huber, W., & Anders, S. (2014). Moderated estimation of fold change and dispersion for RNA-seq data with DESeq2. *Genome Biology*, *15*(12), 550. <https://doi.org/10.1186/s13059-014-0550-8>
- Lu, H., Liu, C., Yang, C., He, Z., Wang, L., & Song, L. (2024). Genome-wide identification of the HSP70 genes in Pacific oyster *Magallana gigas* and their response to heat stress. *Cell Stress and Chaperones*, *29*(4), 589–602. <https://doi.org/10.1016/j.cstres.2024.06.002>
- Lv, X., Yang, W., Guo, Z., Wu, W., Li, Y., Yan, X., Wang, W., Zhang, T., Sun, J., Wang, L., & Song, L. (2022). CgHMGB1 functions as a broad-spectrum recognition molecule to induce the expressions of CgIL17-5 and Cgdefh2 via MAPK or NF- κ B signaling pathway in *Crassostrea gigas*. *International Journal of Biological Macromolecules*, *211*, 289–300. <https://doi.org/10.1016/j.ijbiomac.2022.04.166>
- Maar, M., Larsen, J., Saurel, C., Mohn, C., Murawski, J., & Petersen, J. K. (2021). Mussel transplantation as a tool to mitigate hypoxia in eutrophic areas. *Hydrobiologia*, *848*(7), 1553–1573. <https://doi.org/10.1007/s10750-021-04545-6>
- Mackenzie, C. L., Raap, M. R., Leduc, S., Walker, C. Y. V., Green, T. J., Kim, E., Montgomery, E. M., Gray, S. L. M., Long, A., & Pearce, C. M. (2024). Development of a nature-based

- solution for mitigation of Pacific oyster summer mortality: Use of the intertidal zone to improve resilience to environmental stressors. *Frontiers in Marine Science*, *11*, 1345493. <https://doi.org/10.3389/fmars.2024.1345493>
- Malham, S. K., Cotter, E., O’Keeffe, S., Lynch, S., Culloty, S. C., King, J. W., Latchford, J. W., & Beaumont, A. R. (2009). Summer mortality of the Pacific oyster, *Crassostrea gigas*, in the Irish Sea: The influence of temperature and nutrients on health and survival. *Aquaculture*, *287*(1–2), 128–138. <https://doi.org/10.1016/j.aquaculture.2008.10.006>
- Marks, A. R. (1996). Cellular functions of immunophilins. *Physiological Reviews*, *76*(3), 631–649. <https://doi.org/10.1152/physrev.1996.76.3.631>
- Martenot, C., Gervais, O., Chollet, B., Houssin, M., & Renault, T. (2017). Haemocytes collected from experimentally infected Pacific oysters, *Crassostrea gigas*: Detection of ostreid herpesvirus 1 DNA, RNA, and proteins in relation with inhibition of apoptosis. *PLOS ONE*, *12*(5), e0177448. <https://doi.org/10.1371/journal.pone.0177448>
- Martínez-García, M. F., Ruesink, J. L., Grijalva-Chon, J. M., Lodeiros, C., Arreola-Lizárraga, J. A., De La Re-Vega, E., Varela-Romero, A., & Chávez-Villalba, J. (2022). Socioecological factors related to aquaculture introductions and production of Pacific oysters (*Crassostrea gigas*) worldwide. *Reviews in Aquaculture*, *14*(2), 613–629. <https://doi.org/10.1111/raq.12615>
- Masanja, F., Xu, Y., He, G., Liang, F., Liu, X., Yang, K., Mkuye, R., Liang, J., Deng, Y., & Zhao, L. (2022). Exploring HSP90 as a Biomarker for Marine Heatwaves in *Pinctada maxima*. *Frontiers in Marine Science*, *9*, 913920. <https://doi.org/10.3389/fmars.2022.913920>
- Maulu, S., Hasimuna, O. J., Haambiya, L. H., Monde, C., Musuka, C. G., Makorwa, T. H., Munganga, B. P., Phiri, K. J., & Nsekanabo, J. D. (2021). Climate Change Effects on

- Aquaculture Production: Sustainability Implications, Mitigation, and Adaptations. *Frontiers in Sustainable Food Systems*, 5, 609097.
<https://doi.org/10.3389/fsufs.2021.609097>
- McMahon, R. F. (1988). Respiratory Response to Periodic Emergence in Intertidal Molluscs. *American Zoologist*, 28(1), 97–114. <https://doi.org/10.1093/icb/28.1.97>
- Miao, Z., Xu, D., Cui, M., & Zhang, Q. (2016). High mobility group protein DSP1 negatively regulates HSP70 transcription in *Crassostrea hongkongensis*. *Biochemical and Biophysical Research Communications*, 474(4), 634–639.
<https://doi.org/10.1016/j.bbrc.2016.03.163>
- Michael Beman, J., Arrigo, K. R., & Matson, P. A. (2005). Agricultural runoff fuels large phytoplankton blooms in vulnerable areas of the ocean. *Nature*, 434(7030), 211–214.
<https://doi.org/10.1038/nature03370>
- Miossec, L., Deuff, R.-M. L., & Gouilletquer, P. (2009). *Alien Species Alert: Crassostrea Gigas (Pacific Oyster)*.
- Möller, T., Högner, A. E., Schleussner, C.-F., Bien, S., Kitzmann, N. H., Lamboll, R. D., Rogelj, J., Donges, J. F., Rockström, J., & Wunderling, N. (2024). Achieving net zero greenhouse gas emissions critical to limit climate tipping risks. *Nature Communications*, 15(1), 6192.
<https://doi.org/10.1038/s41467-024-49863-0>
- Moore, C., Morley, J. W., Morrison, B., Kolian, M., Horsch, E., Frölicher, T., Pinsky, M. L., & Griffis, R. (2021). Estimating the Economic Impacts of Climate Change on 16 Major US Fisheries. *Climate Change Economics*, 12(01), 2150002.
<https://doi.org/10.1142/S2010007821500020>

- Moore, S. K., Cline, M. R., Blair, K., Klinger, T., Varney, A., & Norman, K. (2019). An index of fisheries closures due to harmful algal blooms and a framework for identifying vulnerable fishing communities on the U.S. West Coast. *Marine Policy*, *110*, 103543. <https://doi.org/10.1016/j.marpol.2019.103543>
- Mukhopadhyay, I., Nazir, A., Saxena, D. K., & Chowdhuri, D. K. (2003). Heat shock response: *Hsp70* in environmental monitoring. *Journal of Biochemical and Molecular Toxicology*, *17*(5), 249–254. <https://doi.org/10.1002/jbt.10086>
- Murshed-e-Jahan, K., Ahmed, M., & Belton, B. (2010). The impacts of aquaculture development on food security: Lessons from Bangladesh. *Aquaculture Research*, *41*(4), 481–495. <https://doi.org/10.1111/j.1365-2109.2009.02337.x>
- Naylor, R. L., Hardy, R. W., Bureau, D. P., Chiu, A., Elliott, M., Farrell, A. P., Forster, I., Gatlin, D. M., Goldberg, R. J., Hua, K., & Nichols, P. D. (2009). Feeding aquaculture in an era of finite resources. *Proceedings of the National Academy of Sciences*, *106*(36), 15103–15110. <https://doi.org/10.1073/pnas.0905235106>
- Nydahl, A., Panigrahi, S., & Wikner, J. (2013). Increased microbial activity in a warmer and wetter climate enhances the risk of coastal hypoxia. *FEMS Microbiology Ecology*, *85*(2), 338–347. <https://doi.org/10.1111/1574-6941.12123>
- Oh, S. J., Moon, S., Yoon, Y. H., Kim, D. H., Kang, I. J., & Shimasaki, Y. (2021). *Biomonitoring System to Assist in Early Detection of Oxygen-deficient Sea Water using Shell Valve Movements of Pacific Oyster (Crassostrea gigas)* (2). Faculty of Agriculture, Kyushu University. <https://doi.org/10.15017/4486554>
- Oksanen, J., Simpson, G. L., Blanchet, F. G., Kindt, R., Legendre, P., Minchin, P. R., O'Hara, R. B., Solymos, P., Stevens, M. H. H., Szoecs, E., Wagner, H., Barbour, M., Bedward, M.,

- Bolker, B., Borcard, D., Carvalho, G., Chirico, M., De Caceres, M., Durand, S., & Weedon, J. (2001). *vegan: Community Ecology Package* (p. 2.6-8) [Dataset].
<https://doi.org/10.32614/CRAN.package.vegan>
- Oliver, E. C. J., Burrows, M. T., Donat, M. G., Sen Gupta, A., Alexander, L. V., Perkins-Kirkpatrick, S. E., Benthuisen, J. A., Hobday, A. J., Holbrook, N. J., Moore, P. J., Thomsen, M. S., Wernberg, T., & Smale, D. A. (2019). Projected Marine Heatwaves in the 21st Century and the Potential for Ecological Impact. *Frontiers in Marine Science*, *6*, 734. <https://doi.org/10.3389/fmars.2019.00734>
- Oliver, E. C. J., Donat, M. G., Burrows, M. T., Moore, P. J., Smale, D. A., Alexander, L. V., Benthuisen, J. A., Feng, M., Sen Gupta, A., Hobday, A. J., Holbrook, N. J., Perkins-Kirkpatrick, S. E., Scannell, H. A., Straub, S. C., & Wernberg, T. (2018). Longer and more frequent marine heatwaves over the past century. *Nature Communications*, *9*(1), 1324. <https://doi.org/10.1038/s41467-018-03732-9>
- Pace, S. M., Powell, E. N., Soniat, T. M., & Kuykendall, K. M. (2020). How Oyster Health Indices Vary between Mass Mortality Events. *Journal of Shellfish Research*, *39*(3).
<https://doi.org/10.2983/035.039.0308>
- Patterson, H. K., Boettcher, A., & Carmichael, R. H. (2014). Biomarkers of Dissolved Oxygen Stress in Oysters: A Tool for Restoration and Management Efforts. *PLoS ONE*, *9*(8), e104440. <https://doi.org/10.1371/journal.pone.0104440>
- Pecl, G. T., Araújo, M. B., Bell, J. D., Blanchard, J., Bonebrake, T. C., Chen, I.-C., Clark, T. D., Colwell, R. K., Danielsen, F., Evengård, B., Falconi, L., Ferrier, S., Frusher, S., Garcia, R. A., Griffis, R. B., Hobday, A. J., Janion-Scheepers, C., Jarzyna, M. A., Jennings, S., & Williams, S. E. (2017). Biodiversity redistribution under climate change: Impacts on

- ecosystems and human well-being. *Science*, 355(6332), eaai9214.
<https://doi.org/10.1126/science.aai9214>
- Peñaloza, C., Gutierrez, A. P., Eöry, L., Wang, S., Guo, X., Archibald, A. L., Bean, T. P., & Houston, R. D. (2021). A chromosome-level genome assembly for the Pacific oyster *Crassostrea gigas*. *GigaScience*, 10(3), giab020.
<https://doi.org/10.1093/gigascience/giab020>
- Petton, B., Destoumieux-Garzón, D., Pernet, F., Toulza, E., De Lorgeril, J., Degremont, L., & Mitta, G. (2021). The Pacific Oyster Mortality Syndrome, a Polymicrobial and Multifactorial Disease: State of Knowledge and Future Directions. *Frontiers in Immunology*, 12, 630343. <https://doi.org/10.3389/fimmu.2021.630343>
- Piatt, J. F., Parrish, J. K., Renner, H. M., Schoen, S. K., Jones, T. T., Arimitsu, M. L., Kuletz, K. J., Bodenstein, B., García-Reyes, M., Duerr, R. S., Corcoran, R. M., Kaler, R. S. A., McChesney, G. J., Golightly, R. T., Coletti, H. A., Suryan, R. M., Burgess, H. K., Lindsey, J., Lindquist, K., & Sydeman, W. J. (2020). Extreme mortality and reproductive failure of common murrelets resulting from the northeast Pacific marine heatwave of 2014-2016. *PLOS ONE*, 15(1), e0226087. <https://doi.org/10.1371/journal.pone.0226087>
- Piñeiro-Corbeira, C., Barrientos, S., Barreiro, R., & De La Cruz-Modino, R. (2022). Assessing the importance of kelp forests for small-scale fisheries under a global change scenario. *Frontiers in Marine Science*, 9, 973251. <https://doi.org/10.3389/fmars.2022.973251>
- Pörtner, H. O., Peck, L. S., & Hirse, T. (2006). Hyperoxia alleviates thermal stress in the Antarctic bivalve, *Laternula elliptica*: Evidence for oxygen limited thermal tolerance. *Polar Biology*, 29(8), 688–693. <https://doi.org/10.1007/s00300-005-0106-1>

- Pörtner, H.-O., Bock, C., & Mark, F. C. (2017). Oxygen- and capacity-limited thermal tolerance: Bridging ecology and physiology. *Journal of Experimental Biology*, 220(15), 2685–2696. <https://doi.org/10.1242/jeb.134585>
- Quayle, D. B. (1988). *Pacific oyster culture in British Columbia*. Dept. of Fisheries and Oceans.
- Rainier, J. S., & Mann, R. L. (1992). *A comparison of methods for calculating condition index in eastern oysters Crassostrea virginica (Gmelin, 1791)*.
- Raivo Kolde. (2010). *pheatmap: Pretty Heatmaps* (p. 1.0.12) [Dataset]. <https://doi.org/10.32614/CRAN.package.pheatmap>
- Rasmusson, L. M., Buapet, P., George, R., Gullström, M., Gunnarsson, P. C. B., & Björk, M. (2020). Effects of temperature and hypoxia on respiration, photorespiration, and photosynthesis of seagrass leaves from contrasting temperature regimes. *ICES Journal of Marine Science*, 77(6), 2056–2065. <https://doi.org/10.1093/icesjms/fsaa093>
- Reeder-Myers, L., Braje, T. J., Hofman, C. A., Elliott Smith, E. A., Garland, C. J., Grone, M., Hadden, C. S., Hatch, M., Hunt, T., Kelley, A., LeFebvre, M. J., Lockman, M., McKechnie, I., McNiven, I. J., Newsom, B., Pluckhahn, T., Sanchez, G., Schwadron, M., Smith, K. Y., & Rick, T. C. (2022). Indigenous oyster fisheries persisted for millennia and should inform future management. *Nature Communications*, 13(1), 2383. <https://doi.org/10.1038/s41467-022-29818-z>
- Ren, J., Ross, A., & Schiel, D. (2000). Functional descriptions of feeding and energetics of the Pacific oyster *Crassostrea gigas* in New Zealand. *Marine Ecology Progress Series*, 208, 119–130. <https://doi.org/10.3354/meps208119>
- Richter, K., & Buchner, J. (2001). Hsp90: Chaperoning signal transduction. *Journal of Cellular Physiology*, 188(3), 281–290. <https://doi.org/10.1002/jcp.1131>

- Roman, M. R., Brandt, S. B., Houde, E. D., & Pierson, J. J. (2019). Interactive Effects of Hypoxia and Temperature on Coastal Pelagic Zooplankton and Fish. *Frontiers in Marine Science*, 6, 139. <https://doi.org/10.3389/fmars.2019.00139>
- Rouyer, T., Fromentin, J.-M., Hidalgo, M., & Stenseth, N. C. (2014). Combined effects of exploitation and temperature on fish stocks in the Northeast Atlantic. *ICES Journal of Marine Science*, 71(7), 1554–1562. <https://doi.org/10.1093/icesjms/fsu042>
- Roy, S. M., P, J., Machavaram, R., Pareek, C. M., & Mal, B. C. (2021). Diversified aeration facilities for effective aquaculture systems—A comprehensive review. *Aquaculture International*, 29(3), 1181–1217. <https://doi.org/10.1007/s10499-021-00685-7>
- Sabine, C. L., Feely, R. A., Gruber, N., Key, R. M., Lee, K., Bullister, J. L., Wanninkhof, R., Wong, C. S., Wallace, D. W. R., Tilbrook, B., Millero, F. J., Peng, T.-H., Kozyr, A., Ono, T., & Rios, A. F. (2004). The Oceanic Sink for Anthropogenic CO₂. *Science*, 305(5682), 367–371. <https://doi.org/10.1126/science.1097403>
- Sae-Lim, P., Kause, A., Mulder, H. A., & Olesen, I. (2017). Breeding and Genetics Symposium: Climate change and selective breeding in aquaculture. *Journal of Animal Science* 95(4), 1801–1812. <https://doi.org/10.2527/jas.2016.1066>
- Safonova, K., Meier, H. E. M., & Gröger, M. (2024). Summer heatwaves on the Baltic Sea seabed contribute to oxygen deficiency in shallow areas. *Communications Earth & Environment*, 5(1), 106. <https://doi.org/10.1038/s43247-024-01268-z>
- Sampaio, E., Santos, C., Rosa, I. C., Ferreira, V., Pörtner, H.-O., Duarte, C. M., Levin, L. A., & Rosa, R. (2021). Impacts of hypoxic events surpass those of future ocean warming and acidification. *Nature Ecology & Evolution*, 5(3), 311–321. <https://doi.org/10.1038/s41559-020-01370-3>

- Saulnier, D., De Decker, S., Haffner, P., Cobret, L., Robert, M., & Garcia, C. (2010). A Large-Scale Epidemiological Study to Identify Bacteria Pathogenic to Pacific Oyster *Crassostrea gigas* and Correlation Between Virulence and Metalloprotease-like Activity. *Microbial Ecology*, 59(4), 787–798. <https://doi.org/10.1007/s00248-009-9620-y>
- Scanes, E., Parker, L. M., O'Connor, W. A., Dove, M. C., & Ross, P. M. (2020). Heatwaves alter survival of the Sydney rock oyster, *Saccostrea glomerata*. *Marine Pollution Bulletin*, 158, 111389. <https://doi.org/10.1016/j.marpolbul.2020.111389>
- Schmitt, P., Lorgeril, J. D., Gueguen, Y., Destoumieux-Garzón, D., & Bachère, E. (2012). Expression, tissue localization and synergy of antimicrobial peptides and proteins in the immune response of the oyster *Crassostrea gigas*. *Developmental & Comparative Immunology*, 37(3–4), 363–370. <https://doi.org/10.1016/j.dci.2012.01.004>
- Scripps Institution of Oceanography, Cavole, L., Demko, A., Diner, R., Giddings, A., Koester, I., Pagniello, C., Paulsen, M.-L., Ramirez-Valdez, A., Schwenck, S., Yen, N., Zill, M., & Franks, P. (2016). Biological Impacts of the 2013–2015 Warm-Water Anomaly in the Northeast Pacific: Winners, Losers, and the Future. *Oceanography*, 29(2). <https://doi.org/10.5670/oceanog.2016.32>
- Segarra, A., Mauduit, F., Faury, N., Trancart, S., Dégremont, L., Tourbiez, D., Haffner, P., Barbosa-Solomieu, V., Pépin, J.-F., Travers, M.-A., & Renault, T. (2014). Dual transcriptomics of virus-host interactions: Comparing two Pacific oyster families presenting contrasted susceptibility to ostreid herpesvirus 1. *BMC Genomics*, 15(1), 580. <https://doi.org/10.1186/1471-2164-15-580>
- Serpetti, N., Baudron, A. R., Burrows, M. T., Payne, B. L., Helaouët, P., Fernandes, P. G., & Heymans, J. J. (2017). Impact of ocean warming on sustainable fisheries management

- informs the Ecosystem Approach to Fisheries. *Scientific Reports*, 7(1), 13438.
<https://doi.org/10.1038/s41598-017-13220-7>
- Shumway, S. E., Davis, C., Downey, R., Karney, R., Kraeuter, J., Rheault, R., & Wikfors, G. (2003). Shellfish aquaculture—In praise of sustainable economies and environments. *World Aquaculture*, 34(4).
- Shunk, N. P., Mazzini, P. L. F., & Walter, R. K. (2024). Impacts of Marine Heatwaves on Subsurface Temperatures and Dissolved Oxygen in the Chesapeake Bay. *Journal of Geophysical Research: Oceans*, 129(3), e2023JC020338.
<https://doi.org/10.1029/2023JC020338>
- Siboni, N., King, W. L., Williams, N. L. R., Scanes, E., Giardina, M., Green, T. J., Ostrowski, M., O'Connor, W., Dove, M., Labbate, M., & Seymour, J. R. (2024). Increased abundance of potentially pathogenic *Vibrio* and a marine heatwave co-occur with a Pacific Oyster summer mortality event. *Aquaculture*, 583, 740618.
<https://doi.org/10.1016/j.aquaculture.2024.740618>
- Siddique, M. A. B., Ahammad, A. K. S., Mahalder, B., Alam, Md. M., Hasan, N. A., Bashar, A., Biswas, J. C., & Haque, M. M. (2022). Perceptions of the Impact of Climate Change on Performance of Fish Hatcheries in Bangladesh: An Empirical Study. *Fishes*, 7(5), 270.
<https://doi.org/10.3390/fishes7050270>
- Skjæveland, I., Iliev, D. B., Strandskog, G., & Jørgensen, J. B. (2009). Identification and characterization of TLR8 and MyD88 homologs in Atlantic salmon (*Salmo salar*). *Developmental & Comparative Immunology*, 33(9), 1011–1017.
<https://doi.org/10.1016/j.dci.2009.04.007>

- Smale, D. A. (2020). Impacts of ocean warming on kelp forest ecosystems. *New Phytologist*, 225(4), 1447–1454. <https://doi.org/10.1111/nph.16107>
- Smith, K. E., Burrows, M. T., Hobday, A. J., King, N. G., Moore, P. J., Sen Gupta, A., Thomsen, M. S., Wernberg, T., & Smale, D. A. (2023). Biological Impacts of Marine Heatwaves. *Annual Review of Marine Science*, 15(1), 119–145. <https://doi.org/10.1146/annurev-marine-032122-121437>
- Smith, K. E., Burrows, M. T., Hobday, A. J., Sen Gupta, A., Moore, P. J., Thomsen, M., Wernberg, T., & Smale, D. A. (2021). Socioeconomic impacts of marine heatwaves: Global issues and opportunities. *Science*, 374(6566), eabj3593. <https://doi.org/10.1126/science.abj3593>
- Soletchnik, P., Ropert, M., Mazurié, J., Gildas Fleury, P., & Le Coz, F. (2007). Relationships between oyster mortality patterns and environmental data from monitoring databases along the coasts of France. *Aquaculture*, 271(1–4), 384–400. <https://doi.org/10.1016/j.aquaculture.2007.02.049>
- Sone, R., Waku, M., Yamada, S., Miyawaki, D., Ishida, T., Kamohara, S., Inoue, T., & Suzuki, T. (2023). Mass Mortality of Asari Clams (*Ruditapes philippinarum*) Triggered by Wind-Induced Upwelling of Hypoxic Water Masses. *Water*, 15(22), 3997. <https://doi.org/10.3390/w15223997>
- Song, J., Farhadi, A., Tan, K., Lim, L., & Tan, K. (2024). Impact of anthropogenic global hypoxia on the physiological response of bivalves. *Science of The Total Environment*, 926, 172056. <https://doi.org/10.1016/j.scitotenv.2024.172056>
- Song, X., Wang, L., Song, L., Zhao, J., Zhang, H., Zheng, P., Qiu, L., Liu, X., & Wu, L. (2009). A cyclophilin A inducible expressed in gonad of zhikong scallop *Chlamys farreri*.

Molecular Biology Reports, 36(6), 1637–1645. <https://doi.org/10.1007/s11033-008-9363-8>

Sørensen, J. G., Kristensen, T. N., & Loeschcke, V. (2003). The evolutionary and ecological role of heat shock proteins. *Ecology Letters*, 6(11), 1025–1037.

<https://doi.org/10.1046/j.1461-0248.2003.00528.x>

Srisunont, C., Srisunont, T., & Babel, S. (2022). Development of models for sustainable green mussel cultivation under climate change events. *Ecological Modelling*, 473, 110141.

<https://doi.org/10.1016/j.ecolmodel.2022.110141>

Stephens, M. (2016). False discovery rates: A new deal. *Biostatistics*, kxw041.

<https://doi.org/10.1093/biostatistics/kxw041>

Stewart-Sinclair, P. J., Last, K. S., Payne, B. L., & Wilding, T. A. (2020). A global assessment of the vulnerability of shellfish aquaculture to climate change and ocean acidification.

Ecology and Evolution, 10(7), 3518–3534. <https://doi.org/10.1002/ece3.6149>

Štros, M. (2010). HMGB proteins: Interactions with DNA and chromatin. *Biochimica et Biophysica Acta (BBA) - Gene Regulatory Mechanisms*, 1799(1–2), 101–113.

<https://doi.org/10.1016/j.bbagr.2009.09.008>

Sussarellu, R., Dudognon, T., Fabioux, C., Soudant, P., Moraga, D., & Kraffe, E. (2013). Rapid mitochondrial adjustments in response to short-term hypoxia and re-oxygenation in the Pacific oyster *Crassostrea gigas*. *Journal of Experimental Biology*, jeb.075879.

<https://doi.org/10.1242/jeb.075879>

Sussarellu, R., Fabioux, C., Le Moullac, G., Fleury, E., & Moraga, D. (2010). Transcriptomic response of the Pacific oyster *Crassostrea gigas* to hypoxia. *Marine Genomics*, 3(3–4),

133–143. <https://doi.org/10.1016/j.margen.2010.08.005>

- Takahashi, N., Hayano, T., & Suzuki, M. (1989). Peptidyl-prolyl cis-trans isomerase is the cyclosporin A-binding protein cyclophilin. *Nature*, *337*(6206), 473–475.
<https://doi.org/10.1038/337473a0>
- Tang, Q., Zhang, J., & Fang, J. (2011). Shellfish and seaweed mariculture increase atmospheric CO₂ absorption by coastal ecosystems. *Marine Ecology Progress Series*, *424*, 97–104.
<https://doi.org/10.3354/meps08979>
- Teagle, H., Hawkins, S. J., Moore, P. J., & Smale, D. A. (2017). The role of kelp species as biogenic habitat formers in coastal marine ecosystems. *Journal of Experimental Marine Biology and Ecology*, *492*, 81–98. <https://doi.org/10.1016/j.jembe.2017.01.017>
- The State of World Fisheries and Aquaculture 2024*. (2024). FAO.
<https://doi.org/10.4060/cd0683en>
- Tigchelaar, M., Leape, J., Micheli, F., Allison, E. H., Basurto, X., Bennett, A., Bush, S. R., Cao, L., Cheung, W. W. L., Crona, B., DeClerck, F., Fanzo, J., Gelcich, S., Gephart, J. A., Golden, C. D., Halpern, B. S., Hicks, C. C., Jonell, M., Kishore, A., & Wabnitz, C. C. C. (2022). The vital roles of blue foods in the global food system. *Global Food Security*, *33*, 100637. <https://doi.org/10.1016/j.gfs.2022.100637>
- Townhill, B. L., Couce, E., Bell, J., Reeves, S., & Yates, O. (2021). Climate Change Impacts on Atlantic Oceanic Island Tuna Fisheries. *Frontiers in Marine Science*, *8*, 634280.
<https://doi.org/10.3389/fmars.2021.634280>
- Trainer, V. L., Moore, S. K., Hallegraeff, G., Kudela, R. M., Clement, A., Mardones, J. I., & Cochlan, W. P. (2020). Pelagic harmful algal blooms and climate change: Lessons from nature's experiments with extremes. *Harmful Algae*, *91*, 101591.
<https://doi.org/10.1016/j.hal.2019.03.009>

- Troost, K. (2010). Causes and effects of a highly successful marine invasion: Case-study of the introduced Pacific oyster *Crassostrea gigas* in continental NW European estuaries. *Journal of Sea Research*, 64(3), 145–165. <https://doi.org/10.1016/j.seares.2010.02.004>
- United Nations Department of Economic and Social Affairs. (2023). *The Sustainable Development Goals Report 2023: Special Edition*. United Nations. <https://doi.org/10.18356/9789210024914>
- Valenzuela Castillo, A., Sanchez Paz, A., Castro Longoria, R., Lopez Torres, M., & Grijalva Chon, J. (2019). Hsp70 function and polymorphism, its implications for mollusk aquaculture: A review. *Latin American Journal of Aquatic Research*, 47(2), 224–231. <https://doi.org/10.3856/vol47-issue2-fulltext-2>
- Van Der Schatte Olivier, A., Jones, L., Vay, L. L., Christie, M., Wilson, J., & Malham, S. K. (2020). A global review of the ecosystem services provided by bivalve aquaculture. *Reviews in Aquaculture*, 12(1), 3–25. <https://doi.org/10.1111/raq.12301>
- Vaquer-Sunyer, R., & Duarte, C. M. (2008). Thresholds of hypoxia for marine biodiversity. *Proceedings of the National Academy of Sciences*, 105(40), 15452–15457. <https://doi.org/10.1073/pnas.0803833105>
- Vasquez, H. E., Hashimoto, K., Yoshida, A., Hara, K., Imai, C. C., Kitamura, H., & Satuito, C. G. (2013). A Glycoprotein in Shells of Conspecifics Induces Larval Settlement of the Pacific Oyster *Crassostrea gigas*. *PLoS ONE*, 8(12), e82358. <https://doi.org/10.1371/journal.pone.0082358>
- Vergés, A., Doropoulos, C., Malcolm, H. A., Skye, M., Garcia-Pizá, M., Marzinelli, E. M., Campbell, A. H., Ballesteros, E., Hoey, A. S., Vila-Concejo, A., Bozec, Y.-M., & Steinberg, P. D. (2016). Long-term empirical evidence of ocean warming leading to

- tropicalization of fish communities, increased herbivory, and loss of kelp. *Proceedings of the National Academy of Sciences*, 113(48), 13791–13796.
<https://doi.org/10.1073/pnas.1610725113>
- Vezzulli, L., Brettar, I., Pezzati, E., Reid, P. C., Colwell, R. R., Höfle, M. G., & Pruzzo, C. (2012). Long-term effects of ocean warming on the prokaryotic community: Evidence from the vibrios. *The ISME Journal*, 6(1), 21–30. <https://doi.org/10.1038/ismej.2011.89>
- Villasante, S., Macho, G., Silva, M. R. O., Lopes, P. F. M., Pita, P., Simón, A., Balsa, J. C. M., Olabarria, C., Vázquez, E., & Calvo, N. (2022). Resilience and Social Adaptation to Climate Change Impacts in Small-Scale Fisheries. *Frontiers in Marine Science*, 9, 802762. <https://doi.org/10.3389/fmars.2022.802762>
- Walsh, S., Copeland, C., & Westlake, M. (2004). *Major Fish Kills in the Northern Rivers of NSW in 2001: Causes, Impacts & Responses*.
- Wang, T., Meng, J., Li, L., & Zhang, G. (2016). Characterization of CgHIF α -Like, a Novel bHLH-PAS Transcription Factor Family Member, and Its Role under Hypoxia Stress in the Pacific Oyster *Crassostrea gigas*. *PLOS ONE*, 11(11), e0166057.
<https://doi.org/10.1371/journal.pone.0166057>
- Wendling, C. C., & Wegner, K. M. (2013). Relative contribution of reproductive investment, thermal stress and *Vibrio* infection to summer mortality phenomena in Pacific oysters. *Aquaculture*, 412–413, 88–96. <https://doi.org/10.1016/j.aquaculture.2013.07.009>
- Wendling, C. C., & Wegner, K. M. (2015). Adaptation to enemy shifts: Rapid resistance evolution to local *Vibrio* spp. in invasive Pacific oysters. *Proceedings of the Royal Society B: Biological Sciences*, 282(1804), 20142244.
<https://doi.org/10.1098/rspb.2014.2244>

- Wernberg, T., Smale, D. A., Tuya, F., Thomsen, M. S., Langlois, T. J., De Bettignies, T., Bennett, S., & Rousseaux, C. S. (2013). An extreme climatic event alters marine ecosystem structure in a global biodiversity hotspot. *Nature Climate Change*, 3(1), 78–82.
<https://doi.org/10.1038/nclimate1627>
- Wernberg, T., Thomsen, M. S., Baum, J. K., Bishop, M. J., Bruno, J. F., Coleman, M. A., Filbee-Dexter, K., Gagnon, K., He, Q., Murdiyarso, D., Rogers, K., Silliman, B. R., Smale, D. A., Starko, S., & Vanderklift, M. A. (2024). Impacts of Climate Change on Marine Foundation Species. *Annual Review of Marine Science*, 16(1), 247–282.
<https://doi.org/10.1146/annurev-marine-042023-093037>
- White, R. H., Anderson, S., Booth, J. F., Braich, G., Draeger, C., Fei, C., Harley, C. D. G., Henderson, S. B., Jakob, M., Lau, C.-A., Mareshet Admasu, L., Narinesingh, V., Rodell, C., Roocroft, E., Weinberger, K. R., & West, G. (2023). The unprecedented Pacific Northwest heatwave of June 2021. *Nature Communications*, 14(1), 727.
<https://doi.org/10.1038/s41467-023-36289-3>
- Whitney, M. M. (2022). Observed and projected global warming pressure on coastal hypoxia. *Biogeosciences*, 19(18), 4479–4497. <https://doi.org/10.5194/bg-19-4479-2022>
- Whittington, R. J., Ingram, L., & Rubio, A. (2024). Environmental Conditions Associated with Four Index Cases of Pacific Oyster Mortality Syndrome (POMS) in *Crassostrea gigas* in Australia Between 2010 and 2024: Emergence or Introduction of Ostreid herpesvirus-1? *Animals*, 14(21), 3052. <https://doi.org/10.3390/ani14213052>
- Wickham, H., Averick, M., Bryan, J., Chang, W., McGowan, L., François, R., Grolemond, G., Hayes, A., Henry, L., Hester, J., Kuhn, M., Pedersen, T., Miller, E., Bache, S., Müller, K., Ooms, J., Robinson, D., Seidel, D., Spinu, V., & Yutani, H. (2019). Welcome to the

- Tidyverse. *Journal of Open Source Software*, 4(43), 1686.
<https://doi.org/10.21105/joss.01686>
- Witkop, E. M., Proestou, D. A., & Gomez-Chiarri, M. (2022). The expanded inhibitor of apoptosis gene family in oysters possesses novel domain architectures and may play diverse roles in apoptosis following immune challenge. *BMC Genomics*, 23(1), 201.
<https://doi.org/10.1186/s12864-021-08233-6>
- Xie, F., Wang, J., & Zhang, B. (2023). RefFinder: A web-based tool for comprehensively analyzing and identifying reference genes. *Functional & Integrative Genomics*, 23(2), 125. <https://doi.org/10.1007/s10142-023-01055-7>
- Xu, T., Xie, J., Yang, S., Ye, S., Luo, M., & Wu, X. (2016). First characterization of three cyclophilin family proteins in the oyster, *Crassostrea ariakensis* Gould. *Fish & Shellfish Immunology*, 55, 257–266. <https://doi.org/10.1016/j.fsi.2016.05.037>
- Xu, T., Yang, S., Xie, J., Ye, S., Luo, M., Zhu, Z., & Wu, X. (2012). HMGB in Mollusk *Crassostrea ariakensis* Gould: Structure, Pro-Inflammatory Cytokine Function Characterization and Anti-Infection Role of Its Antibody. *PLoS ONE*, 7(11), e50789.
<https://doi.org/10.1371/journal.pone.0050789>
- Xu, Y., Liang, J., He, G., Liu, X., Yang, K., Masanja, F., Deng, Y., & Zhao, L. (2022). Responses of Pearl Oysters to Marine Heatwaves as Indicated by HSP70. *Frontiers in Marine Science*, 9, 847585. <https://doi.org/10.3389/fmars.2022.847585>
- Xu, Y., Wang, Z., Zhang, Y., Liang, J., He, G., Liu, X., Zheng, Z., Deng, Y., & Zhao, L. (2022). Transcriptome analysis reveals acclimation responses of pearl oysters to marine heatwaves. *Science of The Total Environment*, 810, 151189.
<https://doi.org/10.1016/j.scitotenv.2021.151189>

- Yang, B., Zhai, S., Li, X., Tian, J., Li, Q., Shan, H., & Liu, S. (2021). Identification of *Vibrio alginolyticus* as a causative pathogen associated with mass summer mortality of the Pacific Oyster (*Crassostrea gigas*) in China. *Aquaculture*, 535, 736363. <https://doi.org/10.1016/j.aquaculture.2021.736363>
- Yang, C., Gao, Q., Liu, C., Wang, L., Zhou, Z., Gong, C., Zhang, A., Zhang, H., Qiu, L., & Song, L. (2017). The transcriptional response of the Pacific oyster *Crassostrea gigas* against acute heat stress. *Fish & Shellfish Immunology*, 68, 132–143. <https://doi.org/10.1016/j.fsi.2017.07.016>
- Yang, C.-Y., Sierp, M. T., Abbott, C. A., Li, Y., & Qin, J. G. (2016). Responses to thermal and salinity stress in wild and farmed Pacific oysters *Crassostrea gigas*. *Comparative Biochemistry and Physiology Part A: Molecular & Integrative Physiology*, 201, 22–29. <https://doi.org/10.1016/j.cbpa.2016.06.024>
- Yu, H., Fang, G., Rose, K. A., Lin, J., Feng, J., Wang, H., Cao, Q., Tang, Y., & Zhang, T. (2023). Effects of habitat usage on hypoxia avoidance behavior and exposure in reef-dependent marine coastal species. *Frontiers in Marine Science*, 10, 1109523. <https://doi.org/10.3389/fmars.2023.1109523>
- Zarzychny, K. M., Rius, M., Williams, S. T., & Fenberg, P. B. (2024). The ecological and evolutionary consequences of tropicalisation. *Trends in Ecology & Evolution*, 39(3), 267–279. <https://doi.org/10.1016/j.tree.2023.10.006>
- Zhang, G., Fang, X., Guo, X., Li, L., Luo, R., Xu, F., Yang, P., Zhang, L., Wang, X., Qi, H., Xiong, Z., Que, H., Xie, Y., Holland, P. W. H., Paps, J., Zhu, Y., Wu, F., Chen, Y., Wang, J., & Wang, J. (2012). The oyster genome reveals stress adaptation and complexity of shell formation. *Nature*, 490(7418), 49–54. <https://doi.org/10.1038/nature11413>

- Zhang, G., Li, L., Meng, J., Qi, H., Qu, T., Xu, F., & Zhang, L. (2016). Molecular Basis for Adaptation of Oysters to Stressful Marine Intertidal Environments. *Annual Review of Animal Biosciences*, 4(1), 357–381. <https://doi.org/10.1146/annurev-animal-022114-110903>
- Zhang, X., Huang, B.-W., Zheng, Y.-D., Xin, L.-S., Chen, W.-B., Yu, T., Li, C., Wang, C.-M., & Bai, C.-M. (2023). Identification and Characterization of Infectious Pathogens Associated with Mass Mortalities of Pacific Oyster (*Crassostrea gigas*) Cultured in Northern China. *Biology*, 12(6), 759. <https://doi.org/10.3390/biology12060759>
- Zhang, Y., Sun, J., Mu, H., Li, J., Zhang, Y., Xu, F., Xiang, Z., Qian, P.-Y., Qiu, J.-W., & Yu, Z. (2015). Proteomic Basis of Stress Responses in the Gills of the Pacific Oyster *Crassostrea gigas*. *Journal of Proteome Research*, 14(1), 304–317. <https://doi.org/10.1021/pr500940s>
- Zhao, X., Yu, H., Kong, L., Liu, S., & Li, Q. (2014). Comparative Transcriptome Analysis of Two Oysters, *Crassostrea gigas* and *Crassostrea hongkongensis* Provides Insights into Adaptation to Hypo-Osmotic Conditions. *PLoS ONE*, 9(11), e111915. <https://doi.org/10.1371/journal.pone.0111915>